

คุณลักษณะทางกลเชิงความร้อนของโคพอลิเมอร์เบนซอกซาซีน-ยูรีเทน
และวัสดุคอมพอสิตเสริมแรงด้วยเส้นใยไพลอน



นายวันฉัตร บางเสน

ศูนย์วิทยทรัพยากร
จุฬาลงกรณ์มหาวิทยาลัย

วิทยานิพนธ์นี้เป็นส่วนหนึ่งของการศึกษาตามหลักสูตรปริญญาวิศวกรรมศาสตรมหาบัณฑิต

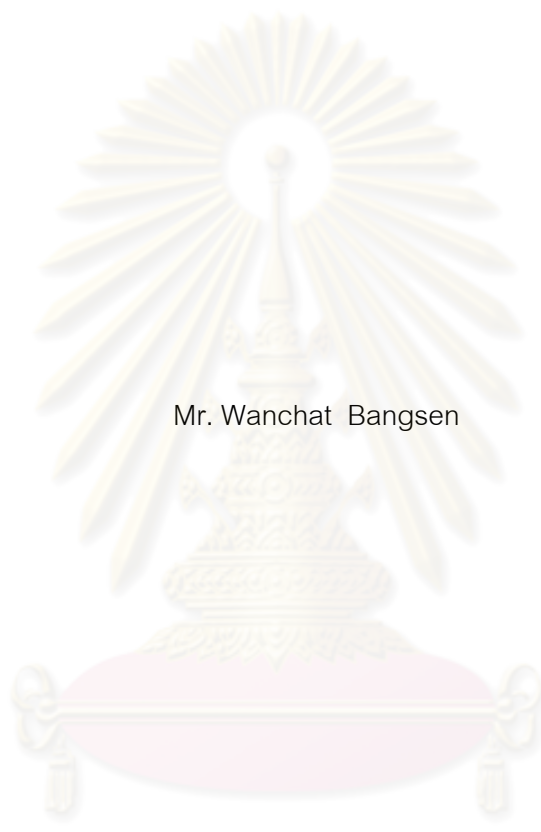
สาขาวิชาวิศวกรรมเคมี ภาควิชาวิศวกรรมเคมี

คณะวิศวกรรมศาสตร์ จุฬาลงกรณ์มหาวิทยาลัย

ปีการศึกษา 2551

ลิขสิทธิ์ของจุฬาลงกรณ์มหาวิทยาลัย

THERMOMECHANICAL CHARACTERISTIC OF BENZOXAZINE-URETHANE
COPOLYMERS AND THEIR ZYLON FIBER-REINFORCED COMPOSITES



Mr. Wanchat Bangsen

ศูนย์วิทยทรัพยากร
จุฬาลงกรณ์มหาวิทยาลัย
A Thesis Submitted in Partial Fulfillment of the Requirements
for the Degree of Master of Engineering Program in Chemical Engineering

Department of Chemical Engineering

Faculty of Engineering

Chulalongkorn University

Academic Year 2008

Copyright of Chulalongkorn University

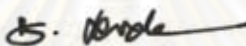
Thesis Title THERMOMECHANICAL CHARACTERISTIC OF BENZOXAZINE-
URETHANE COPOLYMERS AND THEIR ZYLON FIBER-REINFORCED
COMPOSITES

By Mr. Wanchat Bangsen


Field of Study Chemical Engineering

Advisor Associate Professor Sarawut Rimdusit, Ph.D.

Accepted by the Faculty of Engineering, Chulalongkorn University in Partial
Fulfillment of the Requirements for the Master's Degree



..... Dean of the Faculty of Engineering
(Associate Professor Boonsom Lerthirunwong, Dr.Ing.)

THESIS COMMITTEE


..... Chairman
(Associate Professor Chairit Satayaprasert, Ph.D.)


..... Advisor
(Associate Professor Sarawut Rimdusit, Ph.D.)


..... Examiner
(Assistant Professor Anongnat Somwangthanoj, Ph.D.)


..... External Examiner
(Kasinee Hemvichian, Ph.D.)

วันจักร บางเสน : คุณลักษณะทางกลเชิงความร้อนของโคพอลิเมอร์เบนซอกซาซีน-ยูรีเทนและวัสดุคอมพอลิทีเสริมแรงด้วยเส้นใยไครลอน. (THERMOMECHANICAL CHARACTERISTIC OF BENZOXAZINE-URETHANE COPOLYMERS AND THEIR ZYLON FIBER-REINFORCED COMPOSITES) อ. ที่ปรึกษาวิทยานิพนธ์หลัก : รศ.ดร. ศราวุธ ริมดุสิต, 106 หน้า.

งานวิจัยนี้มีจุดมุ่งหมายเพื่อพัฒนาสมบัติของเบนซอกซาซีนอัลลอยเมตริกเพื่อให้มีสมบัติทางกลในช่วงที่กว้างตั้งแต่การใช้งานในรูปพลาสติกแข็งของพอลิเบนซอกซาซีนที่ไม่ได้ผ่านการตัดแปรจนเป็นเมตริกที่มีความยืดหยุ่นสูงขึ้นไปของพอลิเบนซอกซาซีนที่อัลลอยกับยูรีเทนอีลาสโตเมอร์ ซึ่งยูรีเทนอีลาสโตเมอร์มีคุณสมบัติเด่นคือมีความยืดหยุ่นสูง ทำให้ได้พอลิเมอร์ลูกผสมที่มีคุณสมบัติทางกลที่กว้าง อีกทั้งในงานวิจัยนี้ได้พัฒนาวัสดุคอมพอลิทีโดยการเสริมแรงด้วยเส้นใยไครลอน โดยใช้พอลิเบนซอกซาซีนที่อัลลอยกับยูรีเทนอีลาสโตเมอร์เป็นพอลิเมอร์เมตริก เพื่อเพิ่มคุณสมบัติทางกล ซึ่งสามารถปรับให้เหมาะสมกับการใช้งานที่ต้องการรับแรงได้สูง โดยพอลิเบนซอกซาซีนถูกพัฒนาเพื่อให้มีคุณสมบัติเหมาะสมกับการใช้งานเป็นเมตริกของวัสดุประกอบแต่งสมรรถนะสูง พอลิเมอร์ชนิดนี้มีคุณสมบัติที่โดดเด่นหลายประการ เช่น สามารถสังเคราะห์ได้ง่าย รวมทั้งเกิดปฏิกิริยาเชื่อมขวางได้เองโดยไม่ต้องใช้สารปรม มีเสถียรภาพทางความร้อนสูง มีคุณสมบัติเชิงกลที่ดี และความแข็งแรงสูง อีกทั้งเบนซอกซาซีนเรซินยังมีสมบัติเด่นที่สามารถทำพอลิเมอร์อัลลอยร่วมกับเรซินประเภทอื่นเพื่อเพิ่มคุณสมบัติของเมตริกลูกผสมให้กว้างขวางและหลากหลาย จากผลการทดลองพบว่า ช่วงอุณหภูมิในการขึ้นรูปของเรซินผสมเบนซอกซาซีน/ยูรีเทนมีค่ากว้างมากขึ้นเมื่อทำการเพิ่มปริมาณของยูรีเทน สิ่งที่น่าสนใจคือ สามารถสังเกตเห็นการเกิดงานร่วม (synergy) ของอุณหภูมิการเปลี่ยนสถานะคล้ายแก้วได้อย่างชัดเจน นั่นคือ อุณหภูมิการเปลี่ยนสถานะคล้ายแก้วของระบบเบนซอกซาซีน/ยูรีเทน ที่ได้จะมีค่าสูงกว่าของพอลิเบนซอกซาซีน (166 องศาเซลเซียส) และ ยูรีเทนพรีพอลิเมอร์ (-70 องศาเซลเซียส) ปรากฏการณ์ดังกล่าวสามารถอธิบายได้ว่า ยูรีเทนพรีพอลิเมอร์สามารถเพิ่มความหนาแน่นในการเชื่อมขวางโครงสร้างตาข่ายของพอลิเมอร์อัลลอย นอกจากนี้จากการวิเคราะห์ผลการสลายตัวทางความร้อนพบว่าอุณหภูมิการสลายตัวทางความร้อนมีค่าเพิ่มขึ้นจาก 325°C ของพอลิเบนซอกซาซีน เป็น 336°C ในสัดส่วน 60/40 โดยน้ำหนักของ BA-a/PU และยังพบว่าปริมาณแก้วจะสูงขึ้นตามสัดส่วนของเบนซอกซาซีน ส่วนการทดสอบค่าการขยายตัวทางความร้อนพบว่าเกิดงานร่วมที่อัตราส่วนของพอลิเบนซอกซาซีนกับยูรีเทนอีลาสโตเมอร์ที่ 90/10 โดยน้ำหนัก สำหรับการทดสอบสมบัติการรับแรงดัดโค้งของพอลิเมอร์อัลลอย พบว่า ค่ามอดูลัสภายใต้แรงดัดโค้งของพอลิเมอร์ผสมลดลงอย่างเป็นระบบตามปริมาณของยูรีเทนโดยลดลงจาก 5.4 จิกกะปาสคาล ของพอลิเบนซอกซาซีน เป็น 2.1 จิกกะปาสคาล เมื่อทำการเติมพอลิยูรีเทนลงไป 40% โดยน้ำหนัก นอกจากนี้ค่าความแข็งแรงภายใต้แรงดัดโค้งยังพบปรากฏการณ์การเกิดงานร่วมเช่นกันที่อัตราส่วนของพอลิเบนซอกซาซีนกับยูรีเทนอีลาสโตเมอร์ที่ 90/10 โดยน้ำหนัก นอกจากนี้ผลการทดสอบพอลิเมอร์คอมพอลิทีเสริมแรงด้วยเส้นใยไครลอนโดยใช้พอลิเบนซอกซาซีนที่อัลลอยกับยูรีเทนเป็นเมตริก ที่ปริมาณเส้นใย 70%โดยน้ำหนักและทำการจัดเรียงเส้นใยแบบ cross-ply พบว่า ทั้งค่าความแข็งแรงภายใต้แรงดัดโค้งและมอดูลัสภายใต้แรงดัดโค้ง มีค่ามากกว่าพอลิเมอร์เมตริก สุดท้ายคือพบสมบัติการเสริมกันของอุณหภูมิเปลี่ยนสถานะคล้ายแก้วเช่นเดียวกับพอลิเมอร์เมตริก

ภาควิชา..... วิศวกรรมเคมี.....
สาขาวิชา..... วิศวกรรมเคมี.....
ปีการศึกษา..... 2551.....

ลายมือชื่อนิสิต..... วันจักร บางเสน.....
ลายมือชื่อ อ.ที่ปรึกษาวิทยานิพนธ์หลัก.....

5070438121 : MAJOR CHEMICAL ENGINEERING

KEYWORDS : POLYBENZOXAZINE/ URETHANE PREPOLYMER/ ZYLON FIBER
COMPOSITE/ POLYMER ALLOYS

WANCHAT BANGSEN : THERMOMECHANICAL CHARACTERISTIC OF
BENZOXAZINE-URETHANE COPOLYMERS AND THEIR ZYLON FIBER-
REINFORCED COMPOSITES. ADVISOR : ASSOC. PROF. SARAWUT RIMDUSIT,
Ph.D., 106 pp.

The purpose of this research is to improve polybenzoxazine properties by broadening its mechanical property i.e. the rigid polybenzoxazine is toughened by alloying with a highly flexible urethane elastomer. Another objective is to utilize the obtained polymer alloy as a matrix for composite material by reinforcing with Zylon fiber for high mechanical property application. Polybenzoxazine (BA-a) possesses several outstanding properties for being used as a composite matrix such as ease of synthesis, self polymerization upon heating, high thermal stability, good mechanical property and rigidity. In addition, polybenzoxazine can be alloyed with various types of resins to further broaden its useful properties. The experimental results revealed that the processing window of the alloys was widened by the amount of the urethane resin. Interestingly, synergism in glass transition temperature (T_g) was clearly observed, i.e. T_g 's of the BA-a/PU alloys were significantly greater than those of the parent resins, i.e. BA ($T_g = 166^\circ\text{C}$) and PU ($T_g = -70^\circ\text{C}$). The phenomenon was explained by the ability of the PU fraction to substantially enhanced crosslinked density of the resulting polymer alloys thus created the more connected network structure of the obtained alloys. Furthermore, the degradation temperature of the alloys was systematically increased from 325°C of a neat polybenzoxazine to 336°C with the addition of the PU up to 40% by weight while the char yield of the alloys was steadily enhanced with increasing amount of the benzoxazine fraction. Coefficient of thermal expansion of the polymer alloys were found to show a minimum value at BA-a/PU = 90/10. In addition flexural modulus was found to systemically decrease from 5.4 GPa of the neat polybenzoxazine to 2.1 GPa at 40% by weight of the PU. Flexural strength of the alloys, however, showed a synergistic behavior at the BA-a/PU ratio of 90/10. Furthermore, Zylon fiber-reinforced BA-a/PU composites at the fiber content of about 70% in cross-ply orientation showed that both the flexural strength and flexural modulus of Zylon fiber-reinforced BA-a/PU composites expectedly are higher than polymer matrix. Finally, synergistic behavior in T_g of Zylon fiber-reinforced BA-a/PU composites was observed to be similar to that observed in the matrix alloys.

Department : Chemical Engineering
Field of Study : Chemical Engineering
Academic Year : 2008

Student's Signature *Sarawut Rimdusit*
Advisor's Signature *Sarawut Rimdusit*

ACKNOWLEDGEMENTS

I am sincerely grateful to my advisor, Associate Professor Dr. Sarawut Rimdusit, for his invaluable guidance and value suggestions including constant encourage throughout this study. Furthermore, I deeply appreciate all the things. I have learnt from him and for the opportunity to work in his group. I really enjoyed our meetings and pleasure with my thesis. I am also grateful to Associate Professor Dr. Chairit Satayaprasert, as the chairman, Assistant Professor Dr. Anongnat Somwangthanaroj and Dr. Kasinee Hemvichian, who have been members of my thesis committee.

This research is supported by the TRF-MAG scholarship of the Thailand Research Fund. The Center of Excellence on Catalysis and Catalytic Reaction Engineering, Chulalongkorn University is also gratefully acknowledged for the support on the use of thermogravimetric analysis. Additionally, the authors would like to thank Mektec International Corporation (MIC) for the assistance on thermomechanical analysis. Many appreciations are due to Thai Polycarbonate Co., Ltd., South City Groups Co., Ltd., TPI Polyol Co., Ltd. and Toyobo Co., Ltd for providing materials including bisphenol A, toluene diisocyanate, polyols and Zylon fiber for this work.

Additionally, I would like to extend my grateful thanks to all members of Polymer Engineering Laboratory of the Department of Chemical Engineering, Faculty of Engineering, Chulalongkorn University, for their assistance, discussion, and friendly encouragement in solving problems. Finally, my deepest regard to my family and parents, who have always been the source of my unconditional love, understanding, and generous encouragement during my studies. Also, every person who deserves thanks for encouragement and support that cannot be listed.

CONTENTS

	PAGE
ABSTRACT (THAI).....	iv
ABSTRACT (ENGLISH).....	v
ACKNOWLEDGEMENTS.....	vi
CONTENTS.....	vii
LIST OF TABLES.....	xi
LIST OF FIGURES.....	xiv
CHAPTER I INTRODUCTION.....	1
1.1 Overview.....	1
1.2 Objectives.....	3
1.3 Scopes of Research.....	3
CHAPTER II THEORY.....	5
2.1 Benzoxazine Resin.....	5
2.2 Polyurethane.....	7
2.2.1 Isocyanates.....	8
2.2.2 Polyol.....	10
2.3 Network Formation between Benzoxazine Resin and Urethane Prepolymer.....	11
2.4 Advanced Composites Materials.....	12
2.5 Zylon Fiber.....	13
CHAPTER III LITERATURE REVIEWS.....	16

	PAGE
CHAPTER IV EXPERIMENT.....	27
4.1 Materials	27
4.2 Matrix Resin Preparation.....	27
4.2.1 Benzoxazine Resin Preparation.....	27
4.2.2 Urethane Prepolymer Preparation.....	28
4.3 Benzoxazine/Urethane Polymer Alloys Preparation.....	28
4.4 Composite Manufacturing.....	28
4.5 Characterization Methods.....	29
4.5.1 Fourier Transform Infrared Spectroscopy (FT-IR).....	29
4.5.2 Rheological Properties Measurements.....	29
4.5.3 Differential Scanning Calorimetry (DSC).....	29
4.5.4 Density Measurement.....	30
4.5.5 Dynamic Mechanical Analysis (DMA).....	31
4.5.6 Thermogravimetric Analysis (TGA).....	31
4.5.7 Thermomechanical Analysis (TMA).....	32
4.5.8 Universal Testing Machine (Flexural Mode).....	33
4.5.9 Hardness Measurement (Shore D).....	33
4.5.10 Water Absorption Measurement.....	34
4.5.11 Interfacial Bonding Examination.....	34
CHAPTER V RESULTS AND DISCUSSION.....	36
5.1 Benzoxazine/Urethane prepolymers Characterization.....	37
5.1.1 Fourier Transform Infrared Spectroscopic Investigation.....	38
5.1.2 Chemorheological Behaviors	39
5.1.3 Differential Scanning Calorimetry (DSC) for Curing Process Investigation.....	39
5.2 Characterizations of Benzoxazine/Urethane Polymer Alloys.....	40
5.2.1 Density Determination of BA-a/PU Polymer Alloys.....	40
5.2.2 Dynamic Mechanical Analysis of the BA-a/PU Polymer Alloys...	41

	PAGE
5.2.3 Thermal Degradation of BA-a/PU Alloys (TGA).....	46
5.2.4 Coefficient of Thermal Expansion of BA-a/PU Polymer Alloys.....	48
5.2.5 Flexural Properties of BA-a/PU Polymer Alloys.....	48
5.2.6 Hardness of BA-a/PU Polymer Alloys.....	49
5.2.7 Water Absorption of BA-a/PU Polymer Alloys.....	50
5.3 Zylon-Fiber reinforced BA-a/PU Composite Characterization.....	50
5.3.1 Determination of Polymer Matrix Content in the Composites.....	50
5.3.2 Differential Scanning Calorimetry for Curing Condition Examination	51
5.3.3 Density Measurement of Zylon Fiber-Reinforced BA-a/PU Composites.....	52
5.3.4 Dynamic Mechanical Properties of BA-a/PU and Zylon Fiber Composites.....	53
5.3.5 Thermal Degradation of Zylon Fiber-Reinforced BA-a/PU Composites.....	54
5.3.6 Flexural Properties of Zylon Fiber-Reinforced BA-a/PU Composites.....	55
CHAPTER VI CONCLUSIONS.....	90
REFERENCES.....	92
APPENDICES.....	96
Appendix A Thermal Properties of BA-a/PU Alloys.....	97
Appendix B Mechanical Properties of BA-a/PU Alloys.....	99

	PAGE
Appendix C Dynamic Mechanical Properties of BA-a/PU Alloys.....	100
Appendix D Physical Properties of BA-a/PU Alloys.....	101
Appendix E Thermal Properties of Zylon Fiber Reinforced BA-a/PU Composites.....	102
Appendix F Mechanical Properties of Zylon Fiber Reinforced BA-a/PU Composites.....	103
Appendix G Dynamic Mechanical Properties of Zylon Fiber Reinforced BA-a/PU Composites.....	104
Appendix H Physical Properties of Zylon Fiber Reinforced BA-a/PU Composites.....	105
VITAE.....	106



ศูนย์วิทยทรัพยากร
 จุฬาลงกรณ์มหาวิทยาลัย

LIST OF TABLES

	PAGE
Table 2.1 The specification of toluene diisocyanate.....	9
Table 2.2 Comparison Zylon fiber with other high-performance fibers.....	13
Table 2.3 Property comparison between Zylon®AS and Zylon®HM	15
Table 3.1 Tensile strength and modulus of Zylon fiber, Zylon/epoxy and epoxy resin.....	25



คุรุวิทยุทธรัพยากร
จุฬาลงกรณ์มหาวิทยาลัย

LIST OF FIGURES

	PAGE
Figure 2.1 Synthesis of monofunctional benzoxazine monomer.....	5
Figure 2.2 Synthesis of bifunctional benzoxazine monomer based on bisphenol A...	6
Figure 2.3 Urethane linkage.....	8
Figure 2.4 Structure of 2,4 toluene diisocyanate and 2,6 toluene diisocyanate (TDI).....	9
Figure 2.5 Polypropylene glycol used in this study	11
Figure 2.6 Benzoxazine-urethane crosslinked reaction.....	11
Figure 2.7 Synthesis of PBO or Zylon fiber	14
Figure 2.8 Mechanical property comparison of Zylon fiber with other high- performance fibers.....	15
Figure 3.1 Processing windows of benzoxazine/phenolic binary mixtures at various compositions.....	18
Figure 3.2 FT-IR spectra of the compounds of BA-a and BA-a/PU alloy formation.....	19
Figure 3.3 DSC curves of PU/Pa 70/30 treated at various temperatures.....	20
Figure 3.4 Effect of Ba content on the T _g	21
Figure 3.5 TGA analysis of PU/Ba films at various composition.....	21
Figure 3.6 Synergism in the T _g 's of benzoxazine / epoxy / phenolic.....	22
Figure 3.7 Flexural stress and strain of BA-a/PU alloys at various compositions.....	23
Figure 3.8 Shore hardness vs. the content of Al ₂ O ₃ particles.....	23
Figure 3.9 Stress-strain curves of high-performance fibers.....	24
Figure 3.10 Flexural strength of CF/polybenzoxazine-rubber composites.....	26
Figure 5.1 FT-IR spectra of urethane prepolymer.....	57
Figure 5.2 FT-IR Spectra of benzoxazine resin and its polymer.....	58
Figure 5.3 FT-IR Spectra of BA-a/PU resin mixture and its polymer	59

	PAGE
Figure 5.4 Viscosity of BA-a/PU resin at various compositions.....	60
Figure 5.5 Effect of urethane content on viscosity of BA-a/PU resins determined at 120°C	61
Figure 5.6 DSC thermograms of BA-a/PU at various compositions.....	62
Figure 5.7 DSC thermograms of BA-a/PU 60/40 at various curing conditions.....	63
Figure 5.8 DSC thermograms showing glass-transition temperature of BA-a/PU alloys at various compositions	64
Figure 5.9 Density of BA-a/PU alloys at various compositions.....	65
Figure 5.10 Storage modulus of BA-a/PU alloys various PU compositions.....	66
Figure 5.11 Storage modulus at rubbery plateau and crosslink density of BA-a/PU alloys various PU compositions	67
Figure 5.12 Glass transition temperature and the crosslink density of BA-a/PU alloys various PU compositions.....	68
Figure 5.13 Loss modulus of BA-a/PU alloys at various compositions.....	69
Figure 5.14 $\tan \delta$ of BA-a/PU alloys at various compositions.....	70
Figure 5.15 Height of $\tan \delta$ and width at half of BA-a/PU alloys various PU compositions	71
Figure 5.16 Thermal degradation of BA-a/PU alloys at various PU compositions.....	72
Figure 5.17 Thermal degradation of BA-a/PU alloys at various compositions.....	73
Figure 5.18 Effect of urethane content on coefficient of thermal expansion of BA-a/PU alloys at PU various compositions.....	74
Figure 5.19 Effect of urethane content on flexural strength of BA-a/PU alloys at various PU compositions.....	75
Figure 5.20 Effect of urethane content on flexural modulus of BA-a/PU alloys at various PU compositions.....	76
Figure 5.21 Effect of urethane content on surface hardness of BA-a/PU alloys at various PU compositions.....	77
Figure 5.22 Percentage water absorption of BA-a/PU alloys at various PU compositions.....	78

	PAGE
Figure 5.23 DSC thermograms of Zylon fiber composites at various PU compositions in the BA-a/PU alloys.....	79
Figure 5.24 DSC thermograms of Zylon fiber composites at various curing conditions.....	80
Figure 5.25 Density of Zylon fiber at various compositions.....	81
Figure 5.26 Storage modulus of Zylon fiber composites at various PU compositions in the BA-a/PU alloys.....	82
Figure 5.27 Loss modulus of Zylon fiber composites at various PU compositions in the BA-a/PU alloys.....	83
Figure 5.28 $\tan \delta$ of Zylon fiber composites at various PU compositions in the BA-a/PU alloys	84
Figure 5.29 Thermal degradation of Zylon fiber composites at various PU compositions in the BA-a/PU alloys	85
Figure 5.30 Thermal degradation of Zylon fiber composites at PU various compositions in the BA-a/PU alloys	86
Figure 5.31 Effect of urethane content on flexural strength of Zylon fiber composites at various PU compositions in the BA-a/PU alloys	87
Figure 5.32 Effect of urethane content on flexural modulus of Zylon fiber composites at various PU compositions in the BA-a/PU alloys	88
Figure 5.33 SEM micrographs of Zylon fiber-reinforced BA-a/PU composites at various matrix compositions.....	89

CHAPTER I

INTRODUCTION

1.1 Overview

In recent years, processing of thermosetting resins has received strong attention from automotive, aerospace and construction industries because thermosets are plastics that are based on high chemically cross-linked polymers and high molecular weight with high glass-transition temperature of relatively short network chains. The processing of these materials is relatively complicated because of the involvement of chemical reactions [1]. Despite the emergence of several new classes of thermosets, high performance polymers and several other new generation materials that are superior in some respects, phenolic resins retain industrial and commercial interests.

Phenolic resin is used widely as an industrial material because of its good heat resistance, electrical insulation, dimensional stability, and chemical resistance [2]. However, a number of short-comings are also associated with these materials such as their rather brittleness, poor shelf life, and normally acid or base catalysts are involving in the preparation of the resins, which potentially corrode the processing equipments. They usually release small molecule by-products such as water, ammonium compounds, and so forth during curing which sometimes affect the properties of cured resins due to the formation of voids. To overcome those drawbacks of traditional phenolic resins, recently a new type of addition cure phenolic system, a polybenzoxazine, has been developed [3-5].

Polybenzoxazine, which is a novel kind of phenolic resin, is one of new thermosetting plastics. The curing of this resin involves ring-opening polymerization without a catalyst or a curing agent and does not produce any by-products during cure

which might cause void in the products. Polybenzoxazine possesses various useful properties such as high ability to synthesize from inexpensive raw materials, low melt viscosity before cure resulting in its high processability, no by-product during cure, near zero shrinkage after processing, low water absorption, rigidity, high thermal stability and excellent mechanical properties [1, 6-8]. However, the application of this polymer is limited to certain areas due to its high rigidity. To widen the range of its applications, alloying, blending and compositing are normally utilized to improve mechanical properties or thermal stability of polybenzoxazine. This research aims to improve toughness of the rigid polybenzoxazine by alloying with flexible urethane elastomer to widen the useful mechanical properties of the common-typed polybenzoxazine based on bisphenol A and aniline i.e. BA-a.

Urethane elastomer is used to alloy with benzoxazine resin to improve thermal stability and mechanical properties of the resulting materials. Urethane (PU) elastomer is a family of segmented polymers with soft segment derived from polyols and hard segments from isocyanates. PU elastomer represents one of the most attractive elastomers because they have many advantages such as excellent flexibility, high abrasion resistance, good weathering resistance, and transparency [9-11].

In addition, this alloy mixtures of BA-a and PU will be utilized as a matrix of high performance Zylon fiber i.e. tradename of poly-p-phenylene benzobisoxazole (PBO) fiber. Poly-p-phenylene benzobisoxazole (PBO) fiber, or Zylon fiber, has been reported to be the commercial polymeric fiber with highest tensile modulus among different organic fibers, providing outstanding tensile strength, and extremely high thermal stability [12]. The high mechanical and thermal performance of Zylon fiber render great potential applications as reinforcement fibers for composites. As a result, in recent years Zylon fiber has been used to form composites with some polymers such as epoxy to substantially enhance their mechanical properties [13]. In this study, the poly(benzoxazine-urethane) alloys and Zylon fiber-reinforced BA-a/PU alloys will be developed potentially for high mechanical and thermal property applications.

1.2 Objectives

1. To determine the suitable composition ratios of polymeric alloys between benzoxazine resin and urethane prepolymer as matrices for Zylon fiber.
2. To evaluate mechanical and thermal properties of the composites obtained from the suitable alloy matrix in (1).

1.3 Scopes of Research

1. Synthesis of benzoxazine resin by solventless synthesis technology.
2. Synthesis of urethane prepolymer by diol (MW = 2000) and toluene diisocyanate (TDI).
3. Preparation of polymeric alloys between the benzoxazine resin and urethane prepolymers at various weight ratios (BA-a/PU) i.e. 100/0, 90/10, 80/20, 70/30 and 60/40.
4. Evaluation of the curing condition or crosslinking process of the alloys.
 - Finding curing condition by Differential Scanning Calorimeter (DSC) and Rheometer for chemorheological studies.
 - Determining functional groups by Fourier Transform Infrared Spectroscopy (FTIR).
5. Investigation of thermal properties of the alloys.
 - Differential scanning calorimeter (DSC).
 - Thermogravimetric analyzer (TGA).
 - Thermal mechanical analyzer (TMA).
6. Examination of mechanical properties of the alloys.
 - Dynamic mechanical analyzer (DMA).
 - Universal testing machine (flexural mode).
 - Hardness tester (Shore D)
7. Preparation of Zylon fiber-reinforced BA-a/PU alloys at various weight ratios i.e. BA-a/PU = 100/0, 90/10, 80/20, 70/30 and 60/40.

8. Investigation of thermal properties of the Zylon-reinforced BA-a/PU composites.
 - Thermogravimetric analyzer (TGA).
9. Evaluation of mechanical properties of the Zylon fiber composites based on the above alloys.
 - Dynamic mechanical analyzer (DMA).
 - Universal testing machine (flexural mode) .
10. Examination of the obtained polymer composites' fracture surfaces using scanning electron microscope (SEM).



คุรุวิทยาลัยทรัพยากร
จุฬาลงกรณ์มหาวิทยาลัย

CHAPTER II

THEORY

2.1 Benzoxazine Resin

Benzoxazine resin is a novel kind of phenolic resin that can be synthesized from phenol, formaldehyde and primary amines [4]. Solvent or non-solvent systems may be used in its synthesis depending on initiator and heating condition [6]. The resin is developed to provide optimal properties for electronics and other high thermal stability applications. As a novel class of phenolic resins, it has been developed and can be easily modified to overcome various shortcomings of traditional phenolic novolac and resoles. Polybenzoxazines are expected to replace traditional phenolics, polyesters, vinyl esters, epoxies, and polyimides in many respects.

Benzoxazine resins can be classified into monofunctional, bifunctional as well as multifunctional types depending on a type of phenol used. Examples of monofunctional and bifunctional benzoxazine resins are shown in Figure 2.1 and 2.2, respectively.

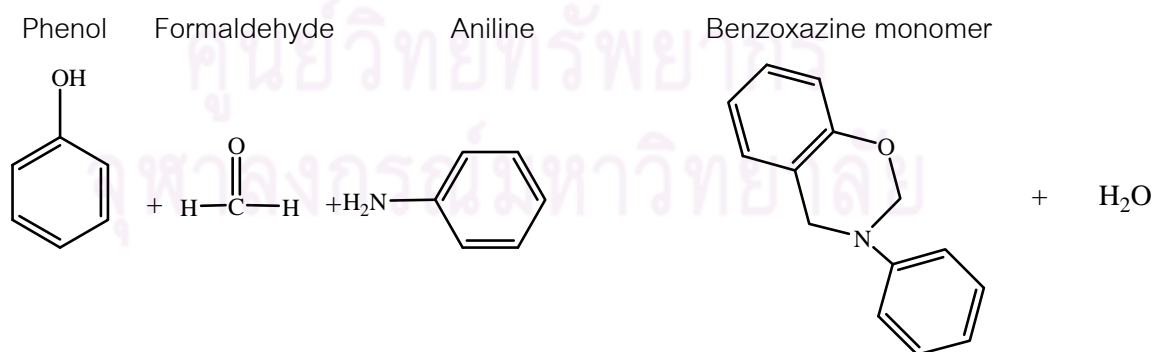


Figure 2.1 Synthesis of monofunctional benzoxazine monomer.

In this work, bifunctional benzoxazine monomer was synthesized and utilized in our laboratory. Raw materials for the synthesis are bisphenol-A, formaldehyde, aniline.

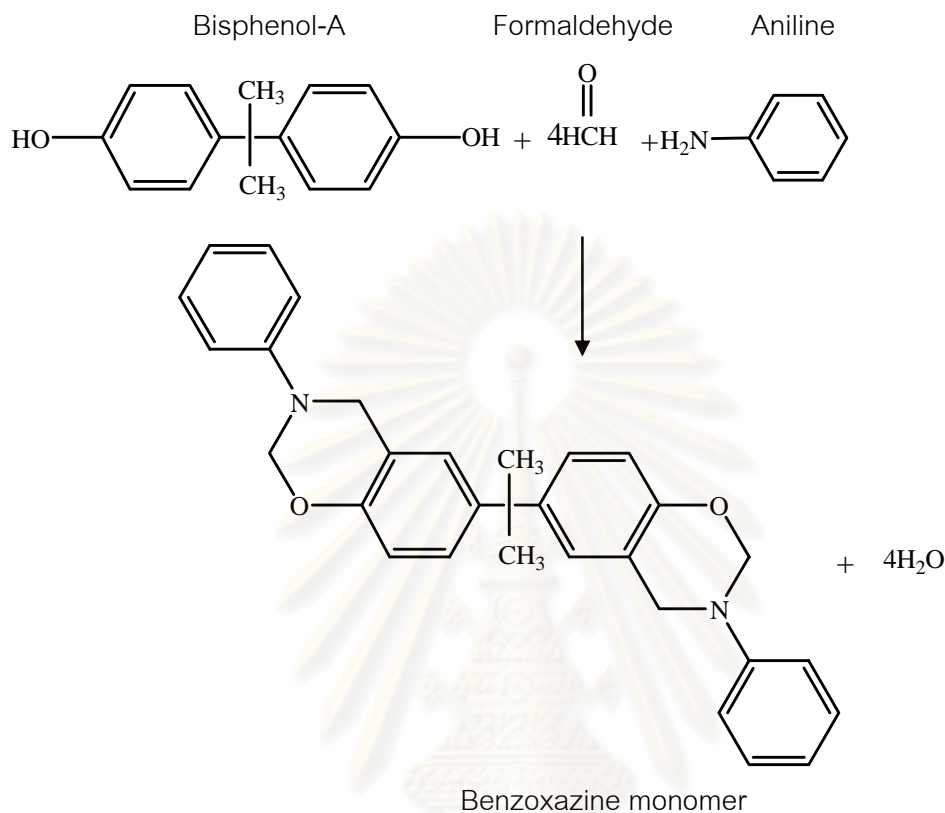


Figure 2.2 Synthesis of bifunctional benzoxazine monomer based on bisphenol A.

These two kinds of polybenzoxazines are different in types of reactants. The monofunctional benzoxazine monomer uses phenol while the bifunctional benzoxazine monomer use bi-phenol for the synthesis. Their properties are also different. The bifunctional benzoxazine monomer can be polymerized to yield a crosslinked network structure whereas the latter can be polymerized, in principle, to yield a linear structure.

The interesting properties of benzoxazine resin are its invented solvent-less synthesis technique that provides almost contaminant-free monomers [6]. Thus, we can neglect a purification process, save a production cost and also decrease pollution

from the use of solvents. The other advantages of benzoxazine resin include good processability, no by-products during cure [14] and low melt viscosity [4].

Polybenzoxazine has been reported to provide self-polymerizability by heating and does not need a catalyst or curing agent for its curing process, near zero mold shrinkage upon polymerization, excellent mechanical integrity e.g. high modulus and strength, high thermal stability including high glass transition temperature and degradation temperature, excellent resistance to chemicals and UV light, no by-product during cure as well as low water absorption [15].

High thermal stability, good mechanical properties and the lack of volatile compounds formation of polybenzoxazine are all attractive for composite material manufacturing. Furthermore, benzoxazine resin is able to be alloyed with several other polymers or resins; therefore rendering a much wider range of the useful properties. Those alloy systems include the alloys of polybenzoxazine with bisphenol A-typed epoxy [14], with flexible epoxy (EPO732) [11], with polyimide [16], with toluene diisocyanates (TDI)/polyethylene adipate polyol-typed urethane resin [10], and with isophorone diisocyanate (IPDI)/polyether polyol-typed urethane resin [11].

2.2 Polyurethane

Polyurethanes are polymer that contain urethane group. These polymers have excellent flexibility, outstanding weathering resistance, as well as high abrasion resistance. Applications of these polymers include shoes soles, solid tire and impeller. Polyurethane elastomers are a family of segmented polymers with soft segments derived from diols and hard segments from isocyanates. The repeating unit of polyurethane is shown in Figure 2.3. Polyurethanes result from the reaction between diols or polyols and isocyanates that contain more than one reactive isocyanate group per molecule (i.e. a diisocyanate or polyisocyanate). This type of polymerization is called addition polymerisation.

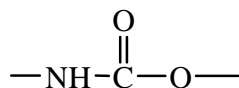
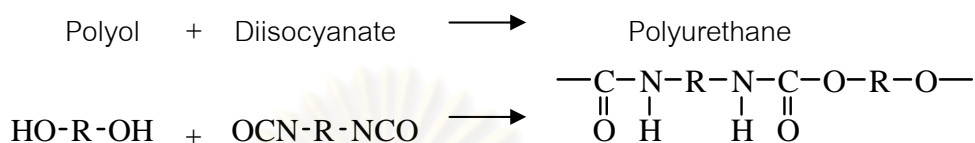


Figure 2.3 Urethane linkage [17].

Polyurethane addition reaction [18-19]



The rate of the polymerisation reaction depends upon the structure of both the isocyanate and the polyol. The functionality of the hydroxy-containing reactant or the isocyanate can be varied. As a result, a wide variety of linear, branched and crosslinked structures can be formed. The hydroxyl-containing components cover a wide range of molecular weights and types, including polyester and polyether polyols. Aliphatic polyols with primary hydroxyl end-groups are the most reactive. They react with isocyanates faster than similar polyols with secondary hydroxyl groups. The polyfunctional isocyanates can be aromatic, aliphatic, cycloaliphatic, or polycyclic in structure and can react with any compound containing “active” hydrogen atoms. This flexibility in the selection of reactants of polyurethane also leads to its wide range of properties.

2.2.1 Raw Materials

Isocyanates

In this work, the raw materials used for the synthesis of PU prepolymer are toluene diisocyanate (TDI) and polyether diol with a molecular weight of 2000.

Toluene diisocyanates (TDI)

TDI is an aromatic diisocyanate. Most of the TDI used is a mixture of the 2,4- and 2,6-isomers. The structure formulae of toluene diisocyanate (TDI) are shown in Figure 2.4.

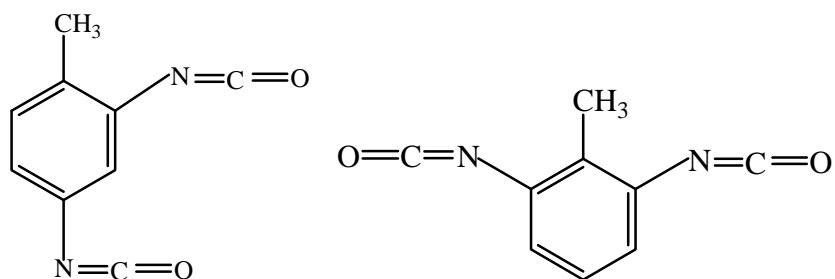


Figure 2.4 2,4 Toluene diisocyanate and 2,6 toluene diisocyanate (TDI) [18-19].

Toluene diisocyanate is prepared by direct nitration of toluene to give a 80:20 mixture of the 2,4- and 2,6-di-nitro derivatives, followed by hydrogenation to the corresponding diaminotoluene. Though toluene diisocyanate (TDI) is stable with a relatively high-flash point, it can be reacted with water, acid, base, organic, and inorganic compounds. The 80:20 mixture of 2,4-TDI and 2,6-TDI is, today, the most important commercial product. The specifications of toluene diisocyanate are shown in Table 2.1.

Table 2.1 The specification of toluene diisocyanate [18-19].

Properties	Value
Molecular weight	174.16
NCO content (% by weight)	48.3
Purity (% by weight)	99.5
Melting point (°C)	19-22
Boiling point (°C)	251
Density (g/cm ³)	1.22 at 20 °C
Viscosity (mPa.s)	3.2 at 20 °C
Vapor pressure (Pa)	3.3 at 25 °C

Polyol

The polyols that are used to make polyurethanes have been developed to possess the required reactivity with commercially available isocyanates and to produce polyurethanes with specific properties. A wide range of polyols is used in polyurethane manufacturing. Most of the polyols used, however, fall into two classes: hydroxyl-terminated polyethers, or hydroxyl-terminated polyesters.

The structure of the polyol plays an important role in determining the properties of the final urethane polymer. The molecular weight and functionality of the polyols are the main factors, but the structure of the polyol chains is also important. In this work, we used polyether polyols with the fixed molecular weight of 2000 to synthesize our urethane prepolymer.

Polyether polyols

Polyether polyols contain the repeating ether linkage $-R-O-R-$ and have two or more hydroxyl groups as terminal functional groups. They are manufactured commercially by the catalyzed addition of epoxies (cyclic ethers) to an initiator. The most important types of the cyclic ethers by far are propylene oxide and ethylene oxide, with smaller quantities of butylene oxide also being consumed. These oxides react with active hydrogen-containing compounds (called initiators), such as water, glycols, polyols and amines; thus, a wide variety of compositions of varying structures, chain lengths and molecular weights is theoretically possible. By selecting the proper oxide (or oxides), initiators, and reaction conditions and catalysts, it is possible to synthesize a series of polyether polyols that range from low-molecular-weight polyglycols to high-molecular-weight resins. Most polyether polyols are produced for polyurethane applications; however, other end uses of the polyols range from synthetic lubricants and functional fluids to surface-active agents. In this work, the polyol used for the synthesis of our urethane prepolymer is polypropylene glycol (MW = 2000). The structure formulae of the polypropylene glycol (MW = 2000) are shown in Figure 2.5.

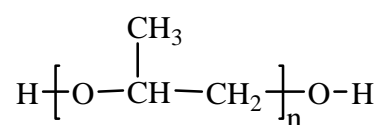


Figure 2.5 Polypropylene glycol used in this study.

2.3 Network Formation between Benzoxazine Resin and Urethane Prepolymer

From previous work, Takeichi and co-workers studied about the synthesis and characterization of poly(urethane-benzoxazine) films. The poly(urethane-benzoxazine) films as novel polyurethane (PU)/phenolic resin alloys were prepared by blending a benzoxazine monomer (BA-a) and TDI-polyethylene adipate polyol (MW = 1000) based PU prepolymer. FT-IR spectroscopic technique was used to investigate the reaction between benzoxazine resin and urethane prepolymer. From the experiment, the mechanism of benzoxazine-urethane alloys was proposed as illustrated in Figure 2.6 [10].

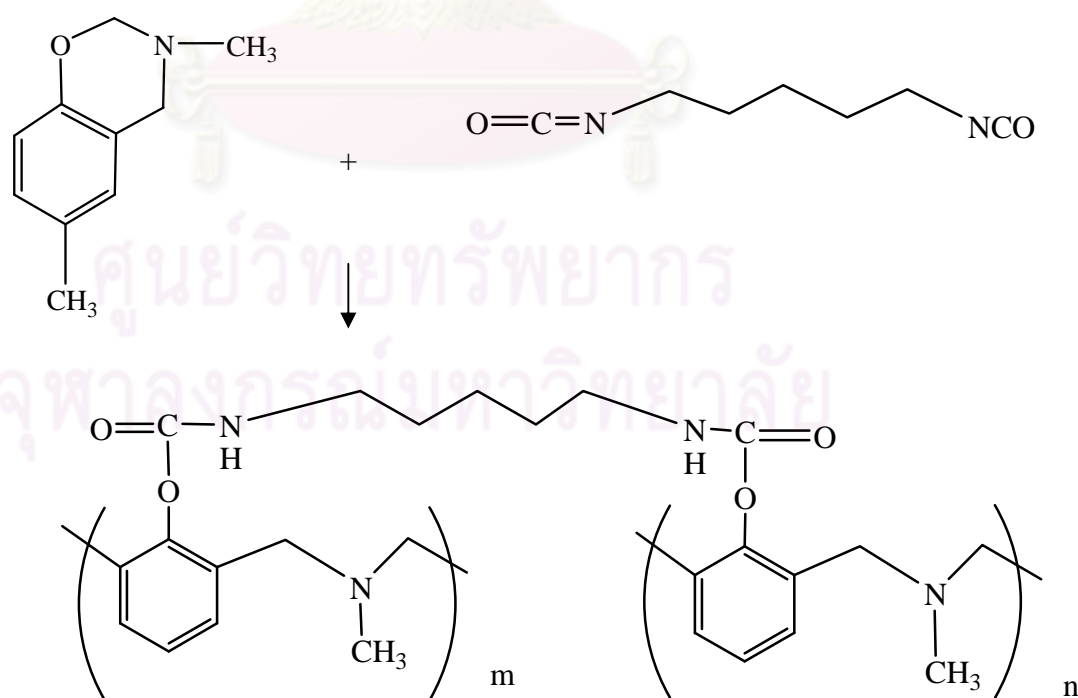


Figure 2.6 Benzoxazine-urethane crosslinked reaction.

2.4 Advanced Composites Materials

Composite materials have been used extensively in many engineering fields. Most composite materials consist of a selected filler or reinforcing material and a compatible resin binder to obtain specific characteristics and properties desired [21]. Depending on type of matrix used, composites may be classified as polymer matrix composites (PMC), ceramic matrix composites (CMC), metal matrix composites (MMC). In addition, based on the form of the dispersed phase, composite materials can also be classified into three commonly accepted types, fibrous composites, laminated composites, and particulate composites [22]. Fiber-reinforced composites consist of continuous or discontinuous fibers in a matrix, while laminated composites consist of layers of various materials whereas particulate composites compose of particles dispersed within a matrix.

Modern structural composites are frequently referred to as advanced composites. The term 'advanced' means the composite materials based on polymer materials with oriented, high-modulus carbon, aramid, glass or ceramic fibers [23]. Composite materials may also be defined as two or more materials that are combined on a microscopic scale to form a useful material. A resinous binder or matrix will hold the fiber in place, distribute or transfer load, protect the dispersed phase either in the structure or before fabrication and control chemical and electrical properties. The fiber is strong and stiff relative to the matrix especially the fiber with a length-to-diameter ratio of over 100. The strength and stiffness of the fiber are generally much greater or multiples of those of the matrix material. The useful application of advanced composite materials is aerospace application (60% capacity) [23]. High-strength fibers used in advanced composites can be the same material or hybrid combination of different materials.

The mechanical properties of typical fiber reinforcement are shown in Table 2.2. Due to its outstanding specific properties, particularly the specific modulus, Zylon fiber was selected as a reinforcing agent for our BA-a/PU alloys. The composite

mechanical and physical properties are also investigated for their potential use as high performance materials.

Table 2.2 Comparison Zylon fiber with other high-performance fibers [9].

	Tensile Strength (GPa)	Tensile Modulus (GPa)	Elongation (%)	Density (g/cm ³)	LOI	Decomposition Temp (°C)
Zylon®AS	5.8	180	3.5	1.54	68	650
Zylon®HM	5.8	270	2.5	1.56	68	650
p-Aramid(HM)	2.8	109	2.4	1.45	29	550
m-Aramid	0.65	17	22	1.38	29	400
Steel Fiber	2.8	200	1.4	7.8	-	-
HS-PE	3.5	110	3.5	0.97	16.5	150
PBI	0.4	5.6	30	1.4	41	550
Polyester	1.1	15	25	1.38	17	260

2.5 Zylon Fiber

One of the most recent developments in the field of soft body armor was that of the high strength Zylon fiber (PBO) in 1998. PBO is currently the highest tensile modulus, highest tensile strength, and most thermally stable commercial polymeric fiber. While the marketing rights to Zylon originally belonged to Dow Chemicals, Dow sold these rights to the Japanese Toyobo Co., Ltd.

Chemical name of Zylon fiber is poly(p-phenylene benzobisoxazole) abbreviated as PBO. The fiber was made from the reaction of 1,3-diamino-4,6-dihydroxybenzene (DADHB) dihydrochloride with terephthalic acid (TA) using poly(phosphoric acid) (PPA) as a catalyst. The reaction scheme for the synthesis is shown in Figure 2.7.

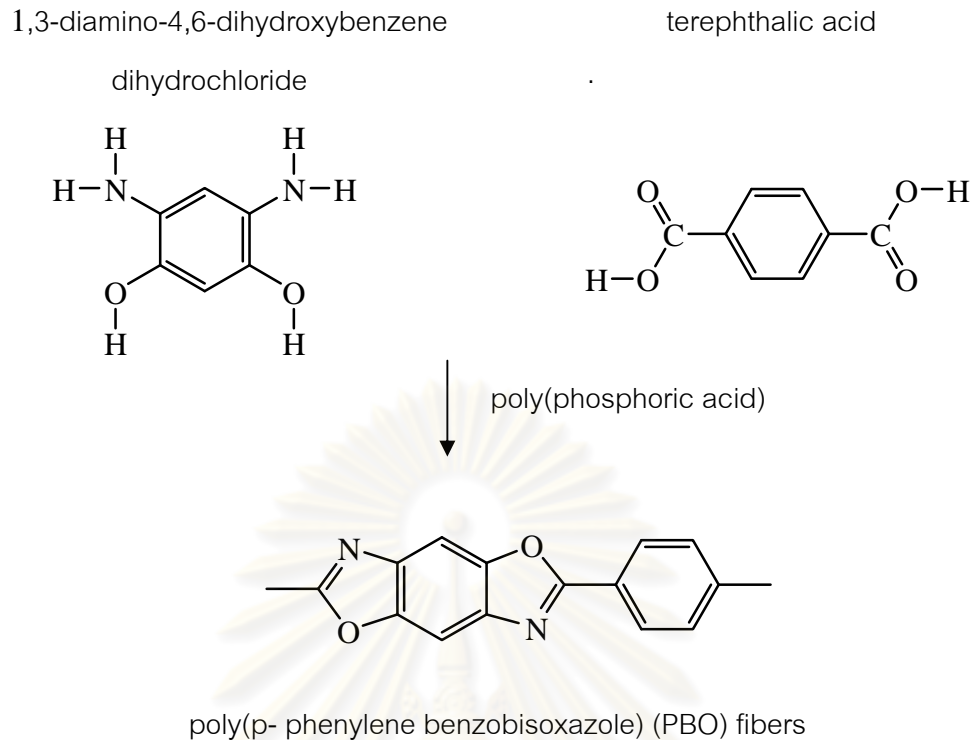


Figure 2.7 Synthesis of PBO or Zylon fiber [12].

It is widely accepted that the excellent mechanical properties of organic polymer fibers are obtained from the rigid nature of the polymer molecules causing the molecules to align in the form of a nematic liquid crystal phase in its solution. During the spinning of the fiber, the molecules are further aligned parallel to the fiber axis, and the coagulation process ensures that this high degree of orientation is maintained in the polymer fiber. This orientation is generally thought to be the main cause of the outstandingly high strength of polymeric fibers such as Zylon [13]. At present, the strength and modulus values of Zylon fiber were reported to be the highest among those organic super fibers as shown in Figure 2.8.

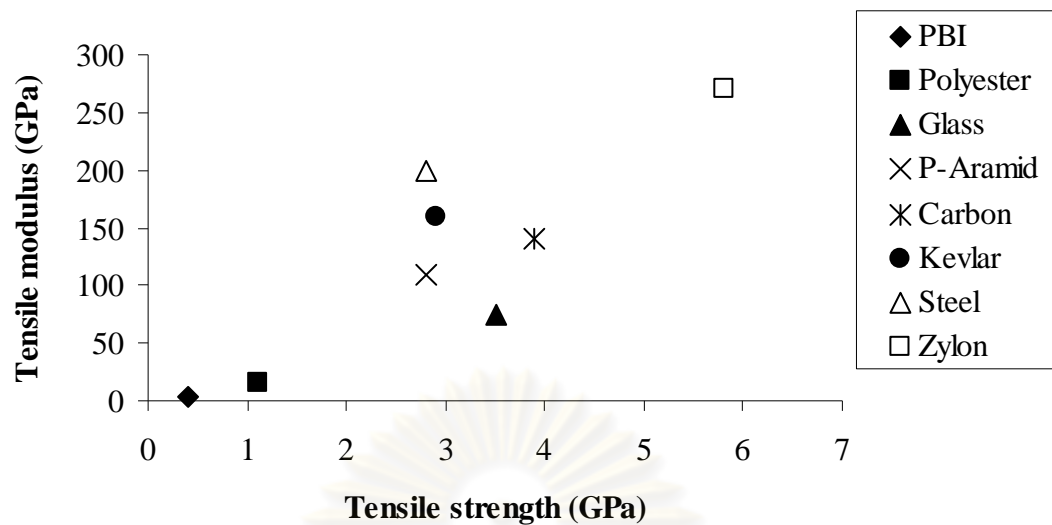


Figure 2.8 Mechanical property comparison of Zylon fiber with other high-performance fibers [12].

There are two types of commercial Zylon fibers i.e. AS (as spun) and HM (high modulus). HM is different from AS type in its modulus, moisture regain etc. as shown in Table 2.3

Table 2.3 Property comparison between Zylon®AS and Zylon®HM [12].

Properties	Zylon®AS	Zylon®HM
Filament decitex	1.7	1.7
Density (g/cm ³)	1.54	1.56
Tensile Strength (GPa)	5.8	5.8
Tensile Modulus (GPa)	180	270
Elongation at break (%)	3.5	2.5
Moisture regain (%)	2.0	0.6
Decomposition Temperature (°C)	650	650
LOI	68	68
Thermal expansion coefficient (ppm/°C)	-	-6

CHAPTER III

LITERATURE REVIEWS

In this work, a new thermosetting resin namely benzoxazine resin is selected to be examined. The polymer possesses various reported outstanding properties. For examples, it can be synthesized from inexpensive raw materials and the polymerization reaction of benzoxazine monomer is initiated merely by heat, without using a curing agent, thereby, it is a good candidate for a wide variety of applications.

Ning and Ishida, 1994 [6] studied the synthesis and characterization of bifunctional benzoxazine precursors. These polyfunctional benzoxazines were found to exhibit excellent mechanical and thermal properties with good handling capability for material processing and composite manufacturing, e.g., the glass transition temperature of 190°C, tensile modulus of 3.2 GPa, and tensile strength of 58 MPa. In addition, the new polymeric systems offered greater flexibility than conventional phenolic resins in terms of molecular design. They do not release by-products during curing reactions and there is no solvent other than for the solvency which the reactants may have for each other. One shortcoming of this resin is its rather high rigidity making it not suitable for some applications.

However, the above shortcoming can be solved effectively from an ability of the resin to be alloyed with several other polymers. For example, Ishida and Allen, 1996 [7] investigated benzoxazine resin combined with epoxy based on DGEBA. The benzoxazine resin was copolymerized with epoxy resin in order to modify their performance. The addition of epoxy to the polybenzoxazine network greatly increased the crosslinked density of the hybrid thermosetting matrix and strongly influenced its mechanical properties. The copolymerization led to significant increase in the glass transition temperature, flexural strength, and flexural strain at break over those of the polybenzoxazine homopolymer with only a minimal loss of stiffness. By understanding

the structural changes induced by variation of epoxy content and their effect on material properties, the network can be tailored to specific performance requirements.

Moreover, Kimura et al., 1999 [24] synthesized terpenediphenol-based benzoxazine from terpenediphenol, formaline and aniline. Curing behavior of the benzoxazine resin with epoxy resin and the properties of the cured resins were investigated. Their study revealed that the curing reaction did not proceed at low temperatures, but it proceeded rapidly at higher temperatures without a curing accelerator. The properties of the cured resin both from the neat resin and from reinforced resin with fused silica were evaluated. The cured resin showed good heat resistance, mechanical properties, electrical insulation, and especially water resistance, compared with the cured resin from bisphenol A-typed novolac and epoxy resin.

Rimdusit et al., 2007 [25] studied rheological behavior on benzoxazine (BA-a) - phenolic novolac resin mixture filled with *Hevea brasiliensis* woodflour. The results revealed that phenolic novolac resin can significantly reduce the curing temperature of the neat benzoxazine resin whereas the benzoxazine resin helped improve mechanical integrity, thermal properties and processing ability of the BA-a-novolac alloy (BP alloy). The complex viscosities of the BA-a, BP91, BP82, and BP73 as a function of temperature are shown in Figure 3.1. The complex viscosities of the alloys, compared at the same temperature, tended to decrease with an increase in the amount of the benzoxazine fraction. Moreover, the liquefying temperatures of these alloys also systematically decreased with increasing benzoxazine content in the alloys. On the other hand, the gel point of these binary mixtures tended to increase with an increase in the amount of the benzoxazine resin in the binary mixtures. This behavior provided sufficiently broad processing window for a compounding process in a composite manufacturing.

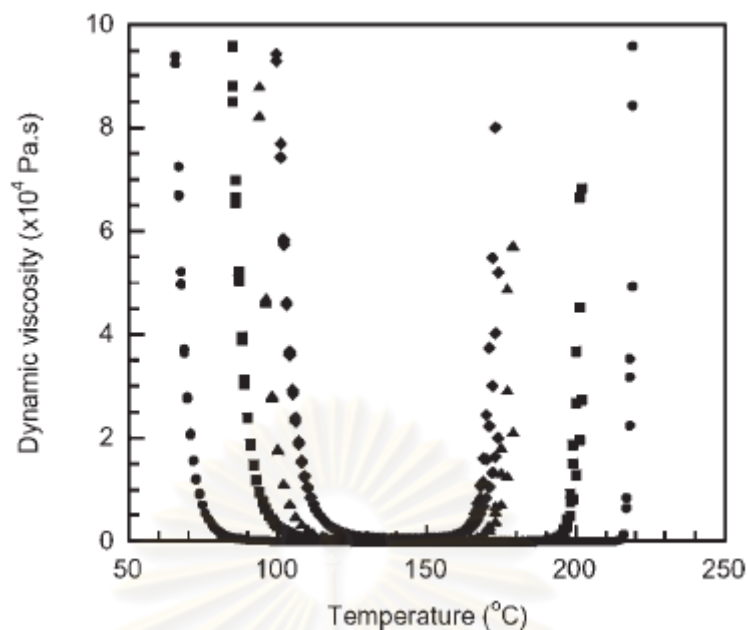


Figure 3.1 Processing windows of benzoxazine / phenolic binary mixtures at a heating rate of 2°C/min : (●) BA-a, (■) BP91, (▲) BP82, (◆) BP73 [25].

Takeichi and Guo, 2001 [9] prepared poly(urethane-benzoxazine) films from blending a monofunctional benzoxazine monomer, 3-phenyl-3,4-dihydro-2H-1,3-benzoxazine, and urethane prepolymer. The prepolymer was synthesized from 2,4-tolulene diisocyanate and polyethylene adipate polyol (MW ca. 1000) in a 2:1 molar ratio followed by casting as films and thermal curing of the films. These elastic films exhibited good resilience with excellent reinstating behavior and swelled in polar organic solvents such as DMSO, DMF and NMP. The reaction between the monofunctional benzoxazine monomer (Pa) and urethane prepolymer (PU) at the mass ratio of 70/30 was investigated by IR as seen in Figure 3.2. Characteristic absorption bands of Pa were found at 942 and 1232 cm^{-1} both assigned to C-O-C vibration (Figure 3.2a). After the thermal treatment at 190°C for 1h (Figure 3.2b), the ring opening polymerization of benzoxazine monomer occurred. Characteristic absorption bands of polybenzoxazine (PPa) situated at 942 and 1232 cm^{-1} disappeared and an intensive absorption appeared at 3498 cm^{-1} was assigned to the phenolic hydroxyl group. These indicated that Pa thermally polymerized through its ring opening reaction to give PPa. Additionally, the blend of Pa and PU prepolymer contained both benzoxazine and isocyanate characteristic

absorptions such as 942 and 1232 cm^{-1} from benzoxazine structure, and 2281 cm^{-1} from NCO group of PU prepolymer (Figure 3.2c). After cure at 190°C for 1 h, the absorptions due to NCO (2281 cm^{-1}) and benzoxazine (942 and 1232 cm^{-1}) disappeared completely (Figure 3.2e), suggesting the formation of PU/Pa network.

The curing behavior of PU/Pa at 70/30 mass ratio were also followed by DSC and the results are shown in Figure 3.3. The exothermic peak due to the ring opening of Pa was clearly seen. Compared with pristine Pa, the overall amount of exotherm of PU/Pa films decreased in proportion to the weight ratio of Pa. Furthermore, the ring opening polymerization of PU/Pa 70/30 occurred above 150°C and the exothermic peak was disappeared at 240°C. Similar DSC behavior was observed for PU/Pa films at different ratios.

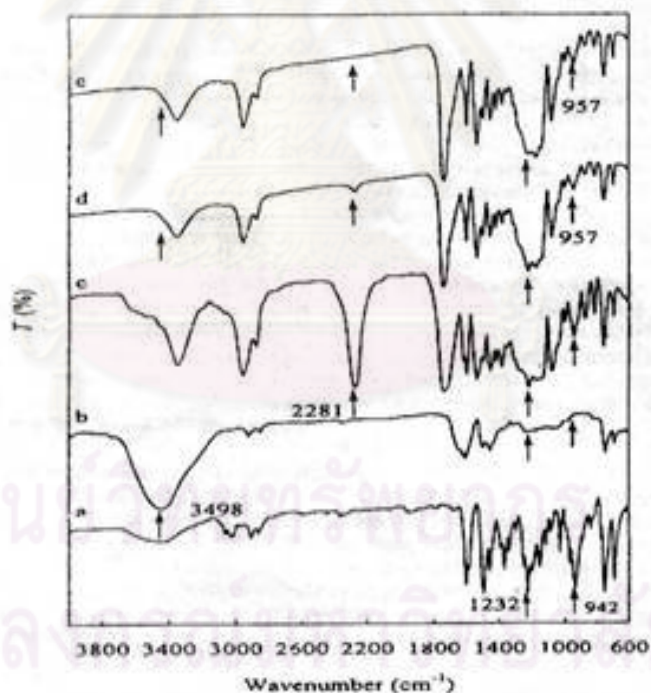


Figure 3.2 IR spectra of PU/Pa compounds : (a) Pa, (b) PPa, (c) alloy of PU and Pa prepolymer, (d) PU/Pa treated at 150°C for 1 h, (e) 190°C for 1 h [9].

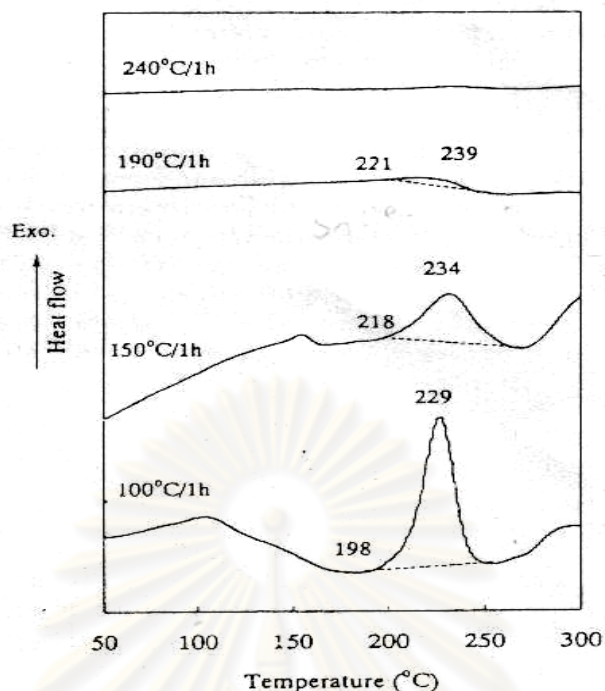


Figure 3.3 DSC curves of PU/Pa 70/30 treated at various temperatures [9].

Takeichi et al., 2000 [10] prepared poly(urethane-benzoxazine) films as novel polyurethane/phenolic resin alloys from blending a benzoxazine monomer (Pa) and urethane prepolymer (PU) that was synthesized from 2,4-tolulene diisocyanate (TDI) and polyethylene adipate polyol (MW ca. 1000) in 2:1 molar ratio. Thermal properties of the alloys were investigated by dynamic mechanical analysis (DMA) and thermogravimetric analysis (TGA). All the films had one glass transition temperature (T_g) from viscoelastic measurements, indicating no phase separation in poly(urethane-benzoxazine) due to the in-situ polymerization. The T_g increased with the increase of benzoxazine content as shown in Figure 3.4. Moreover, Figure 3.5 shows TGA profile of polyurethane and bifunctional polybenzoxazine (PU/Ba) films. The results suggested that initial decomposition temperatures (5% weight loss) of PU/Ba films were higher than that of the PU itself and increased to a higher decomposition temperature with the Ba content. Thus, introducing polybenzoxazine (PBa) into PU can be an effective way to an improvement on the thermal stability of the PU. Furthermore, tensile properties were found to change dramatically with the content of the polybenzoxazine. Finally, as the

content of the polybenzoxazine increased, both the modulus and tensile strength of the alloys increased.

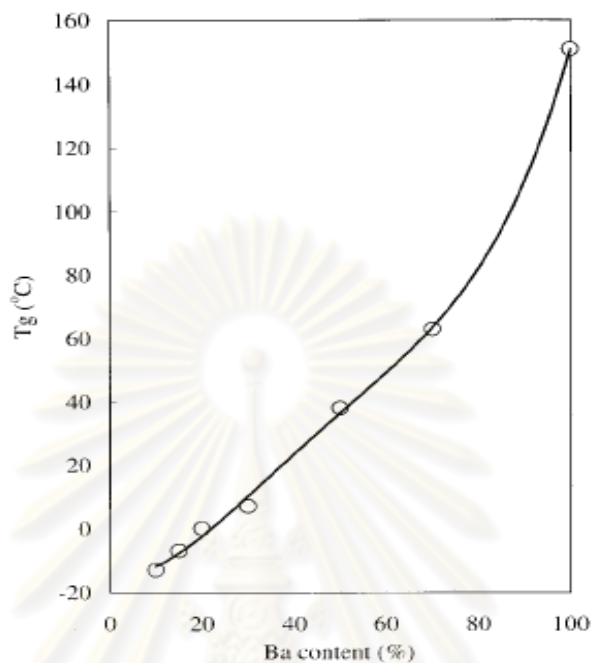


Figure 3.4 Effect of bifunctional polybenzoxazine content on the alloy Tg [10].

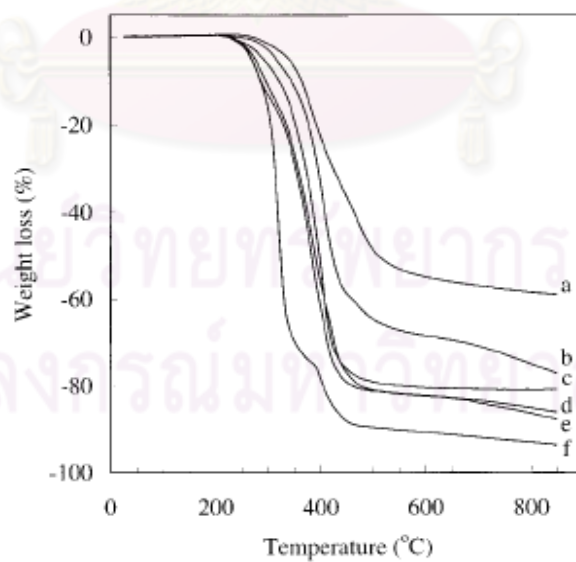


Figure 3.5 TGA analysis of PU/Ba films : (a) PU/Ba 0/100, (b) PU/Ba 70/30, (c) PU/Ba 80/20, (d) PU/Ba 85/15, (e) PU/Ba 90/10 and (f) PU/Ba 100/0 [10].

Rimduisit and Ishida, 2000 [26] observed synergism in glass-transition temperature (T_g) of ternary systems based on benzoxazine, epoxy, and phenolic resins. Figure 3.6 revealed the maximum T_g up to about 180°C in benzoxazine / epoxy / phenolic at a 5 / 4 / 1 mass ratio. The molecular rigidity from benzoxazine structure and the improved crosslink density from epoxy contributed to the observed synergistic behavior. The mechanical relaxation spectra of the fully cured ternary systems in a temperature range of -140 to 350°C showed four types of relaxation transitions : gamma transition at -80 to -60°C, beta transition at 60-80°C, α_1 transition at 135-190°C, and α_2 transition at 290-300°C.

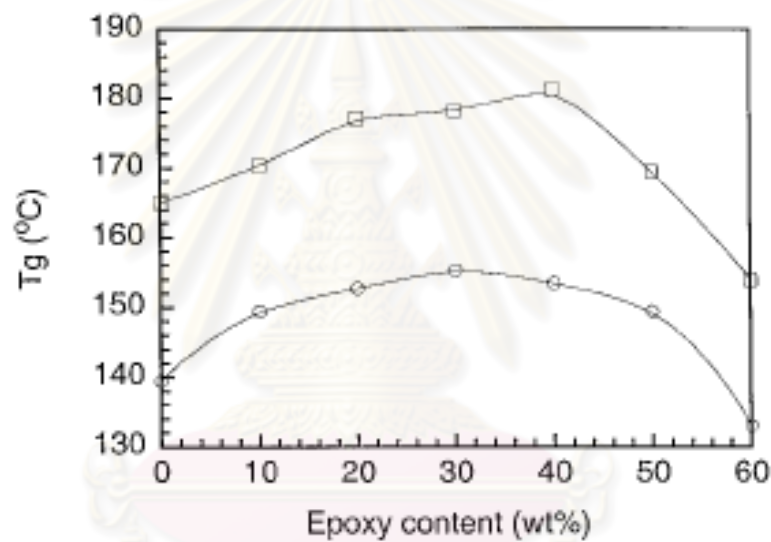


Figure 3.6 Synergism in the T_g 's of benzoxazine / epoxy / phenolic ternary systems:

(○) DSC T_g 's , (□) DMA T_g 's [26].

Rimduisit et al., 2005 [11] demonstrated the toughening of polybenzoxazine by alloying with urethane prepolymer (PU) from isophorone diisocyanate (IPDI) system and with flexible epoxy (EPO732). The transition temperatures were determined from loss modulus curves of DMA. The T_g 's of the polyurethane elastomer and bisphenol A-based polybenzoxazine (BA-a) used were reported to be about -70 to -20°C and 160 to 170°C, respectively. The T_g 's of BA-a/PU binary systems were found to increase with the mass fraction of PU. At 30 wt% of the

PU, the corresponding T_g was about 220°C which was significantly greater than its parent polymers. Effects of the urethane prepolymer (PU) on flexural properties are also shown in Figure 3.7. The flexural strength of the BA-a/PU at a 90/10 weight ratio was slightly higher than that of the polybenzoxazine homopolymer. The flexural strength then decreased with the mass fraction of the PU when the amount of the PU was greater than 20 wt%. Whereas the flexural modulus of these alloys decreased monotonically with the amount of the PU.

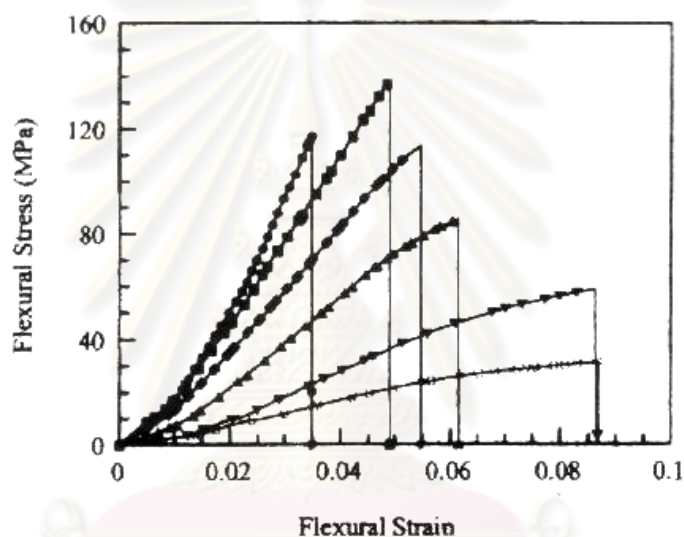


Figure 3.7 Flexural stress and strain of BA-a/PU alloys at various compositions :

(●) 100/0, (■) 90/10, (◆) 80/20, (▲) 70/30, (▼) 60/40 and (○) 50/50 [11].

ศูนย์วิจัยทรัพยากร
จุฬาลงกรณ์มหาวิทยาลัย

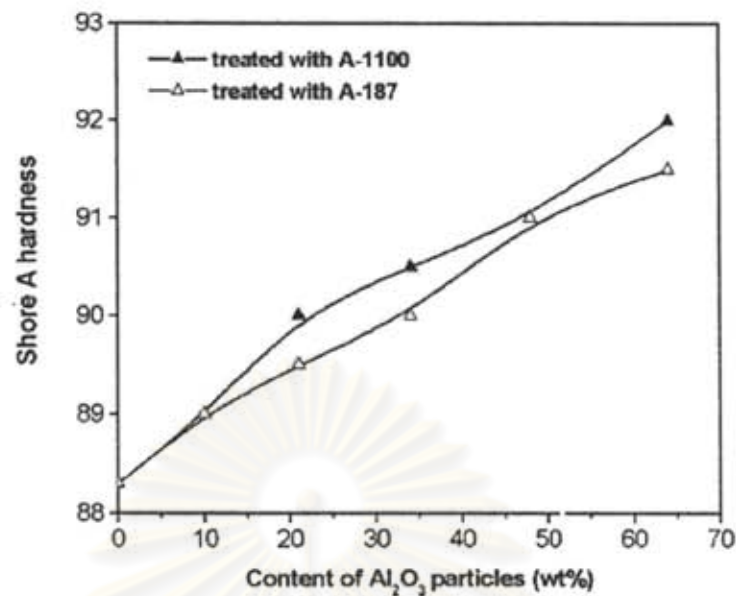


Figure 3.8 Shore A hardness of polyurethane elastomer at various compositions of Al₂O₃ particles [27].

Hardness of polyurethane matrix composites reinforced with aluminum oxide (Al₂O₃) particles was investigated by R. Zhou et al., 2005 [27]. The effects of Al₂O₃ content (0–64 wt%) on mechanical properties of the composites were also investigated. According to the results, the hardness increased gradually with the alumina content as shown in Figure 3.8. However, both the tensile strengths and the elongations at rupture of the composites were found to increase with the content of urethane.

Zylon fiber-reinforced composite materials have been used extensively in many engineering fields, especially in civilian and military aircraft, on account of their high specific strength and specific modulus. The composites used for structural applications require excellent mechanical properties. In 2007, Toyobo Co., Ltd., [12] disclosed technical information of Zylon@HM fiber which possessed the highest tensile strength and tensile modulus among various high-performance fibers. Figure 3.9 shows the stress-strain curves of some major reinforced fibers. The tensile strength of about 5.8 GPa and tensile modulus of about 270 GPa were reported for the ZYLON@HM fiber. Zylon fiber also possesses outstanding thermal properties with a decomposition

temperature of about 650°C and the limiting oxygen index about 68, which is the highest among organic super fibers.

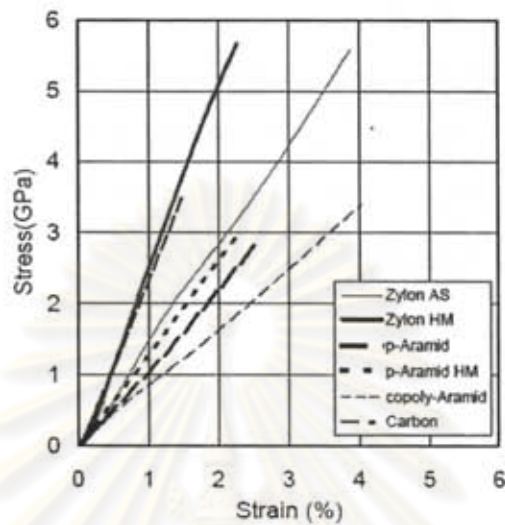


Figure 3.9 Stress-strain curves of some high-performance fibers [12].

Huang et al., 2001 [28] investigated mechanical properties of Zylon/epoxy composites. The composite was prepared from Zylon fiber with epoxy (Stycast 1266). Table 3.1 exhibits the tensile strength and tensile modulus of Zylon fiber, Zylon/epoxy, and epoxy binder. The tensile modulus and tensile strength of the zylon reinforced composite (filling factor = 67.3%) were much greater than those of epoxy because of the high mechanical properties of the zylon fiber used. The filling factor of the zylon fiber/epoxy composite sample was calculated using the formula nA_1/A when n is the number of zylon fiber bundled, A_1 is the cross sectional area of one bundled, and A is the cross sectional area of the sample)

Table 3.1 Tensile strength and modulus of Zylon fiber, Zylon/epoxy, and epoxy [28].

	Tensile strength (GPa)	Tensile modulus (GPa)
Epoxy	0.05	3.1
Zylon fiber	5.80	280
Zylon/epoxy	2.60	152

Jang and Yang, 2000 [29] investigated the effect of rubber modification on carbon fiber/polybenzoxazine composites. The flexural strength of these composites with varied rubber content from 0 to 20 phr was found to show a relatively constant value of about 390 MPa using ATBN (amine-terminated buta-diene acrylonitrile) rubber system. However, a substantial decrease in the flexural strength using CTBN (carboxyl terminated butadiene acrylonitrile) system i.e. 140 MPa with CTBN content of 20 phr was also observed. No study on thermal stability of the composites was reported. The flexural strength at various compositions is shown in Figure 3.10.

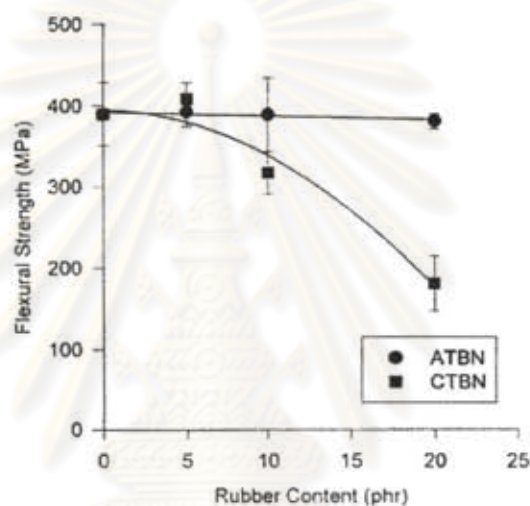


Figure 3.10 Flexural strength of CF/polybenzoxazine-rubber composites [29].

For high performance composites, Ishida and Chaisuwan, 2003 [30] improved the mechanical properties of carbon fiber-reinforced polybenzoxazine composites by rubber interlayering. The resin used is BA-35X because the material rendered the highest thermal stability achieved from neat polybenzoxazine based on bisphenol-A and the aniline derivatives ($T_g = 236^\circ\text{C}$ of BA-35X and $T_g = 170^\circ\text{C}$ of BA-a). The fiber content of the composite was about 60% by volume. They reported the optimal concentration of ATBN rubber provided the mechanical properties comparable or superior to those of modified epoxy and phenolic matrices i.e. flexural strength: ~800 MPa of rubber interlayered BA-35X, 780 MPa of modified epoxy, and 650 MPa of modified phenolic and the flexural modulus: of 58 GPa of rubber interlayered BA-35X, 58 GPa of modified epoxy, and 56 GPa of modified phenolic.

CHAPTER IV

EXPERIMENTAL

4.1. Materials

Materials used in this research are benzoxazine resin, urethane prepolymer and Zylon fiber. Benzoxazine resin is based on bisphenol-A, aniline and formaldehyde. The bisphenol-A (polycarbonate grade) was supported by Thai Polycarbonate Co.,Ltd. (TPCC). Para-formaldehyde (AR grade) was purchased from Merck Company and aniline (AR grade) was contributed by Panreac Quimica S.A. Company. Urethane prepolymer was prepared using polypropylene glycol polyol at a molecular weight of 2000 with toluene diisocyanate (TDI). The toluene diisocyanate was obtained from the South City Group whereas the polypropylene glycol polyol at a molecular weight of 2000 was kindly supplied by TPI Polyol Co., Ltd. Dibutyltin dilaurate (DBTL) is the catalyst for the urethane prepolymer preparation. Finally, Zylon fiber for composite reinforcement was kindly contributed by Toyobo Co., Ltd., Japan.

4.2 Matrix Resin Preparation

4.2.1 Benzoxazine Resin Preparation

Benzoxazine monomer (BA-a) was synthesized from bisphenol A, aniline, and paraformaldehyde at a 1:2:4 molar ratio. The mixture was constantly stirred at about 110°C for approximately 30 minutes to yield a light yellow and low viscosity liquid monomer. This resin was prepared based on a patented solventless method [7]. The resulting benzoxazine monomer is solid at room temperature with transparent yellow color. The as-synthesized monomer was ground into fine powder and were taken for material characterization.

4.2.2 Urethane Prepolymer Preparation

The urethane prepolymer (PU) was prepared by reacting polypropylene glycol polyol (molecular weight of 2000) with toluene diisocyanate (TDI). Small amount of dibutyltin dilaurate (DBDT) was used as a catalyst for the synthesis. The two reactants for urethane resin preparation were mixed in a four-necked round bottomed flask and the mixture at a 2:1 molar ratio of TDI:polyol was stirred under a nitrogen stream at 70°C for 2 hour. 0.075% by weight of dibutyltin dilaurate was used as a catalyst. After the completion of the reaction, the obtained clear and viscous urethane prepolymers were cooled to room temperature and kept in a nitrogen-purged, closed container.

4.3 Benzoxazine/Urethane Polymer Alloys Preparation

The benzoxazine monomer (BA-a) was blended with the urethane prepolymers (PU) to provide BA-a/PU mixtures. Preparation of the benzoxazine resin and the urethane prepolymers was made at various weight ratios of the benzoxazine resin and urethane prepolymers i.e. 100/0, 90/10, 80/20, 70/30 and 60/40. The mixture was typically heated to about 100°C in an aluminum pan and mixed thoroughly for at least 5-10 minutes or until a homogeneous resin mixture was obtained. The molten resin mixture was poured into an aluminum mold and step-cured in an air-circulated oven at 150, 170, 180, 190°C for 1 hour each and 200°C for 2 hours. Part of the mixture was taken for differential scanning analysis. The specimen was finally left to cool down to room temperature and was then ready for material characterizations.

4.4 Zylon Fiber-reinforced BA-a/PU Composite Manufacturing

The Zylon fiber was pre-impregnated with the BA-a/PU binary mixture using the hand-lay up procedure. Twenty plies of the prepregs were laminated in a (0°/90°) arrangement and were cured at 150, 170, 180, 190°C for 1 hour at each temperature and at 200°C for 2 hours by hot pressing in a compression molder at a

pressure of 10 MPa. The specimens were finally left to cool down to room temperature and were ready for the characterizations.

4.5 Characterization Methods

4.5.1 Fourier Transform Infrared Spectroscopy (FT-IR)

Fourier transform infrared spectra of all samples under various curing conditions were acquired by using a Spectrum GX FT-IR spectrometer from Perkin Elmer with an ATR accessory. All spectra were taken as a function of time with 32 scans at a resolution of 4 cm^{-1} and a spectral range of $4000\text{-}650\text{ cm}^{-1}$. For urethane prepolymer before and after synthesis, a small amount of a viscous liquid sample was casted as thin film on a potassium bromide (KBr) window.

4.5.2 Chemorheological Properties Measurement

Chemorheological properties of each alloy were examined using a Rheometer (Haake Rheo Stress 600, Thermo Electron Cooperation) equipped with parallel plate geometry. The measuring gap was set at 0.5 mm. The experiment was performed under an oscillatory shear mode at 1 rad/s. For processing window evaluation of the resin mixture, a sample mass of about 3-5 g was used in each test. The testing temperature program was ramped from room temperature at a heating rate of $2^{\circ}\text{C}/\text{min}$ to a temperature beyond the gel point of each resin and the dynamic viscosity was recorded.

4.5.3 Differential Scanning Calorimetry (DSC)

The curing behavior and glass transition temperature of benzoxazine resins alloyed with urethane elastomer and Zylon-reinforced BA-a/PU composites at various weight ratios of the polymer mixtures were examined using a differential scanning calorimeter (DSC) model 2910 from TA Instruments. All samples were put in

aluminum pans with lids. The thermogram was obtained using a heating rate of 10°C/min from room temperature to 300°C under nitrogen atmosphere. The purge nitrogen gas flow rate was maintained to be constant at 50 ml/min. The sample with a mass in a range of 3-5 mg was sealed in an aluminum pan with lid. The glass transition temperature was obtained from the temperature at half extrapolated tangents of the step transition midpoint.

4.5.4 Density Measurement

The densities of benzoxazine resins alloyed with urethane prepolymer and of their Zylon fiber composites were determined by water displacement method according to the ASTM D 792-91 (Method A). The dimension of specimens was in rectangular shape 25×50×2 mm³. All measurements were performed at room temperature. The density is calculated by a following equation:

$$\rho = \left(\frac{A}{A - B} \right) \times \rho_o \quad (4.1)$$

Where

ρ = Density of the specimen, g/cm³

A = Weight of the specimen in air, g

B = Weight of the specimen in liquid, g

ρ_o = Density of the liquid at the given temperature, g/cm³

The average value from three specimens was calculated.

The theoretical density by mass of benzoxazine-urethane alloys can be calculated as follow

$$\textit{Theoretical.density} = (\rho_B \cdot X_B) + (\rho_U \cdot X_U) \quad (4.2)$$

where

ρ_B = density of benzoxazine, g/cm³

ρ_U = density of urethane prepolymer, g/cm³

X_B = benzoxazine weight fraction

X_U = urethane prepolymer weight fraction

4.5.5 Dynamic Mechanical Analysis (DMA)

The dynamic mechanical analyzer (DMA) model DMA242 from NETZSCH was used to investigate the dynamic mechanical properties and relaxation behaviors of BA-a/PU polymer alloys and the Zylon-reinforced BA-a/PU composites. The dimension of specimens was 10×50×2 mm³. The test was performed in a three-point-bending mode. In a temperature sweep experiment, a frequency of 1 Hz and a strain value of 0.1% were applied. The temperature was scanned from -150°C to the temperature beyond the glass transition temperatures (T_g) of each specimen with a heating rate of 2°C /min under nitrogen atmosphere. The storage modulus (E'), loss modulus (E''), and loss tangent or damping curve (tan δ) were then obtained. The glass transition temperature (T_g) was taken as the maximum point on the loss modulus curve in the DMA thermogram.

4.5.6 Thermogravimetric Analysis (TGA)

The degradation temperature (T_d) and char yield of the benzoxazine alloys at various mass fractions of urethane prepolymers as well as those of Zylon-reinforced BA-a/PU composites were studied using a DSC-TGA Q600 SDT from TA Instruments. The testing temperature program was ramped at a heating rate of 20°C/min from room temperature to 900°C under nitrogen atmosphere. The purge nitrogen gas flow rate was maintained to be constant at 100 ml/min. The sample mass used was measured to be approximately 10-20 mg. Weight loss of the samples was measured as a function of temperature. The degradation temperatures (T_d) of BA-a/PU polymer alloys

and the Zylon-reinforced BA-a/PU composites were reported at their 5% weight loss and char yields of the above specimens were also reported at 800°C.

4.5.7 Thermomechanical Analysis (TMA)

The coefficient of thermal expansion (CTE) was measured with a Perkin Elmer Instrument Technology SII Diamond thermal mechanical analyzer (TMA). The dimension of specimens was 2×2×2 mm³ and had flat surfaces. During the TMA measurement, the specimen was heated from room temperature to the temperature beyond the glass transition temperature at a heating rate of 10°C/min. The linear coefficient of thermal expansion (CTE) describes by how much a material will expand for each degree of temperature increase was determined by the following relationship:

$$\alpha = \frac{(\Delta L / L_o)}{\Delta T} \quad (4.3)$$

where

α = linear coefficient of thermal expansion

ΔL = a change in length of material in the direction being measured

L_o = initial specimen length

ΔT = a change in temperature over which ΔL was measured

Although a ratio is dimensionless, thermal expansion has a unit of 1/°C, and is normally quoted in parts per million per °C rise in temperature. Generally, a thermal expansion increases with an increase in temperature and the CTE were calculated from the slope of the thermogram. An abrupt change in slope of the expansion curve indicates a transition of the material from a glassy state to a rubber state.

4.5.8 Universal Testing Machine (Flexural Mode)

The flexural strength and flexural modulus of the BA-a/PU polymer alloys and the Zylon-reinforced BA-a/PU composites were determined using a universal testing machine (model 5567) from Instron Co., Ltd. The test method was a three-point-bending mode with a supporting span of 32 mm and tested at a crosshead speed of 0.85 mm/min. The dimension of the specimens is 25×50×2 mm³. The flexural properties were determined based on ASTM D790M-93. The flexural strength and modulus were calculated by the following equations:

$$E_B = \frac{L^3 m}{4bd^3} \quad (4.4)$$

$$S = \frac{3PL}{2bd^2} \quad (4.5)$$

where

E_B = flexural modulus, GPa

S = flexural strength, MPa

P = load at a given point on the load-deflection curve, N

L = support span, mm

b = width of beam tested, mm

d = depth of beam tested, mm

m = slope of the tangent to the initial straight-line portion of the load-deflection curve, N/mm

4.5.9 Hardness Measurement (Shore D)

The Shore hardness is the resistance measurement of a material imposed to penetration of a needle under a defined spring force. The two most common scales of hardness tester are the A and D scales. The Shore A scale is used for 'softer' rubbers while the Shore D scale is used for 'harder' ones. The scale results are given in

a value between 0 and 100, with higher values indicating a harder material. In the present research, shore D scale was used to represent the hardness of all the specimens because of a relatively rigid nature of all polybenzoxazines and their alloys. The hardness of polymer alloys samples was also measured using a shore D hardness tester (model ES-720G) from Micro Photonics. The specimens were 25×50×2 mm³, and had flat surfaces following ASTM D2240. Five values of hardness at different positions on each specimen were performed and an average of those values was reported as the Shore D hardness of the specimen.

4.5.10 Water Absorption Measurement

Water absorption measurement was conducted in accordance with ASTM D570 using a specimen dimension of 25×50×2 mm³. Three samples of each composition were submerged in de-ionized water. The specimens were periodically removed and dried by wiping for weight measurements after which they were immediately returned to the water bath. The amount of absorbed water was calculated as the difference between the mass at each of this measurement and the initial conditioned mass. The water absorption was calculated by the following equation:

$$\% \text{ water absorption} = \left(\frac{\text{wet weight} - \text{dried weight}}{\text{dried weight}} \right) \times 100 \quad (4.6)$$

where

wet weight = weight of specimen after water immersion at various time

dried weight = weight of dry specimen before water immersion at a certain period of time.

4.5.11 Composite Interfacial Bonding Examination

Interfacial bonding of the BA-a/PU composite was observed with a scanning electron microscope (SEM) at an acceleration voltage of 15 kV. All specimens were coated with thin gold film using a JEOL ion sputtering device (model JFC-1100E)

for 4 minutes to obtain a thickness of approximately 30Å and the micrographs of the specimen's fracture surface were taken. The obtained micrographs were used to qualitatively evaluate the interfacial interaction between the BA-a/PU matrix resin and the Zylon fiber.



ศูนย์วิทยทรัพยากร
จุฬาลงกรณ์มหาวิทยาลัย

CHAPTER V

RESULTS AND DISCUSSION

5.1 Benzoxazine/Urethane Prepolymer Characterizations

5.1.1 Fourier Transform Infrared Spectroscopic Investigation

In this study, urethane (PU) prepolymer was prepared by reacting polypropylene glycol polyol at a fixed molecular weight of 2000 with toluene diisocyanate (TDI). The basic structure of the urethane prepolymer was studied by FT-IR spectroscopic technique. The important functional groups of the urethane prepolymer are N=C=O and NH-COO [9] which were the characteristic of the urethane prepolymer in the polymerization reaction. In general, the absorption band around 2280-2240 cm^{-1} was assigned to the N=C=O of isocyanate structure while several O-H bands of the polyol were located at a wavenumber range of 3200-3600 cm^{-1} . In addition, the observed urethane absorption band (NH-COO), suggesting the existence of the reaction of the isocyanate group with the hydroxyl group of the polyol in order to form a urethane prepolymer, was observed at 1730-1700 cm^{-1} [10].

Figure 5.1 shows the FT-IR spectra of polypropylene glycol and toluene diisocyanate (TDI) mixture before and after their urethane prepolymer formation. In this study, the urethane prepolymer was obtained after heating the above starting materials for 2 hour at 70°C under a nitrogen atmosphere using dibutyltin dilaurate as a catalyst. The result in this figure indicated the appearance of the absorption band at 1730 cm^{-1} due to the formation of the NH-COO group. The band tended to increase to maximum after the mixture reacted completely. Moreover, the characteristic absorption band at 3400 cm^{-1} of the O-H group disappeared and the peak height at the wavenumber of 2242 cm^{-1} corresponded to the N=C=O decreased with the progress of the reaction to form the urethane prepolymer. Therefore, the formation reaction of the urethane prepolymer was confirmed to be completed under the condition as mentioned above.

FT-IR spectra of benzoxazine resin (BA-a) and polybenzoxazine are shown in Figure 5.2. Characteristic absorption bands of the BA-a resin were found at 942 and 1232 cm^{-1} both assigned to C-O-C stretching mode of benzoxazine ring (Figure 5.2 a). As the curing process proceeded, an infinite three dimensional network was formed upon benzoxazine ring opening by the breakage of C-O bond and then the benzoxazine molecule transformed from a ring structure to a network structure. During this process, the tri-substituted benzene ring (1496 cm^{-1}), backbone of benzoxazine ring, became tetra-substituted benzene ring (1477 cm^{-1}) which led to the formation of a phenolic hydroxyl group-based polybenzoxazine (PBA-a) structure. These absorption bands disappeared after fully thermally cured at temperature of 150°C, 170°C, 180°C, 190°C for 1 hour at each temperature and at 200°C for 2 hours as shown in Figure 5.2 b. In addition, an indication of ring opening reaction of BA-a upon thermal treatment can be observed from the appearance of a broad peak about 3400 cm^{-1} which was assigned to the phenolic hydroxyl groups formation. The result is evident that benzoxazine monomer (BA-a) thermally polymerized through its ring opening reaction to the corresponding polybenzoxazine (PBA-a) [7].

The reaction between benzoxazine resin (BA-a) and urethane prepolymer (PU) could also be analyzed by FT-IR technique. Figure 5.3 reveals the FT-IR spectra of BA-a/PU resin mixture and BA-a/PU polymer alloy at a mass ratio of 60/40. From the figure, the spectrum of the BA-a/PU monomer with the characteristic peaks at 942 and 1232 cm^{-1} , which were the C-O-C stretching mode of the benzoxazine resin, and the absorption band at 2242 cm^{-1} of the N=C=O stretching of the urethane prepolymer was investigated. After being fully-cured, these absorption bands disappeared while the absorption wavenumber of the phenolic hydroxyl groups was observed instead at 3498 cm^{-1} . This peak was, however, clearly indicated in the polybenzoxazine. This observation suggested that the ring opening polymerization of BA-a occurred at those curing temperatures and the phenolic hydroxyl groups from the ring-opened structure of the benzoxazine resin then reacted with the NCO groups simultaneously. Our result is also in good agreement with the result previously reported by Takeichi et al., 2000 [9-10].

5.1.2 Chemorheological Behaviors

The effect of BA-a/PU resin mass ratios on chemorheology of the resin mixtures, which are miscible giving homogenous and transparent liquid, is shown in Figure 5.4. In the rheograms, the complex viscosity of these resin mixtures at various urethane prepolymer contents was reported as a function of the temperature. The specimen temperature was ramped from about 30°C up to the temperature beyond the gel point of each sample. From the figure, all resin mixtures showed a relatively high viscosity at room temperatures due to the solid state nature of these resin mixtures. They were transformed into liquid when the temperature was raised to their liquefying point (i.e. left side of the rheograms). At this point, the complex viscosity of all resin mixtures rapidly decreased. For consistency, the temperature at the viscosity value of 1000 Pa.s was investigated as a liquefying temperature of each resin [25, 31]. From the figure, it can be seen that the increasing urethane polymer fraction in the resin mixtures led to the lowering of their liquefying temperatures. This is due to the fact that the urethane prepolymer used is liquid while the BA-a resin is solid at room temperature. Therefore, the addition of the liquid urethane prepolymer in the solid BA-a resin caused the shifting of the transition from solid state to liquid state to lower temperature. From the above convention, the liquefying temperature of BA-a resin, BA-a/PU 90/10, BA-a/PU 80/20, BA-a/PU 70/30 and BA-a/PU 60/40 resins were determined to be 71, 67, 60, 57 and 51°C, respectively. All resin mixtures became liquid after liquefying point that was the lowest viscosity of each resin system and is normally termed the A-stage viscosity. Lowering the resin liquefying temperature obviously enables the use of lower processing temperature of a compounding process, which is desirable in various composite applications.

Furthermore, at the end of the A-stage viscosity or at higher temperature, the resin mixtures underwent crosslinking reactions past their gel points, which was defined as a transition of liquid (sol) to solid (gel), (i.e. the right side of the rheograms), resulting in a sharp increase in their viscosities. In this case, the maximum temperature at which the viscosity was rapidly raised above 1000 Pa.s was used as gel temperature

of each resin [25, 31]. From the figure, the gel point of the BA-a/PU resin mixture increased with increasing mass fraction of the urethane prepolymer. The gel temperature of BA-a resin, BA-a/PU 90/10, BA-a/PU 80/20, BA-a/PU 70/30 and BA-a/PU 60/40 resins were determined to be 196, 205, 210, 216 and 219°C, respectively. These results suggested that the urethane prepolymer had effect on the curing reaction of the benzoxazine monomer. In other words, the processing window of the BA-a/PU resin mixtures was widened with an addition of the urethane prepolymer. Therefore, one advantage of adding urethane into BA-a/PU resin mixtures was to modify chemorheological behaviors of the benzoxazine resin. The widest processing window was approximately 70°C to 215°C for BA-a/PU of 60/40 compared to the range of 90°C to 195°C of the neat BA-a. This behavior provides BA-a/PU resins with sufficiently broad processing window for a typical compounding process in a composite manufacturing.

Figure 5.5 exhibits the effect of urethane prepolymer content on complex viscosity of BA-a/PU resin mixtures determined at 120°C. From the experiment, the complex viscosity of the benzoxazine-urethane resin mixtures significantly increased with increasing the amount of the urethane prepolymer as the urethane resin had much higher melt viscosity than that of the neat benzoxazine resin. This might be due to the higher molecular weight of the urethane prepolymer compared with that of the benzoxazine resin. The complex viscosity of BA-a/PU resin mixture at 0%, 10%, 20%, 30% and 40% mass fractions of the PU were determined to be 0.11 Pa.s, 0.21 Pa.s, 0.44 Pa.s, 0.78 Pa.s and 1.01 Pa.s, respectively. In practice, the lower viscosity of the resin can enhance the ability of the resin to accommodate greater amount of filler and increase filler wettability of the resin during the compounding process in a composite material preparation [25, 31].

5.1.3 Differential Scanning Calorimetry (DSC) for Curing Process Investigation

The curing reaction of the binary mixtures of BA-a and PU at various PU compositions by differential scanning calorimetry using a heating rate of 10°C/min at a temperature range of 30-300 °C is shown in Figure. 5.6. From the DSC thermograms,

only a single dominant exothermic peak of the curing reaction in each resin composition was observed. The exothermic peak of the neat benzoxazine resin was located at 224°C which is characteristic of the thermal curing of this resin. The curing peak maximum was observed to shift to a higher temperature when the PU fraction in the resin mixtures increased. In Figure 5.6, the positions of the exothermic peaks of BA-a/PU resin mixtures at 90/10, 80/20, 70/30 and 60/40 mass fractions were found to be 234°C, 244°C, 245°C and 246°C, respectively. Additionally, the shifting to high temperature of the exothermic peaks of the mixtures also exhibited a similar trend to the gel temperature of the resin mixtures i.e. the degree of curing retardation increased with an increasing fraction of the PU. In principle, the reactions between the BA-a and the PU were expected to comprise of at least two reactions; the first reaction is the exothermic curing peak among the benzoxazine monomers, while the second one should be the reaction between isocyanate group on the PU and phenolic hydroxyl group on the polybenzoxazine [9-11]. Takeichi and coworkers proposed that the reaction between the isocyanate group on the PU and the phenolic hydroxyl group on the polybenzoxazine was expected to proceed after the generation of hydroxyl group by the ring opening of the benzoxazine monomers. The isocyanate of the PU then could react with the hydroxyl group of the polybenzoxazine.

Considering the breadth of the exotherms, the curing peaks of the binary mixtures became broader when the urethane content increased. Moreover, The decrease of an area under the exothermic peak with the mass fraction of the PU was also observed. The heat of reaction values of the BA-a/PU resin mixtures determined from the area under the exothermic peak, were 270.7 J/g in BA-a/PU 100/0, 229.3 J/g in BA-a/PU 90/10, 207.5 J/g in BA-a/PU 80/20, 165.4 J/g in BA-a/PU 70/30 and 155.5 J/g in BA-a/PU 60/40. The phenomenon was possibly due to the reaction of the BA-a with the PU rendering a lower heat of reaction per mole of the specimen than the reaction of the neat BA-a. These can be attributed to the changes in the number of mole and the functional groups of each component in polymer alloys. At equal mass, the number of molecules of the PU were lower than that of benzoxazine monomers. In addition, a benzoxazine monomer is tetrafunctional while difunctional urethane prepolymer can only

react with two hydroxyl groups of the polybenzoxazine. Thus, we can observe the decreasing of the heat of reaction with decreasing benzoxazine monomers in the binary mixtures.

The curing condition of benzoxazine-urethane resins at a fixed mass ratio of 60/40, which required the highest curing temperature among the investigated resin mixtures, was depicted in Figure 5.7. The fully cured stage of the polymer in our case corresponded to the disappearance of the exothermic heat of reaction as determined from the residual area of the exothermic DSC peak. In theory, the fully cured stage has been reported to provide a polymer with desirable properties including sufficiently high thermal and mechanical integrity. The heat of reaction determined from the area under the exothermic peak was 155.5 J/g (0% conversion) for the uncured 60/40 of BA-a/PU mixture. The heat of reaction reduced to 111.0 J/g (28% conversion) after the thermal curing at 150°C for 1 hour, and decreased to 107.1 J/g (31% conversion) after further thermal curing at 170°C for 1 hour and 26.6 J/g (83% conversion) at 180°C for 1 hour. The heat of reaction decreased to 19.45 J/g (88% conversion) for further thermal curing at 190°C for 1 hour. Finally, after thermal post cure at 200°C for another 2 hours, the exothermic heat of reaction disappeared corresponding to the fully cured stage of the alloys. The degree of conversion of the sample was calculated according to the following relationship.

$$\% \text{ conversion} = \left(1 - \frac{H_{rxn}}{H_o} \right) \times 100 \quad (5.1)$$

where H_{rxn} is a heat of reaction of a partially cured specimen.
 H_o is a heat of reaction of an uncured resin.

Both H_{rxn} and H_o values can be obtained from DSC experiments. The calculated conversion suggested that the curing reaction of BA-a/PU mixtures could rapidly occur at high temperature above 150°C. As a consequence, the curing temperature at 150°C for 1 hour, 170°C for 1 hour, 180°C for 1 hour, 190°C for 1 hour

and 200°C for 2 hours was chosen as an optimum curing condition of all BA-a/PU resin mixtures.

Figure 5.8 presents glass transition temperatures (T_g) from DSC of the fully cured BA-a/PU alloys. In this experiment, the T_g values were taken as the midpoint temperature of the change in specific heat in the transition region. From room temperature up to 300°C, there existed only single T_g in each of these BA-a/PU alloys. Additionally, the T_g 's of the polymer alloys between the BA-a and the PU were found to systematically increase with the mass fraction of the PU. The T_g of the fully cured BA-a/PU alloys were observed to be 156°C in BA-a/PU 100/0, 165°C in BA-a/PU 90/10, 180°C in BA-a/PU 80/20, 222°C in BA-a/PU 70/30 and 239°C in BA-a/PU 60/40. However, T_g of the polyurethane elastomer and the polybenzoxazine were reported to be about -70 to -20°C [9-10] and 160 to 170°C [7, 15], respectively. This is the unique characteristic of these polymer alloys as it exhibited synergistic behaviors in their glass transition which makes the systems highly attractive for high temperature application. The enhancement in the T_g of the polybenzoxazine by alloying or blending with other polymers has also been reported elsewhere [8, 25-26]. This is possibly due to an enhancement in crosslinked density of the BA-a/PU binary systems when the urethane prepolymer was added.

5.2 Characterizations of Benzoxazine/Urethane Polymer Alloys

5.2.1 Density Measurement of BA-a/PU Polymer Alloys

In this work, density measurement of all fully cured BA-a/PU specimens was performed to investigate the presence of void in the specimens. Figure 5.9 shows the density of specimens with various urethane contents comparing with their theoretical density. The actual density of the polymer alloys was calculated using equation (4.1) and the theoretical density of the polymer alloys was calculated from equation (4.2). The calculated one was based on the basis that the densities of the urethane prepolymer and polybenzoxazine were 1.06 g/cm³ [32] and 1.19 g/cm³ [33], respectively.

Furthermore, the theoretical densities of the BA-a/PU polymer alloys were determined to be 1.190 g/cm³ in BA-a/PU 100/0, 1.177 g/cm³ in BA-a/PU 90/10, 1.164 g/cm³ in BA-a/PU 80/20, 1.151 g/cm³ in BA-a/PU 70/30 and 1.138 g/cm³ in BA-a/PU 60/40. Whereas the measured densities at 100/0, 90/10, 80/20, 70/30 and 60/40 mass ratios of the BA-a/PU alloys were found to be 1.188, 1.177, 1.160, 1.148 and 1.133 g/cm³, respectively. In the result, the densities of the polymer alloys were observed to systematically decrease with increasing PU fraction suggesting that the theoretical and actual density of the BA-a/PU alloys followed the rule of mixture. Moreover, it can be observed that the actual densities were about the same with the values slightly lower than those of the theoretical densities. Because of the rather high melt viscosity of the urethane prepolymer, adding more urethane prepolymer directly affected on the mixing behavior and the obtained densities were normally slightly lower than the theoretical values. The phenomenon is likely to be caused by the presence of voids in the specimens as a result of mixing difficulty from an addition of the more viscous PU fraction into the benzoxazine resin.

5.2.2 Dynamic Mechanical Analysis of the BA-a/PU Polymer Alloys

Transition temperatures of all BA-a/PU polymer alloys were also determined using DMA since the technique is highly sensitive to even minor transitions or relaxations. DMA senses any change in molecular mobility in the sample when temperature is raised or lowered. The dynamic modulus is one of the most important properties of materials for structural applications. Typically, mechanical damping is often the most sensitive indicator in determining all kinds of molecular motions, which are taking place in polymeric materials particularly in solid state. Figure 5.10 shows the dynamic mechanical properties of BA-a/PU alloys at various compositions which had been fully cured to yield the crosslinked structures of the infinite network. The experiment was performed on a bending mode as a function of temperature from -160 to 300°C. The specimen's compositions were ranging from 0-40% by weight of PU fraction. From Figure 5.10, three areas including the glassy state, the transition region and the rubbery plateau were obtained for each sample. Ordinarily, the storage modulus of the

materials decreased with increasing temperature. At room temperature, the storage modulus in a glassy state of the BA-a/PU binary systems was expectedly found to systematically decrease with increasing PU mass fraction. We can see that the storage modulus of the BA-a/PU alloys were reduced from 5.2 GPa to 1.8 GPa with the addition of the PU from 0 to 40% by weight. As a consequence, the presence of the more flexible PU in the copolymers was resulted in the more flexible polymer hybrids as seen from the lower room temperature modulus.

Effects of urethane prepolymer on the storage modulus in the rubbery plateau region of their polymer alloys are illustrated in Figure 5.11. From the figure, the storage modulus in the rubbery plateau region tended to increase with the mass fraction of the PU which was an opposite trend to the storage modulus in the glassy state. The storage moduli in the rubbery plateau region were systematically increased from 56 MPa to 148 MPa with an addition of the PU fraction from 0 to 40% by weight. This suggested that the increase in the PU content in the polymer alloys possibly resulted in an enhancement of the crosslinked density of the fully cured specimens which was closely related to the rubber plateau modulus. Crosslinked density of a polymer network can be estimated from the theory of rubber elasticity by knowing its rubbery plateau modulus as suggested by Nielson [34-35].

$$\log\left(\frac{E'}{3}\right) = 7.0 + 293(\rho_x) \quad (5.2)$$

From Nielson's equation above, E' is a storage modulus in a rubbery plateau region, ρ_x is a crosslinked density that is the mole number of network chains per unit volume of the polymers. The crosslinked density of our polymer alloys was found to increase with the mass fraction of the urethane prepolymer. The crosslinked density determined from Nielson's equation of the BA-a/PU polymer alloys was 4,661 mol/m³ in BA-a/PU 100/0, 5,202 mol/m³ in BA-a/PU 90/10, 5,613 mol/m³ in BA-a/PU 80/20, 5,833 mol/m³ in BA-a/PU 70/30 and 7,955 mol/m³ in BA-a/PU 60/40.

In addition, the effect of a crosslinked density on a Tg of the polymer network can be accounted for using the Fox-Loshaek equation [32].

$$Tg = Tg(\infty) - \frac{k}{M_n} + k_x \rho_x \quad (5.3)$$

where $Tg(\infty)$ is the glass transition temperature of infinite molecular weight linear polymer, k and k_x are the numerical constants, M_n is the number averaged molecular weight which equals infinity in the cross-linked system, therefore, this term can be neglected and ρ_x is the crosslinked density. According to the Fox-Loshaek equation, the cross-linked density is one key parameter affecting Tg of the polymer networks. Figure 5.12 illustrates the Tg and cross-linked density of BA-a/PU alloys at various compositions. As seen from this figure, The Tg of the polymer network increased when its cross-linked density in the alloys increased, which is in good agreement with our DMA results.

Figure 5.13 plots the loss modulus (E'') curves of the benzoxazine-urethane alloys as a function of temperature. The Tg of the alloys can be roughly estimated from the maximum peak temperature in the loss modulus curve of each specimen. From the figure, we can see that the Tg of the neat polybenzoxazine was determined to be 165°C whereas those of the polymer alloys were about 177°C in BA-a/PU 90/10, 192°C in BA-a/PU 80/20, 220°C in BA-a/PU 70/30 and 245°C in BA-a/PU 60/40. Therefore, adding PU into the polybenzoxazine can substantially increase the Tg of the polymer alloys. Synergistic behavior of the Tg of the alloys was evidently observed i.e. Tg's of all alloys were greater than those of the BA-a and the PU i.e. 165°C and -70°C, respectively. The Tg of the PU domain in the alloys can also be observed from the decrease of the storage modulus values at about -70°C. And the E' decrease was also found to be more pronounced with the amount of PU. Moreover, it can be noticed that the glass transition temperatures observed from DMA thermograms exhibited the same trend as those obtained by DSC (Figure 5.8). An ability of the urethane prepolymer to

enhance crosslinked density of polybenzoxazine was attributed to the observed synergy in T_g as explained above.

Tan δ or loss tangent curves, obtained from the ratio of energy loss or viscous part (E'') to storage energy or elastic part (E') of dynamic modulus of material, are shown in Figure 5.14. The T_g of the polymer alloys can also be determined from the maximum peak temperature on the tan δ curve of each sample. As shown in the figure, T_g's of the alloys were observed to shift to higher temperature when the urethane prepolymer content in the alloys increased. These results were in good agreement with the previous DSC investigation. However, the values of the T_g's obtained from the DSC experiment were about 10-20°C lower than those obtained from the DMA measurement. Chartoff [36] reviewed the discrepancies of the T_g values measured by DSC and DMA and pointed out that the DSC T_g value is always lower than the DMA value determined by either tan δ or E'' maximum peaks. In addition, the frequency of 1 Hz used in DMA experiment may correspond to a DSC heating rate of about 20-40°C/min range. DMA is approximately 1000 times more sensitive than DSC in terms of baseline deflection for detecting T_g and renders more useful mechanical property data, though larger sample size is required. Furthermore, Figure 5.15 illustrates the magnitude of the tan δ peak maximum reflecting the large scale mobility associated with alpha relaxation. The peak height of the tan δ was found to decrease with increasing the mass fraction of the PU. This confirmed the reduction in segmental mobility of polymer chains with increasing crosslinked density as PU fraction in the alloy increased. The width at half height of the tan δ relates to the network homogeneity. The width at half height of the tan δ curves of our BA-a/PU polymer alloys were broader in the PU rich systems implying network heterogeneity to be more pronounced with an increasing amount of the PU [7].

5.2.3 Thermal Degradation of BA-a/PU Polymer Alloys (TGA)

Thermal degradation of BA-a/PU polymers were investigated by thermogravimetric analysis (TGA). The degradation temperature (T_d) is one of the key parameters needed to be determined for thermal stability of polymers. Figure 5.16

shows TGA profiles of the neat polybenzoxazine, neat polyurethane and benzoxazine-urethane polymer alloys at various urethane contents under nitrogen atmosphere. The Td, in this case, is defined as the temperature at 5% weight loss of the specimens. As evidently seen in the thermograms, the thermal decomposition in each alloy was found to show a single stage weight loss and the Td's of the polymer alloys were found to be slightly higher than that of the neat polybenzoxazine. Both the Td and char yield values of the BA-a/PU alloys are plotted in Figure 5.17. The Td's of the neat polybenzoxazine and the urethane prepolymer were determined to be 325°C and 305°C whereas their alloys showed the Td values of 326°C in BA-a/PU 90/10, 327°C in BA-a/PU 80/20, 334°C in BA-a/PU 70/30 and 336°C in BA-a/PU 60/40. Consequently, synergistic behavior of Td of these alloys were also observed i.e. the Td's of all alloys were greater than that of the neat BA-a (325°C) and the neat PU (305°C). Therefore, an incorporation of the PU into the polybenzoxazine was found to enhance thermal stability of the polybenzoxazine. These results might be due to the reaction of the isocyanate in urethane prepolymer and the hydroxyl of the polybenzoxazine to increase a crosslinked density of the polymer alloys as aforementioned.

Another interesting feature in the TGA thermograms (Figure 5.15) is the percent residual weight of our polybenzoxazine alloys. The char yield, which reported at 800°C under N₂ atmosphere, of our polybenzoxazine alloys was illustrated in Figure 5.17. It can be seen that the residual weight of the BA-a/PU alloys were found to systematically decrease with increasing PU fraction. This is due to the fact that polybenzoxazine possessed higher char yield value of about 29% while no char residue was found for the polyurethane used. The chemical structure of the polyurethane composed of a less thermally stable aliphatic structure of the polypropylene glycol polyol compared to the prevalent benzene rings in the molecular structure of the polybenzoxazine. The char yields of BA-a/PU alloys at 10%, 20%, 30% and 40% mass fractions of the PU were determined to be 24.1 wt%, 23.4 wt%, 20.7 wt% and 18.7 wt%, respectively. This result is also consistent with those reported by Takeichi et al, 2000 [10].

5.2.4 Coefficient of Thermal Expansion of BA-a/PU Polymer Alloys

During heat transfer, the energy that is stored in the intermolecular bonds between atoms changes. When the stored energy increases, so does the length of the molecular bonds. As a result, solids typically expand in response to heating and contract on cooling. This dimensional response to temperature change is expressed by its coefficient of thermal expansion (CTE). Figures 5.18 exhibits the CTE characteristics of BA-a/PU alloy specimens at various urethane mass fractions. The CTE values of BA-a/PU 100/0, BA-a/PU 90/10, BA-a/PU 80/20, BA-a/PU 70/30, and BA-a/PU 60/40 were determined to be 57.7, 44.7, 53.0, 82.8, and 90.2 ppm/°C, respectively. It was clearly observed the CTE of our alloys did not show a linear relationship with the composition of the alloys but also exhibited a synergistic behaviour with the minimum CTE value at BA-a/PU 90/10 mass fraction. The CTE of BA-a/PU at 90/10 and 80/20 weight ratios were found to be lower than that of the neat polybenzoxazine and increased to higher values when the amount of PU fraction was greater than 20 wt%. In principle, the addition of the PU which is more expansible than BA-a due to its elastomeric nature, the resulting BA-a/PU alloys should result in an increase in their CTE values as observed in the PU content of greater than 20% by weight region. The observed synergistic behavior in CTE of these polymer alloys in the vicinity of 10-20% by weight implied that the effect of crosslinked density enhancement in the alloy's CTE dominated the effect of the higher expansion of the PU provided that the PU mass fraction was maintained below 20% by weight.

5.2.5 Flexural Properties of BA-a/PU Polymer Alloys

In this investigation, the specimens for flexural analysis were loaded until failure and the stress-strain curves were obtained for each sample. The flexural strength of a thermosetting resin is influenced by a number of interrelated system parameters including T_g , molecular weight between crosslinks, crosslink density, free volume, chemical structure, network irregularity and perfection, and many other contributing factors [37]. Flexural properties of BA-a/PU polymer alloys were exhibited in Figures

5.19 and 5.20. Figure 5.19 illustrates flexural strength of the BA-a/PU alloys at various mass fractions of PU. The flexural strength of the neat polybenzoxazine was determined to be 130 MPa. Interestingly, the strength values of the BA-a/PU alloys were observed to exhibit also a synergistic behavior with the maximum flexural strength value of 142 MPa observed at the BA-a/PU mass ratio of 90/10. In addition, with an increase of the PU fraction (i.e. 20wt%, 30wt% and 40wt%), the flexural strength values were found to decrease systematically. Those flexural strengths of the BA-a/PU alloys were determined to be 120 MPa in BA-a/PU 80/20, 89 MPa in BA-a/PU 70/30 and 60 MPa in BA-a/PU 60/40. This finding coincides with the phenomenon found in CTE and T_g as discussed earlier.

Figure 5.20 shows the flexural modulus of BA-a/PU alloys at various PU mass fractions. The maximum flexural modulus value of 5.5 GPa belonged to neat polybenzoxazine. The flexural modulus was also found to linearly decrease with increasing amount of PU for all BA-a/PU alloy systems. The flexural modulus values of BA-a/PU alloys were 4.1 GPa, 3.4 GPa, 2.5 GPa and 2.1 GPa for BA-a/PU of 90/10, 80/20, 70/30, and 60/40 mass ratios, respectively. The flexural modulus shows a behavior nearly identical to that of the storage modulus determined by DMA as explained in section 5.2.2. This phenomenon was due to the fact that the addition of the softer urethane resin into the benzoxazine resin was expected to lower the stiffness of the polybenzoxazine alloys as a result of an elastomeric nature of the PU used [10].

5.2.6 Surface Hardness of BA-a/PU Polymer Alloys

Hardness is defined as the resistance offered by a specimen to the penetration of a hardened steel truncated cone (Shore-A), pointed cone (Shore-D) or a spherical or flat indenter (foam hardness). In this study, Shore-D hardness was measured on a scale that was graduated from 0 to 100 divisions; 0 denoting the lowest and 100 the highest degree of hardness. In Figure 5.21, the surface hardness (Shore D) values of the BA-a/PU polymer alloys at different PU content were presented. As expected, the surface hardness of the polymer alloys was found to systematically

decrease with increasing PU fraction. An addition of PU to BA-a was found to diminish the resistance of the BA-a deformation. The surface hardness values of the fully cured BA-a/PU alloys were observed to be 86 shore D in BA-a/PU 100/0, 77 shore D in BA-a/PU 90/10, 73 shore D in BA-a/PU 80/20, 69 shore D in BA-a/PU 70/30, and 68 shore D in BA-a/PU 60/40. The surface hardness of the urethane was reported to be approximately 40 shore D [38]. As a consequence, the hardness of the BA-a/PU alloys tended to follow a simple rule of mixture. This phenomenon was similar to hardness values of polyurethane reinforced with aluminum oxide (Al_2O_3) particles reported by R. Zhou et al, 2005 [27].

5.2.7 Water Absorption of BA-a/PU Polymer Alloys

Figure 5.22 shows percent water absorption of BA-a/PU alloys versus time. It can be seen in this figure that the percent water absorption value of BA-a alloyed with the PU tended to increase with an addition of the PU. Moreover, the percent water absorption was observed to increase sharply in the first 24 hours of the test, and reach a plateau value of 1.3% in BA-a/PU 100/0, 2.0% in BA-a/PU 90/10, 2.8% in BA-a/PU 80/20, and 4.3% in BA-a/PU 70/30, and 4.7% in BA-a/PU 60/40. The reason for this phenomenon was explained as due to the greater number of hydroxyl group from the incorporation of the PU fraction and was confirmed by the FT-IR measurement (Figures 5.2 and 5.3). The more the hydroxyl group presented, the higher the polarity of the polymer alloys thus resulting in the greater water absorption of the alloys.

5.3 Zylon Fiber-Reinforced BA-a/PU Composites Characterizations

5.3.1 Determination of Polymer Matrix Content in the Composites

In principle, a knowledge of polymer matrix content in a polymer composite is the most important factor related to the performance of composite materials. The optimal fiber volume fraction in Zylon fiber-reinforced composites was

reported to be about 67% in epoxy systems [28]. The fiber volume fraction (V_f) was calculated from the following equation

$$V_f = \frac{W_f / \rho_f}{(W_f / \rho_f) + (1 - W_f) / \rho_m} \quad (5.4)$$

Where W_f is the fiber weight fraction, $(1 - W_f)$ is the matrix weight fraction, ρ_f is the fiber density (density of Zylon fiber = 1.56 g/cm³) and ρ_m was the matrix density (density of matrix is approximately 1.10 g/cm³). From equation 5.4, we can determine the value of W_f to be about 74%. As a result, the fiber weight fraction at about 70% (i.e. Zylon fiber = 70% by weight and BA-a/PU matrix = 30% by weight) was chosen as an optimal fiber content of all Zylon fiber-reinforced BA-a/PU composites in our study.

5.3.2 Differential Scanning Calorimetry for Curing Condition Examination

Figure 5.23 exhibits the effect of PU content on curing behaviors of Zylon fiber-reinforced BA-a/PU prepregs. The exothermic peak of Zylon fiber-reinforced BA-a/PU prepregs was observed to systematically shift to higher temperature with an addition of the PU fraction in the matrix resin. The peak temperatures of the Zylon fiber-reinforced BA-a/PU with BA-a/PU equal 100/0, 90/10, 80/20, 70/30 and 60/40 mass ratios were 233°C, 240°C, 245°C, 247°C and 251°C, respectively. In addition, the heat of reaction values of the Zylon fiber-reinforced BA-a/PU prepregs determined from the area under the DSC exothermic peak were 69.4 J/g in BA-a/PU 100/0, 51.3 J/g in BA-a/PU 90/10, 46.6 J/g in BA-a/PU 80/20, 32.7 J/g in BA-a/PU 70/30 and 24.2 J/g in BA-a/PU 60/40. The exothermic curing peak and the heat of reaction of the Zylon fiber-BA-a/PU prepregs showed the characteristics similar to those of the neat matrix alloys.

Figure 5.24 illustrates DSC thermograms of Zylon-reinforced BA-a/PU 60/40 prepregs. The composition at 60/40 was selected to represent all composites for

determining the full cured condition as the ratio required the most curing temperature to achieve the fully cured stage. The Zylon-reinforced BA-a/PU 60/40 prepregs possessed the curing exotherms with the same characteristics as those of the matrix as shown in Figure 5.6. This characteristic indicated that the Zylon fiber used had no effect on the curing reaction either retarding or accelerating the curing reaction of the matrix resin. In other words, the fiber is chemically inert to the benzoxazine curing reaction. The processing condition of the Zylon fiber-reinforced BA-a/PU prepregs was thus chosen to be the same as that of the unreinforced resins. The condition was also selected to ensure that the fully cured stage was obtained in every tested BA-a/PU mixtures. After post curing at 200°C for 2 hours, the exothermic heat of reaction totally disappeared corresponding to the fully cured stage of the Zylon fiber-reinforced composites. Therefore, the curing condition of Zylon fiber-reinforced BA-a/PU prepregs at different urethane contents was the same as the condition used to cure the matrices which was by heating at 150°C for 1 hour, 170°C for 1 hour, 180°C for 1 hour, 190°C for 1 hour and 200°C for 2 hours using a hydraulic hot-press machine.

5.3.3 Density Measurement of Zylon Fiber-Reinforced BA-a/PU Composites

Figure 5.25 illustrates densities of all composite specimens at various PU content comparing with their theoretical densities. The theoretical densities of the polymer composites were calculated from equation (4.2) and the actual densities of the composites were calculated by equation (4.1). The calculation was based on the basis that the densities of the Zylon fiber and the BA-a/PU polymer matrix were 1.56 g/cm³ [16] and 1.10 g/cm³, respectively. The theoretical densities of the BA-a/PU polymer composites were determined to be 1.449 g/cm³ in BA-a/PU 100/0, 1.445 g/cm³ in BA-a/PU 90/10, 1.441 g/cm³ in BA-a/PU 80/20, 1.437 g/cm³ in BA-a/PU 70/30, and 1.433 g/cm³ in BA-a/PU 60/40. While the measured densities of the composites at 100/0, 90/10, 80/20, 70/30 and 60/40 mass ratios of the BA-a/PU were 1.414, 1.404, 1.398, 1.379 and 1.372 g/cm³, respectively. These results indicated that theoretical and actual density values of Zylon fiber-reinforced BA-a/PU composites tended to decrease with an addition of the PU following the rule of mixture.

5.3.4 Dynamic Mechanical Properties of BA-a/PU and Zylon Fiber Composites

Figures 5.26 to 5.28 illustrate dynamic mechanical properties of Zylon fiber-reinforced composites with the PU content in the range of 0 to 40% by weight. From Figure 5.26, the storage modulus in a glassy state of the Zylon fiber-reinforced composites decreased when the PU fraction increased as a result of the incorporation of the more flexible PU molecule in the composite as already explained in the previous section. At room temperature, the storage moduli of the Zylon fiber-reinforced composites were systematically reduced from 31 GPa to 14 GPa with the addition of the PU from 0 to 40% by weight.

Loss modulus (E'') from DMA measurement of the Zylon fiber-reinforced BA-a/PU composites at various PU contents is shown in Figure 5.27. T_g of a sample was defined as the temperature at the maximum of the loss modulus curve. It can be seen that the addition of the PU into the matrix composites was found to increase the T_g of the Zylon fiber composites. The result is consistent with the trend observed in DSC and DMA thermograms of the neat matrix alloys. Finally, the T_g values of the Zylon fiber composites tended to be similar to those of the matrix alloys.

The α -relaxation peaks of the loss factor or $\tan \delta$ of the composites are shown in Figure 5.28. The magnitude of $\tan \delta$ was observed to decrease with increasing mass fraction of the PU and the peak maxima shifted to higher temperature. In addition, the peak height of the $\tan \delta$ was observed to be smaller with the amount of PU. Since $\tan \delta$ is a ratio of a viscous to an elastic component of dynamic moduli of a specimen, it can be surmised that its decreasing height with the PU content around T_g is associated with a lower segmental mobility, and thus is indicative of a higher degree of crosslinking for the urethane-rich samples as observed in our BA-a/PU alloy systems.

5.3.5 Thermal Degradation of Zylon Fiber-Reinforced BA-a/PU Composites

Figure 5.29 exhibits TGA thermograms of Zylon fiber-reinforced BA-a/PU composites at various PU content. Thermal decomposition in all composites was observed to occur in two stages. The first stage occurred at temperature between 300°C and 500°C corresponded to the decomposition temperature of the polymer matrix whereas the second stage from the thermogram corresponded to the decomposition temperature of Zylon fiber which was approximately 600-800°C. The degradation temperatures at 5% weight loss of our Zylon fiber-reinforced composites were found to decrease systematically with increasing mass fraction of the PU in the alloys. In this figure, the degradation temperatures of the Zylon fiber-reinforced composites with the PU compositions of 0 to 40 % by weight was ranging from 384°C to 344°C. However, Zylon fiber-reinforced BA-a/PU composites exhibited higher degradation temperatures than those of the polymer matrices due to the effect of high degradation temperature of the Zylon fiber i.e. approximately at 678°C. The greater Td of the composite with higher amount of the benzoxazine fraction in the matrix alloys suggested the stronger interaction between the Zylon fiber and the polybenzoxazine than between the PU portion.

Another important feature in the thermograms is the weight residue at 800°C or the char yield of the composites which is related to the flammability of material. From Figure 5.30, the char yields of the composites was found to systematically reduce from 57.8% to 51.7% with an incorporation of the PU from 0 to 40% by weight. The values were all greater than those of the matrix alloys comparing at the same PU content. This is due to the fact that the char yields of the composites also included the additional residue of the high char yield Zylon fiber which was approximately 68.2%. One benefit of composing Zylon fiber with BA-a/PU as a matrix is thus to improve the thermal stability of the composite.

Thermogravimetric analyzer was also used to determine the polymer matrix content in the composites. In this research, the polymer matrix content in the composites was calculated using the resulting char yields from thermogravimetric analysis (TGA) of the BA-a/PU alloys as a polymer matrix. The percent of matrix content of 26% in BA-a/PU 100/0, 25wt% in BA-a/PU 90/10, 28wt% in BA-a/PU 80/20, 30wt% in BA-a/PU 70/30 and 33wt% in BA-a/PU 60/40 were obtained. The calculated results confirmed that the Zylon fiber content in each composite was about 30% by weight as prepared in the pre-impregnation stage.

5.3.6 Flexural Properties of Zylon Fiber-Reinforced BA-a/PU Composites

The mechanical properties of fiber reinforced composite depend on several factors such as mechanical properties of the reinforced fiber and polymer matrix, the fiber volume fraction. One of the important factors is adhesion between the fiber and matrix. Flexural properties of the Zylon fiber-reinforced composites were depicted in Figures 5.31 and 5.32. From Figure 5.31, flexural strengths of the Zylon fiber composites at various PU mass fractions were found to be 330.9 MPa in BA-a/PU 100/0, 303.5 MPa in BA-a/PU 90/10, 240.0 MPa in BA-a/PU 80/20, 172.1 MPa in BA-a/PU 70/30 and 143.2 MPa in BA-a/PU 60/40. Moreover, it was also observed that the flexural strengths of the composites tended to decrease in a linear manner with the amount of PU in the matrix alloys. Additionally, the flexural moduli of the composites were found to significantly decrease with increasing amount of PU.

In Figure 5.32, flexural moduli of the Zylon-reinforced composites at 0%, 10%, 20%, 30% and 40% mass fractions of the PU were determined to be 28.0 GPa, 24.5 GPa, 21.9 GPa, 17.8 GPa and 15.1 GPa, respectively. The phenomenon was due to the fact that the addition of the elastomeric PU into the adamantine polybenzoxazine was able to lower both the strength or the stiffness of the resulting polybenzoxazine alloys as clearly seen in both figures.

From the micrographs, it was obvious that wettability of BA-a resin was greater than the others which contained more PU. This good fiber wet-out property of BA-a resin compared with that of the BA-a/PU resin mixtures thus rendered the highest mechanical properties of their Zylon fiber-reinforced composites.



ศูนย์วิทยทรัพยากร
จุฬาลงกรณ์มหาวิทยาลัย

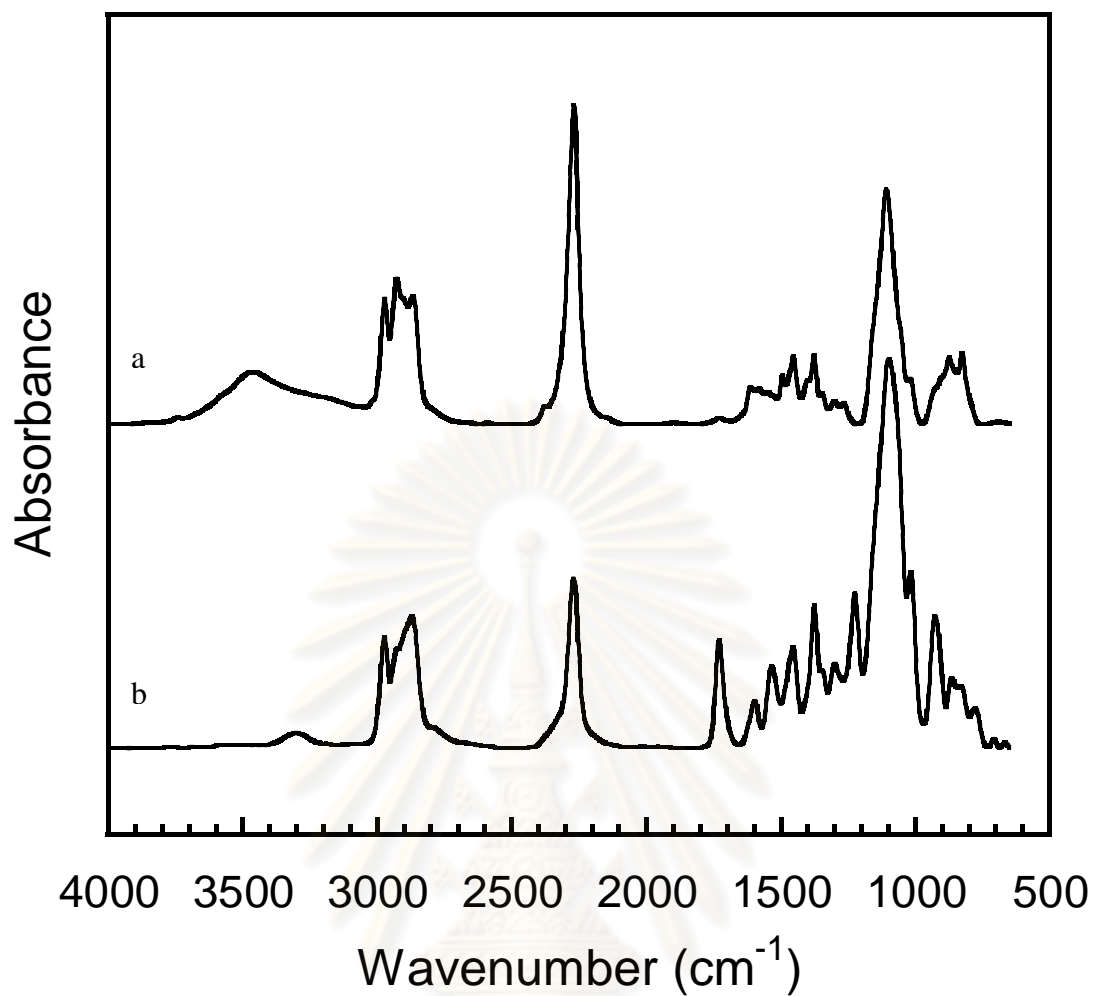


Figure 5.1 FT-IR spectra of polyurethane prepolymer
a) TDI+Diol before synthesis, b) TDI+Diol after synthesis.

ศูนย์วิทยทรัพยากร
จุฬาลงกรณ์มหาวิทยาลัย

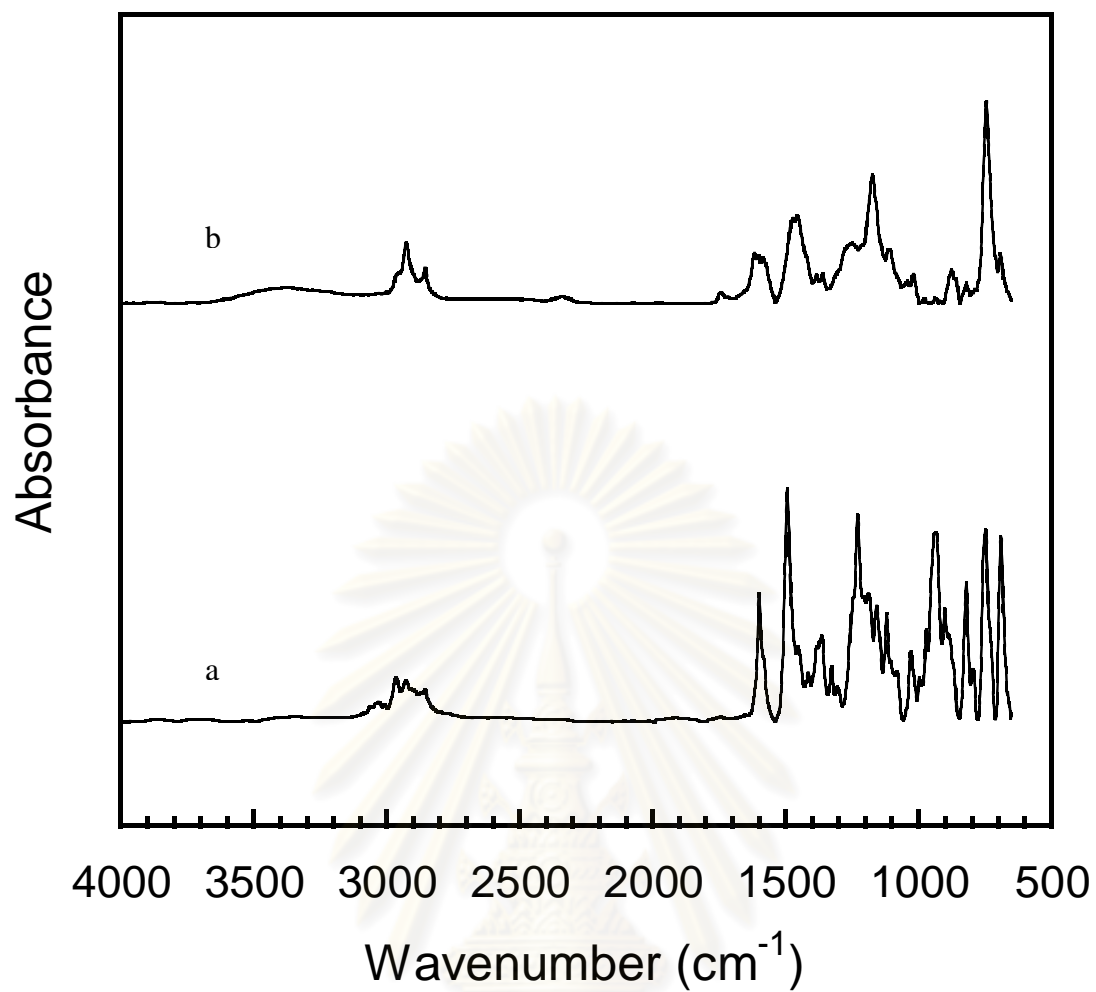


Figure 5.2 FT-IR Spectra of benzoxazine resin and its polymer :

(a) Benzoxazine monomer (BA-a), (b) Polybenzoxazine (PBA-a).

ศูนย์วิทยทรัพยากร
จุฬาลงกรณ์มหาวิทยาลัย

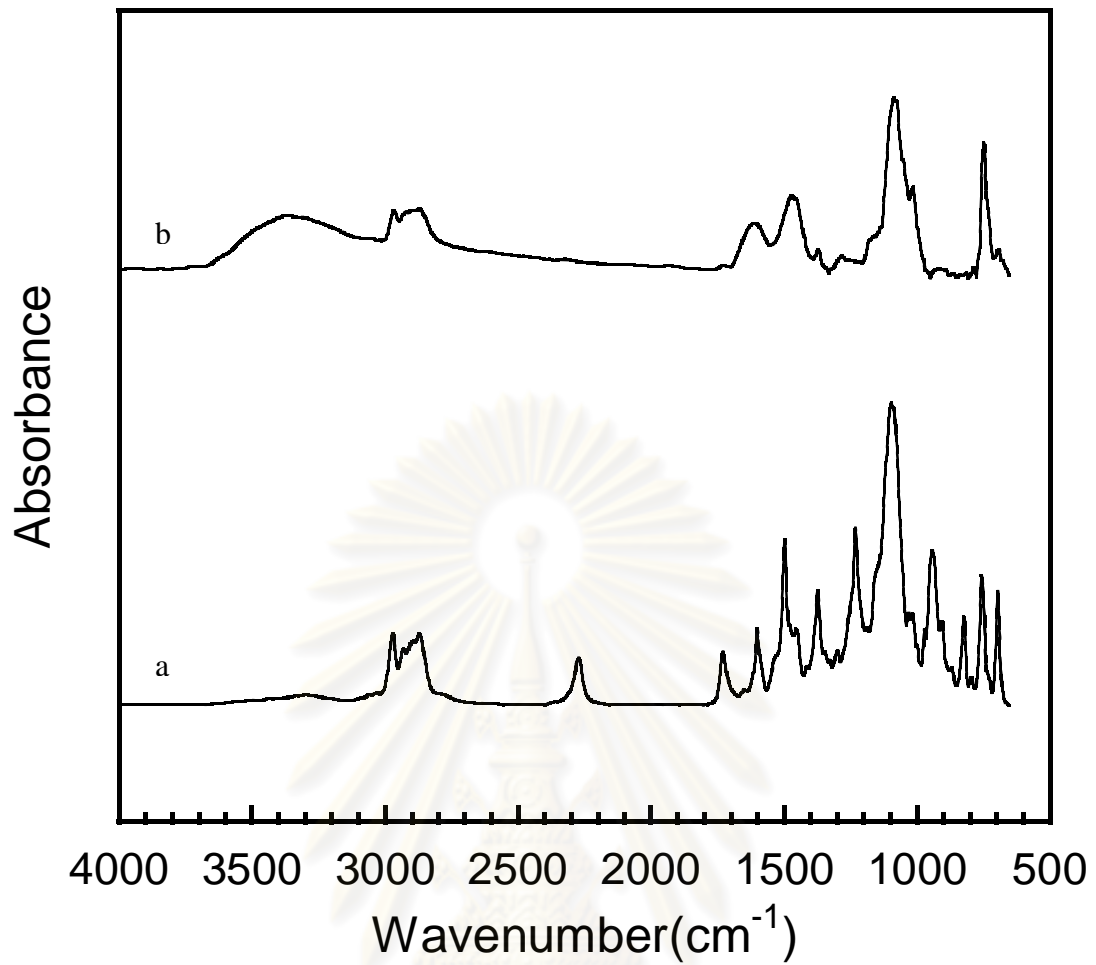


Figure 5.3 FT-IR Spectra of BA-a/PU resin mixture and its polymer :

(a) BA-a/PU 60/40 uncured, (b) BA-a/PU 60/40 fully cured.

ศูนย์วิทยทรัพยากร
จุฬาลงกรณ์มหาวิทยาลัย

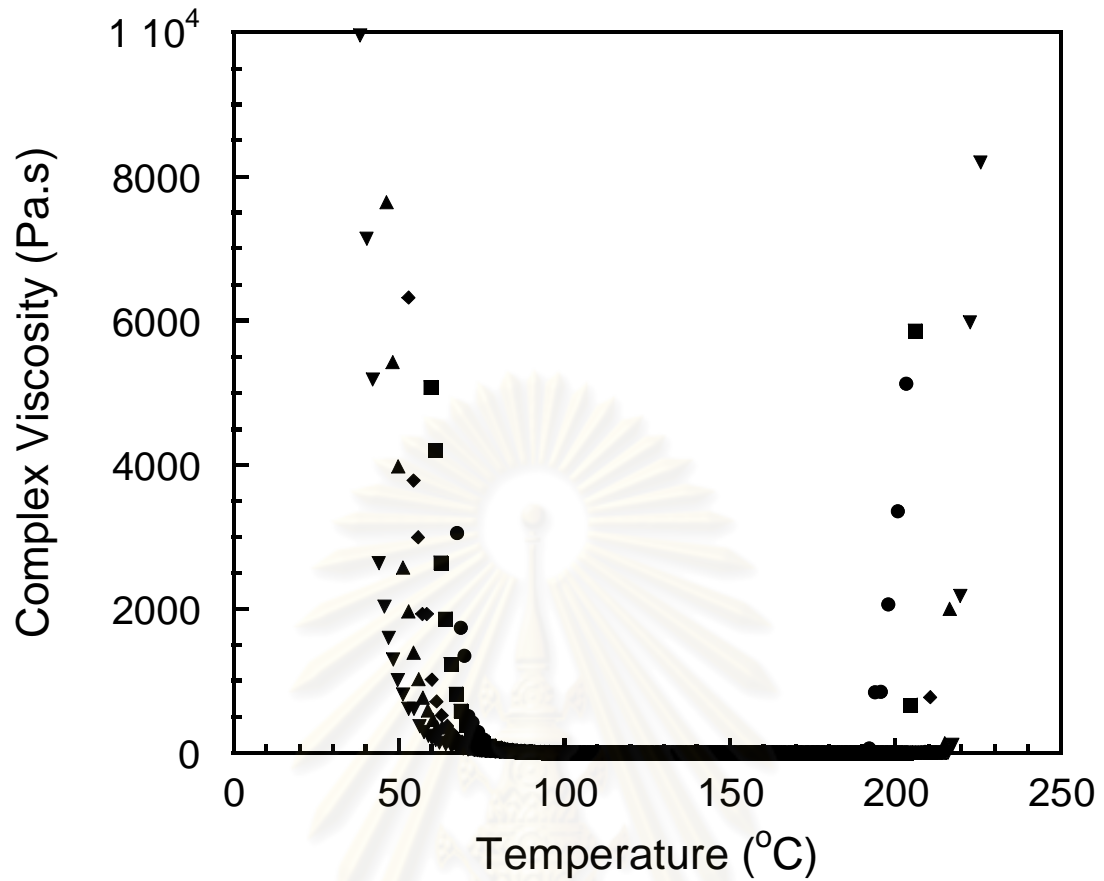


Figure 5.4 Viscosity of BA-a/PU resin at various compositions : (●) BA-a/PU 100/0, (■) BA-a/PU 90/10, (◆) BA-a/PU 80/20, (▲) BA-a/PU 70/30 and (▼) BA-a/PU 60/40.

ศูนย์วิทยทรัพยากร
จุฬาลงกรณ์มหาวิทยาลัย

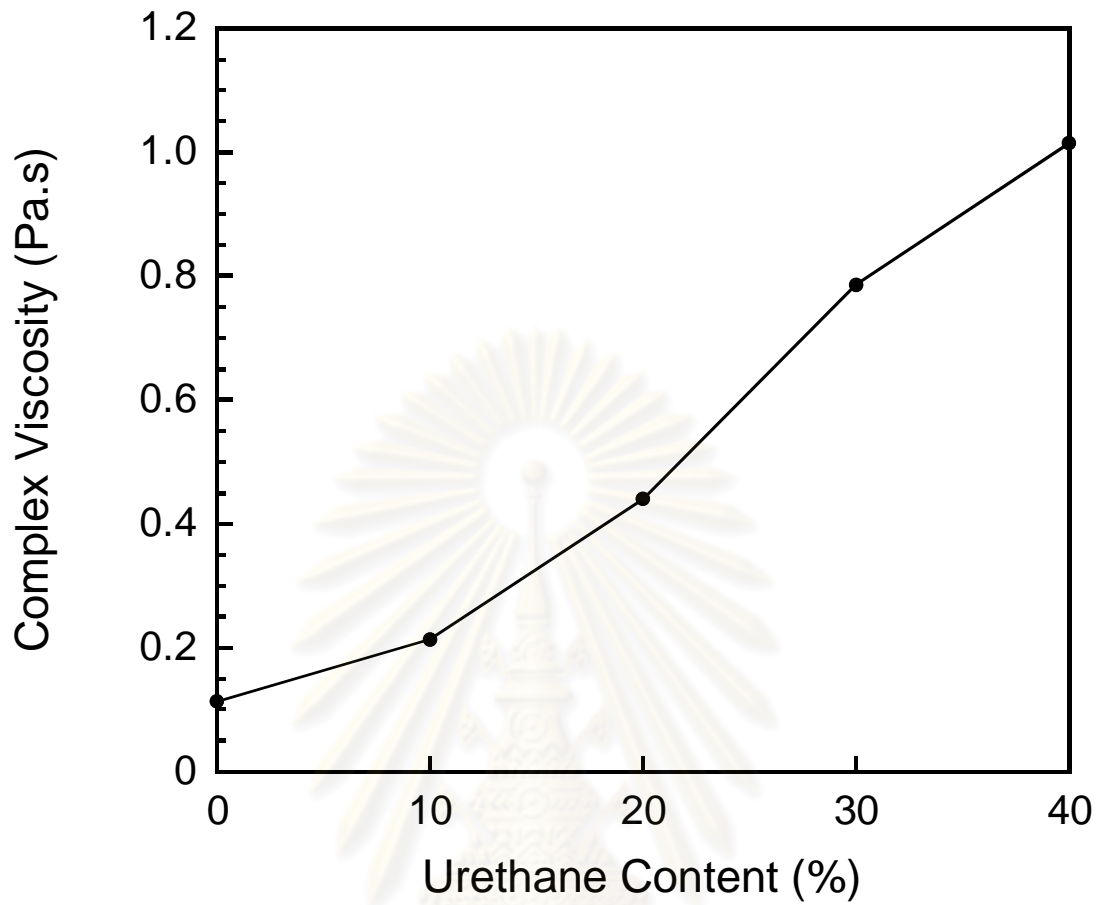


Figure 5.5 Effect of urethane content on viscosity of BA-a/PU resins determined at 120°C.

ศูนย์วิทยทรัพยากร
จุฬาลงกรณ์มหาวิทยาลัย

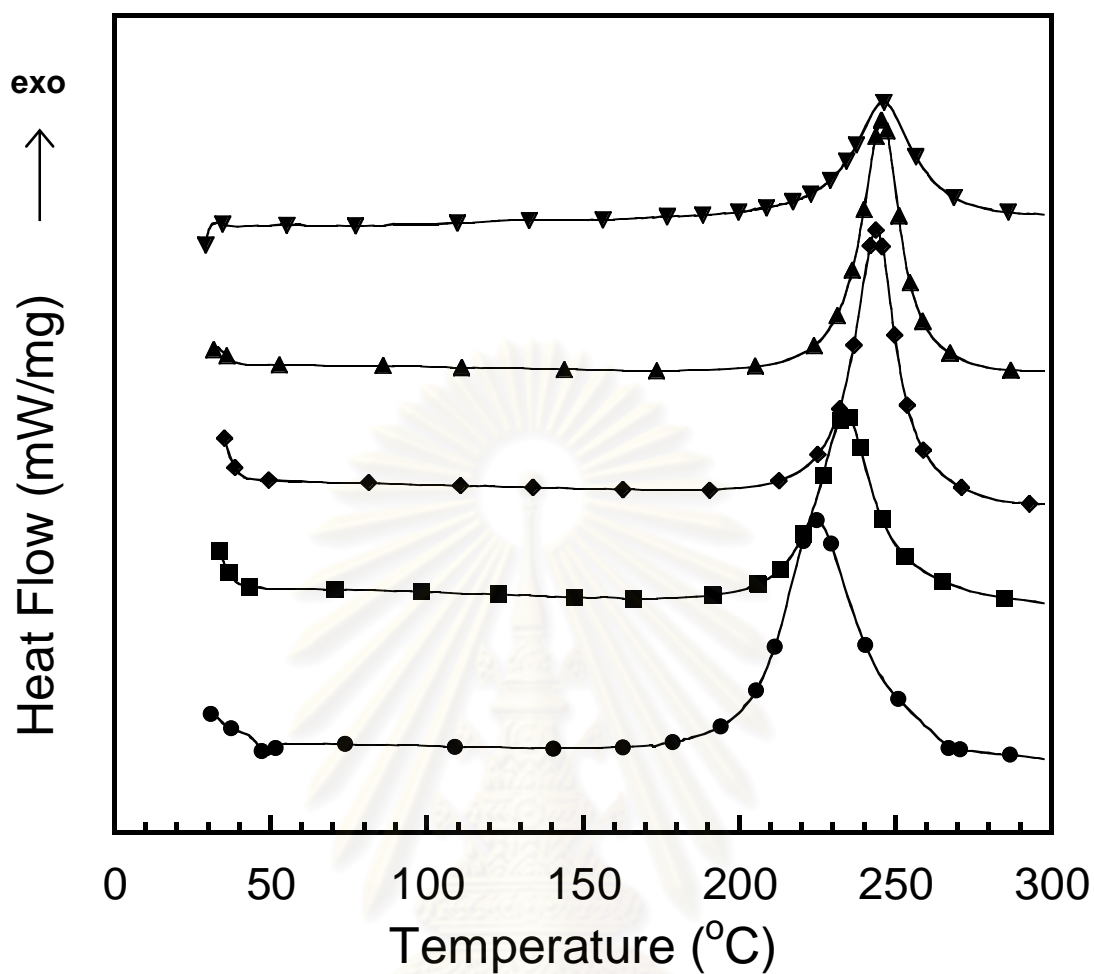


Figure 5.6 DSC thermograms of BA-a/PU resin at various compositions :

- (●) BA-a/PU 100/0, (■) BA-a/PU 90/10, (◆) BA-a/PU 80/20, (▲) BA-a/PU 70/30
and (▼) BA-a/PU 60/40.

ศูนย์วิทยทรัพยากร
จุฬาลงกรณ์มหาวิทยาลัย

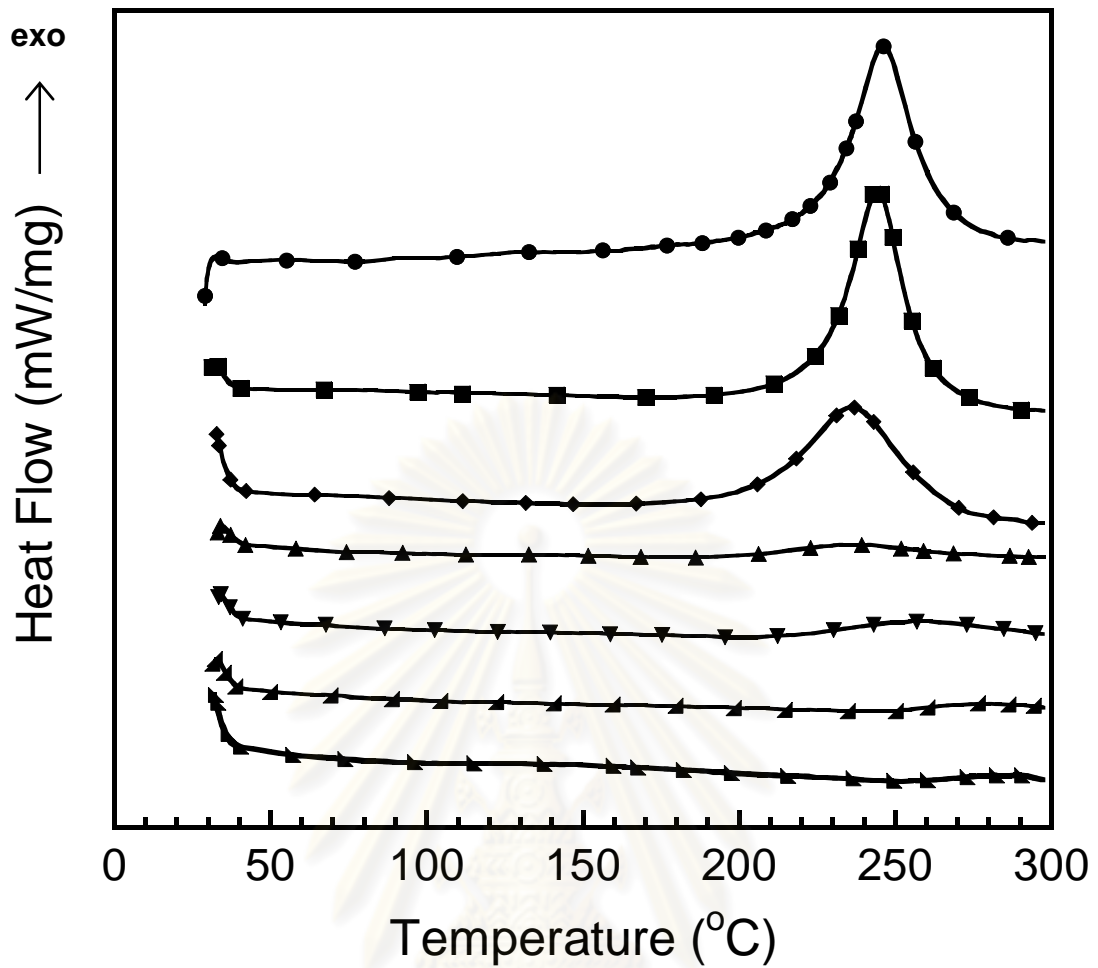


Figure 5.7 DSC thermograms of BA-a/PU 60/40 at various curing conditions :

(●) uncured, (■) 150°C/1h, (◆) 170°C/1h, (▲) 180°C/1h, (▼) 190°C/1h, (◄) 200°C/1h
and (►) 200°C/2h.

ศูนย์วิทยทรัพยากร
จุฬาลงกรณ์มหาวิทยาลัย

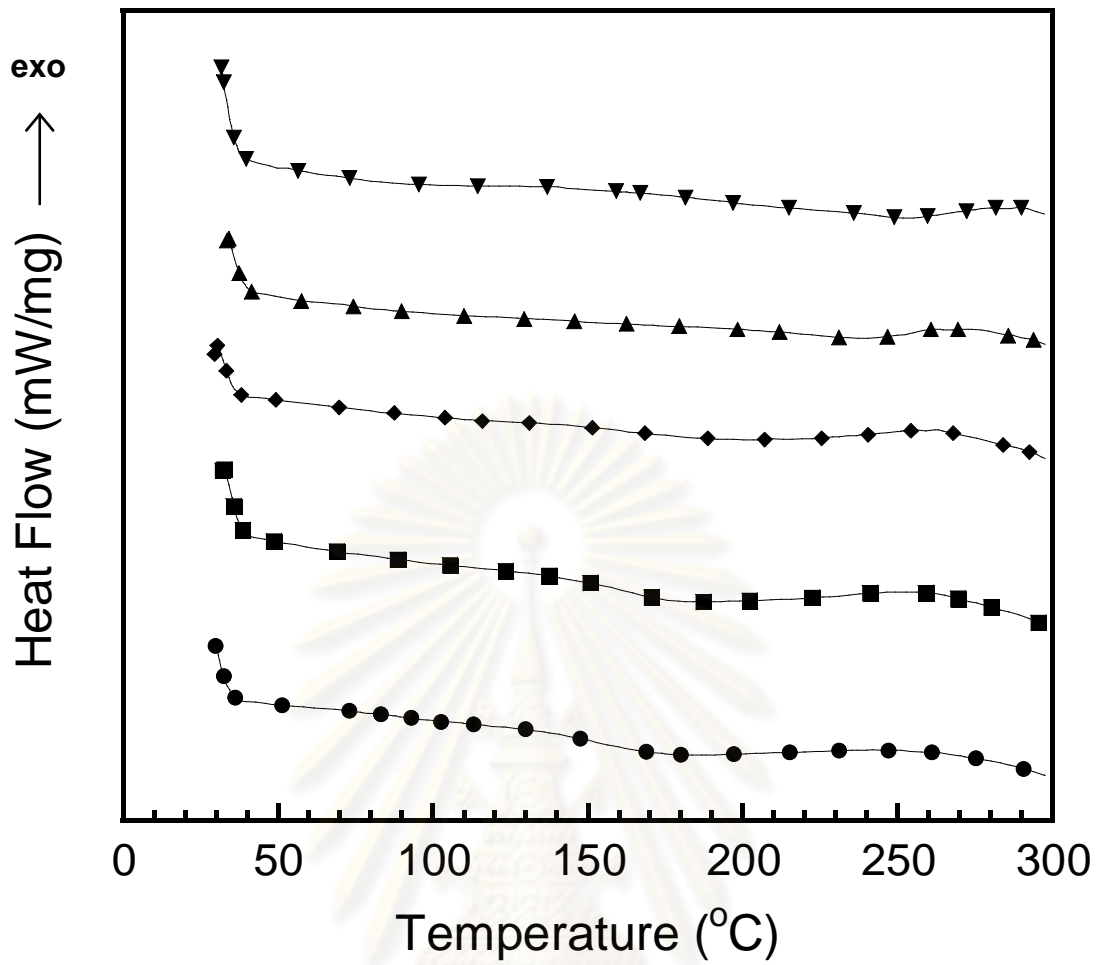


Figure 5.8 DSC thermograms showing glass-transition temperature of BA-a/PU alloys at various compositions : (●) BA-a/PU 100/0, (■) BA-a/PU 90/10, (◆) BA-a/PU 80/20, (▲) BA-a/PU 70/30 and (▼) BA-a/PU 60/40.

ศูนย์วิทยทรัพยากร
จุฬาลงกรณ์มหาวิทยาลัย

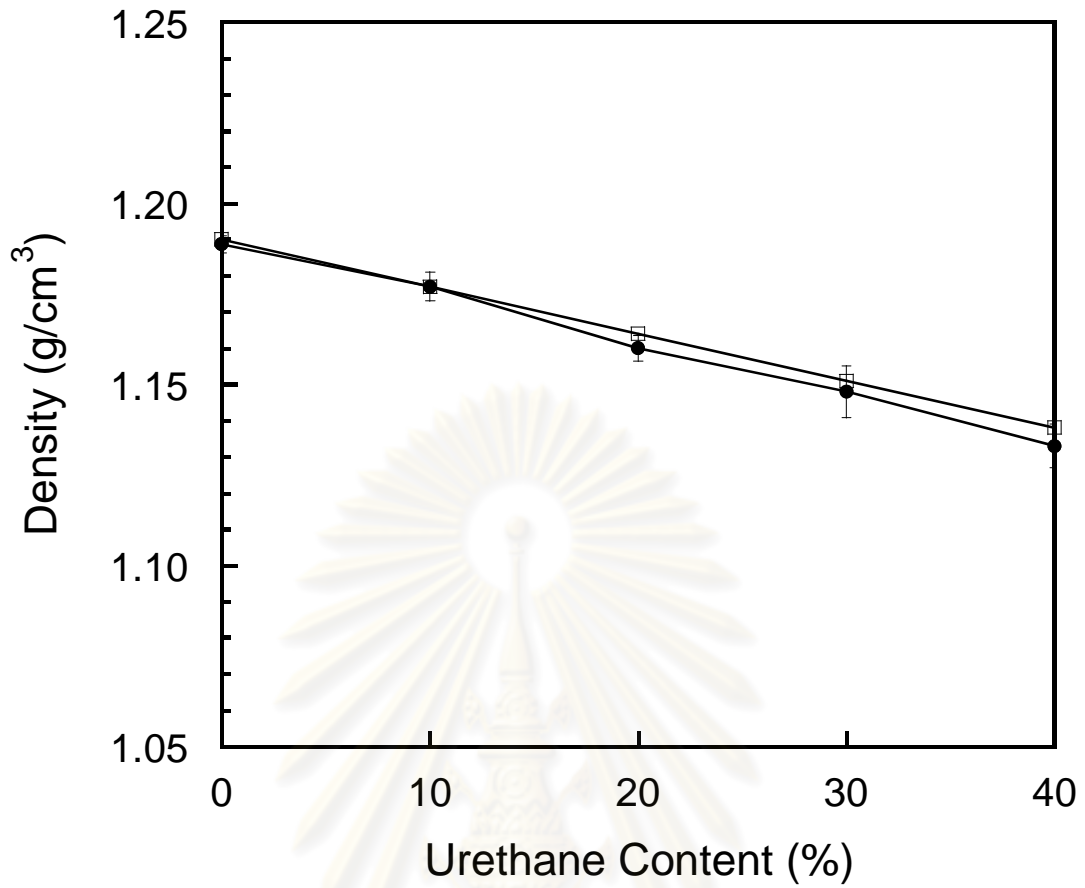


Figure 5.9 Density of BA-a/PU alloys at various PU compositions :

(□) Theory density and (●) Actual density.

ศูนย์วิทยทรัพยากร
จุฬาลงกรณ์มหาวิทยาลัย

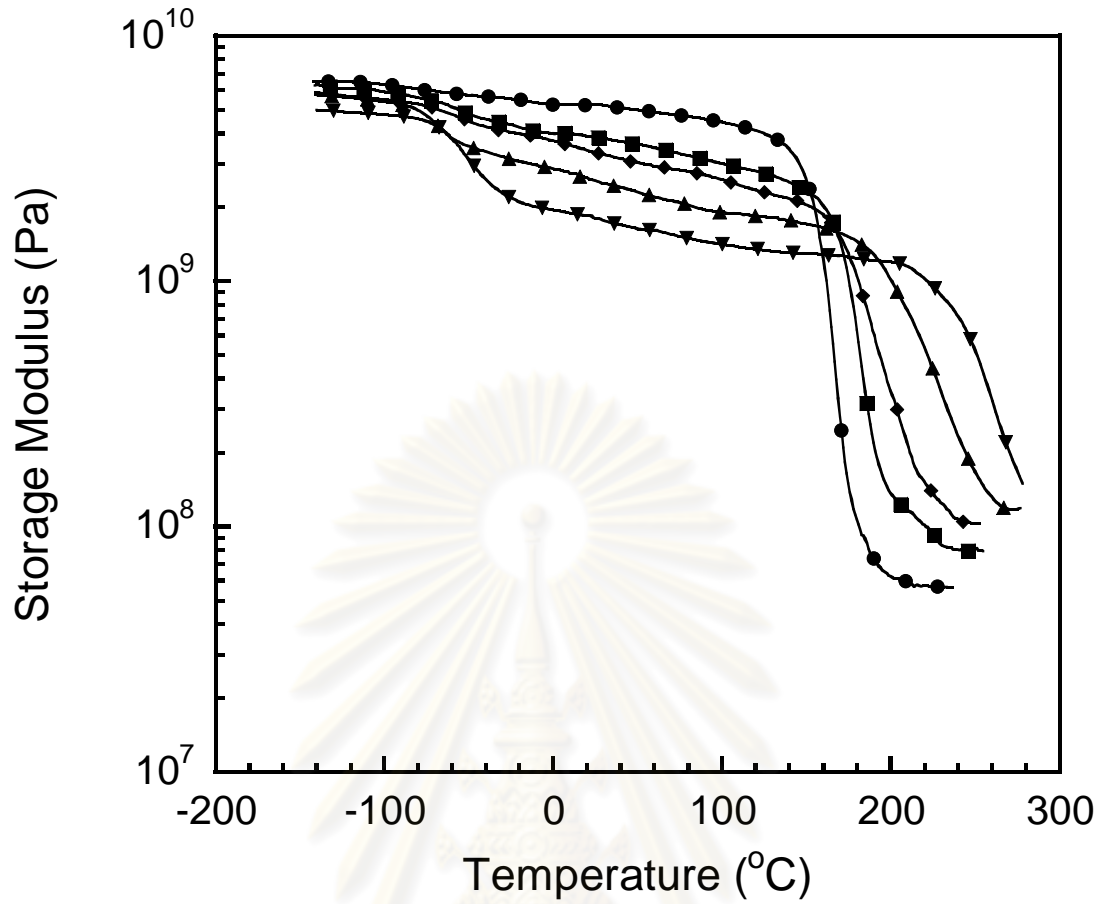


Figure 5.10 Storage modulus of BA-a/PU alloys at various PU compositions : (●) BA-a/PU 100/0, (■) BA-a/PU 90/10, (◆) BA-a/PU 80/20, (▲) BA-a/PU 70/30 and (▼) BA-a/PU 60/40.

ศูนย์วิทยทรัพยากร
จุฬาลงกรณ์มหาวิทยาลัย

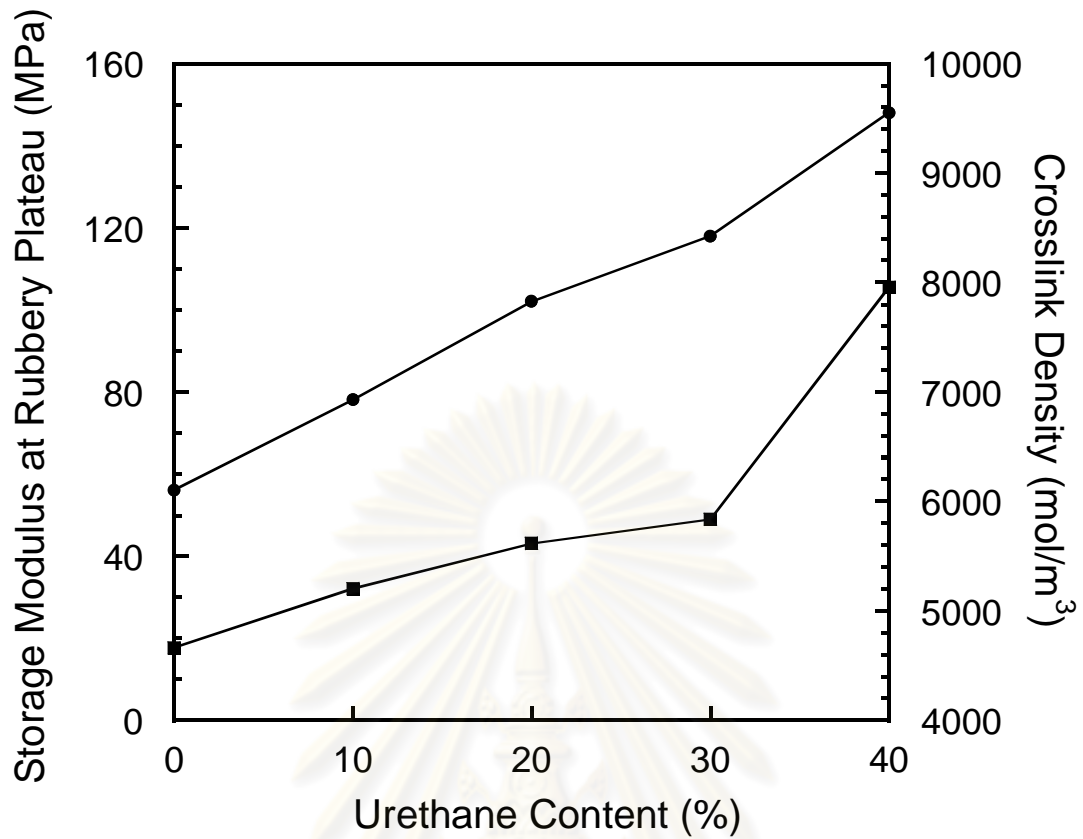


Figure 5.11 Storage modulus at rubbery plateau and crosslink density of BA-a/PU alloys at various PU compositions : (●) Storage modulus at rubbery plateau, (■) Crosslink density.

ศูนย์วิทยทรัพยากร
จุฬาลงกรณ์มหาวิทยาลัย

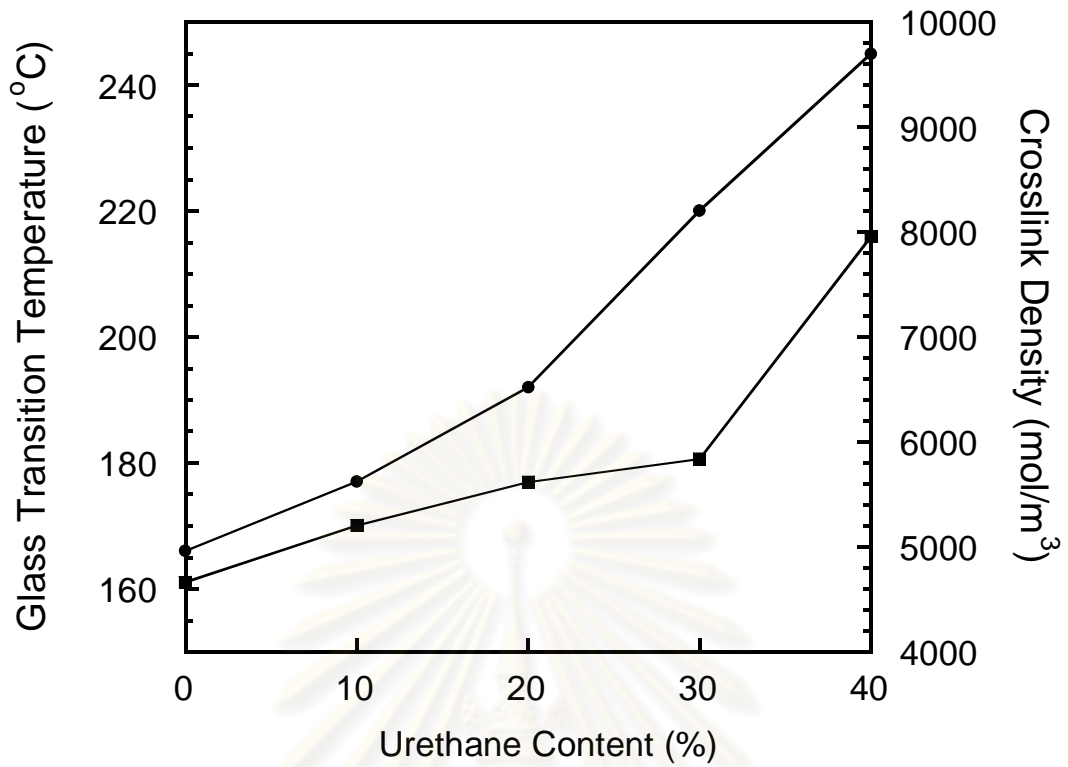


Figure 5.12 Glass transition temperature and the crosslink density of BA-a/PU alloys at various PU compositions : (●) Glass transition temperature, (■) Crosslink density.

ศูนย์วิทยทรัพยากร
จุฬาลงกรณ์มหาวิทยาลัย

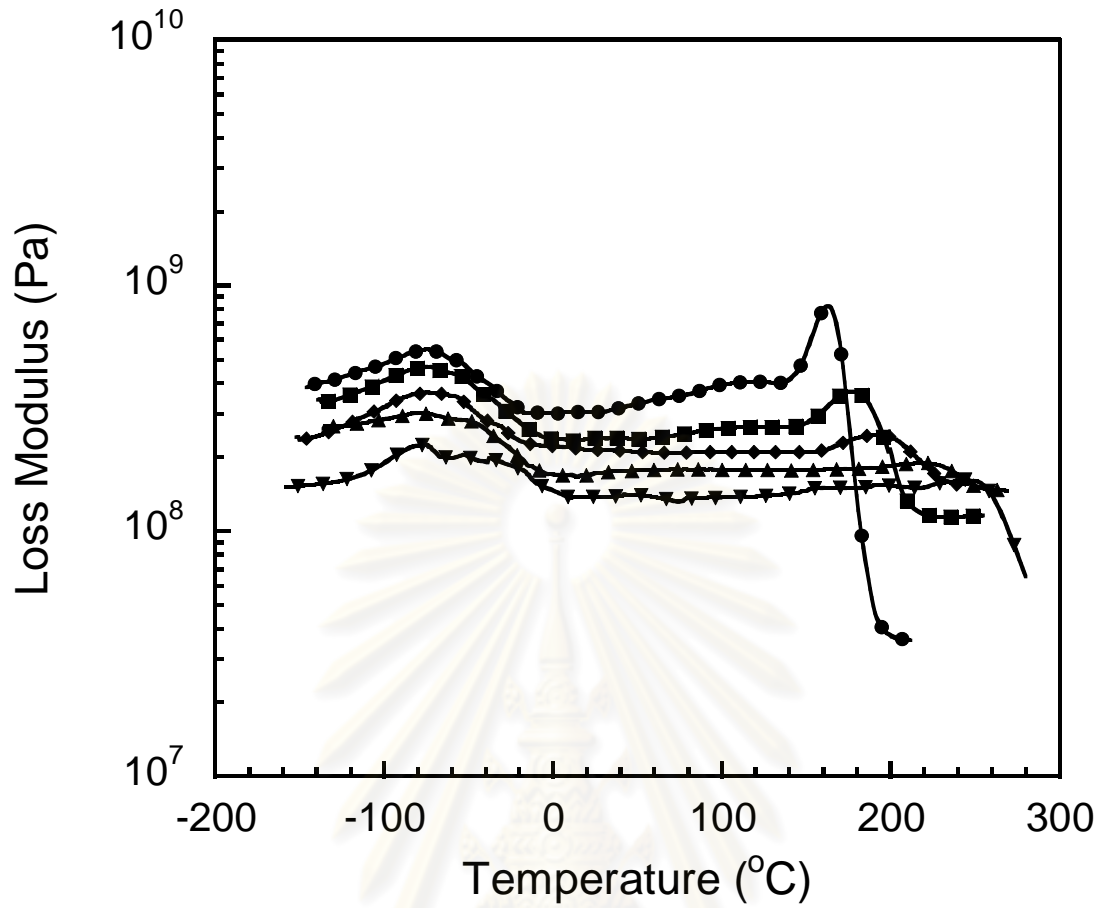


Figure 5.13 Loss modulus of BA-a/PU alloys at various compositions : (●) BA-a/PU 100/0, (■) BA-a/PU 90/10, (◆) BA-a/PU 80/20, (▲) BA-a/PU 70/30 and (▼) BA-a/PU 60/40.

ศูนย์วิทยทรัพยากร
จุฬาลงกรณ์มหาวิทยาลัย

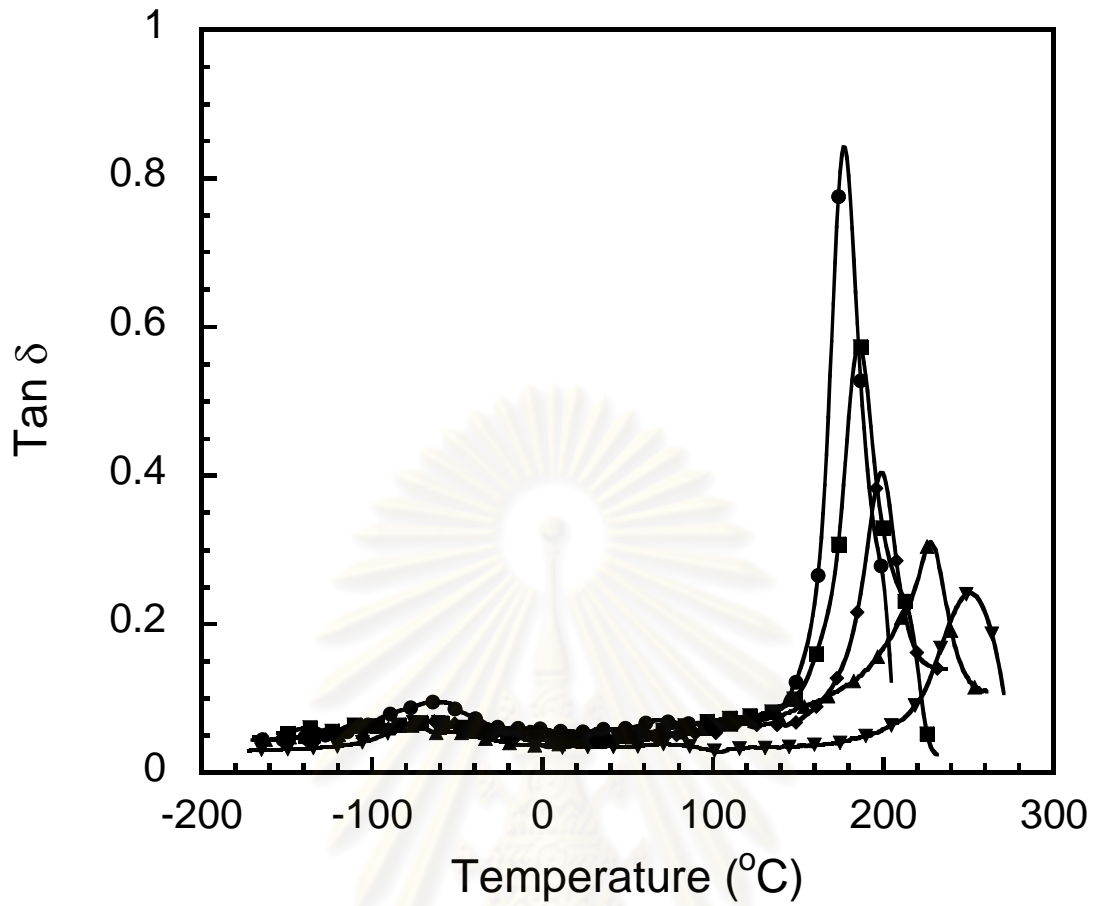


Figure 5.14 Tan δ of BA-a/PU alloys at various compositions : (●) BA-a/PU 100/0, (■) BA-a/PU 90/10, (◆) BA-a/PU 80/20, (▲) BA-a/PU 70/30 and (▼) BA-a/PU 60/40.

ศูนย์วิทยทรัพยากร
จุฬาลงกรณ์มหาวิทยาลัย

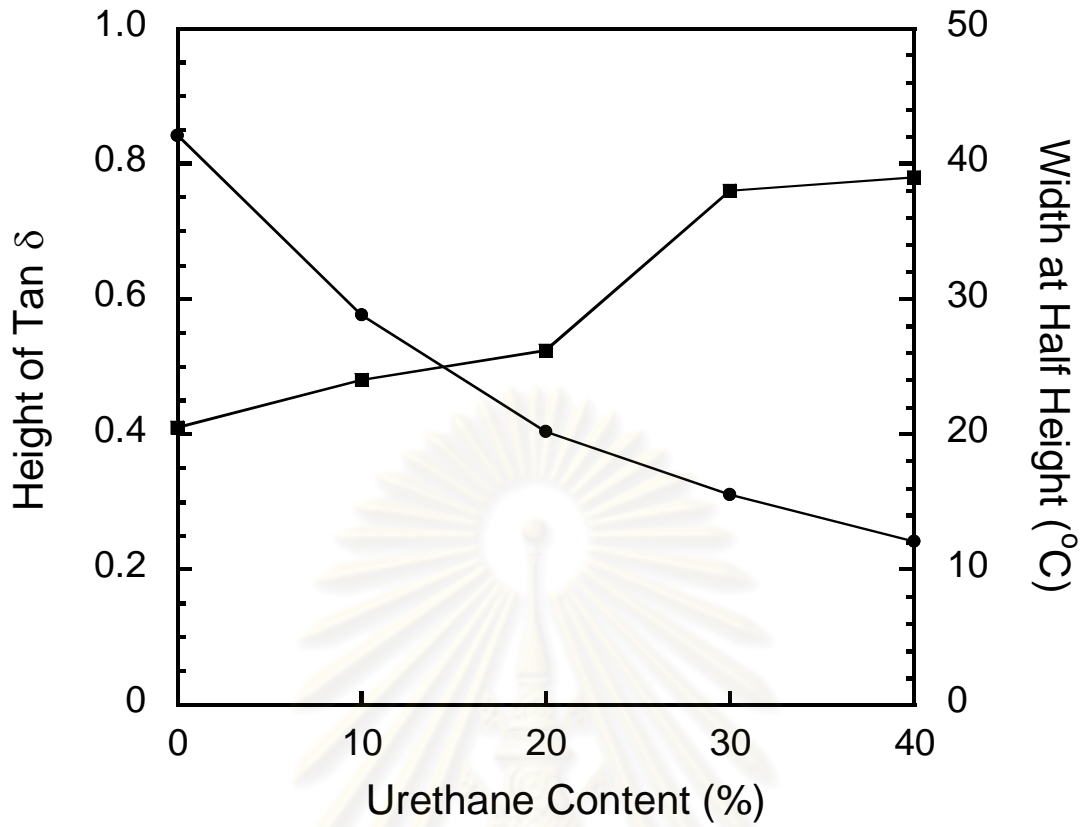


Figure 5.15 Height of Tan δ and width at half of BA-a/PU alloys at various PU compositions :

(●) Height of Tan δ , (■) Width at half.

ศูนย์วิทยทรัพยากร
จุฬาลงกรณ์มหาวิทยาลัย

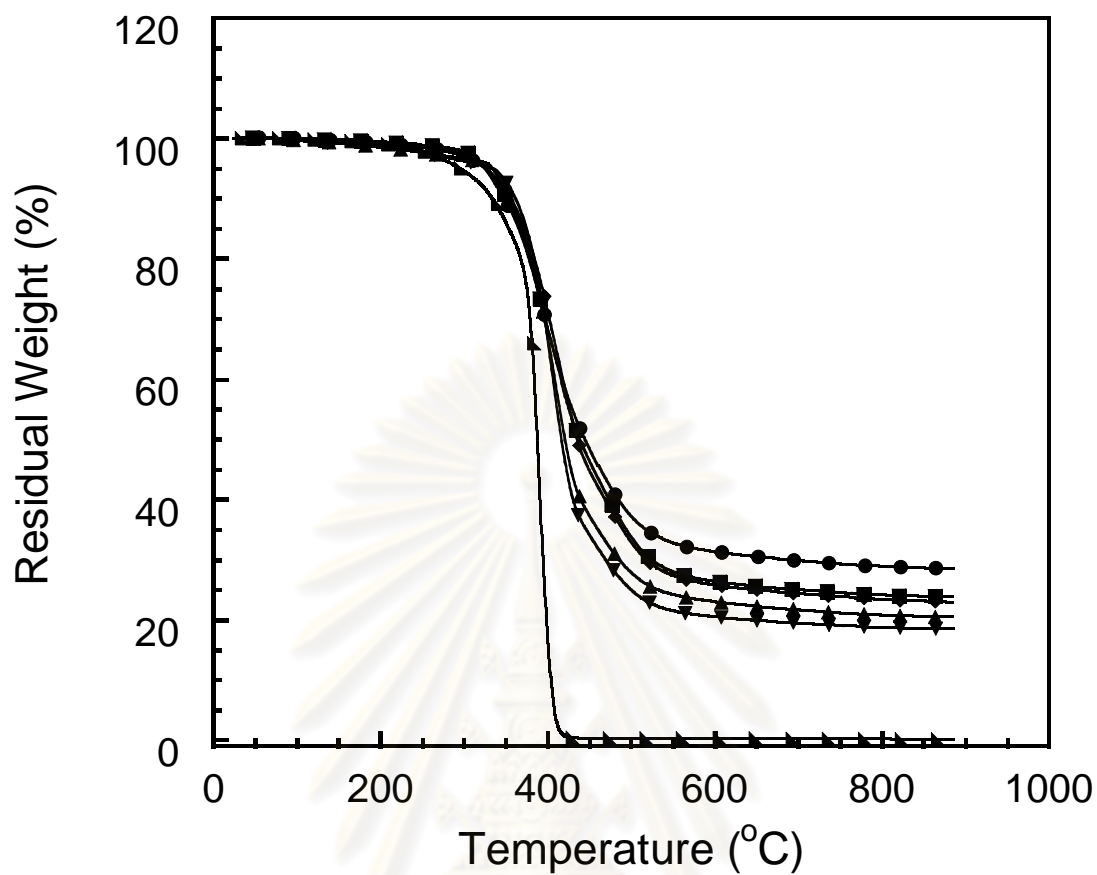


Figure 5.16 Thermal degradation of BA-a/PU alloys at various compositions :

(●) BA-a/PU 100/0, (■) BA-a/PU 90/10, (◆) BA-a/PU 80/20, (▲) BA-a/PU 70/30 and (▼) BA-a/PU 60/40 and (▴) Polyurethane.

ศูนย์วิทยทรัพยากร
จุฬาลงกรณ์มหาวิทยาลัย

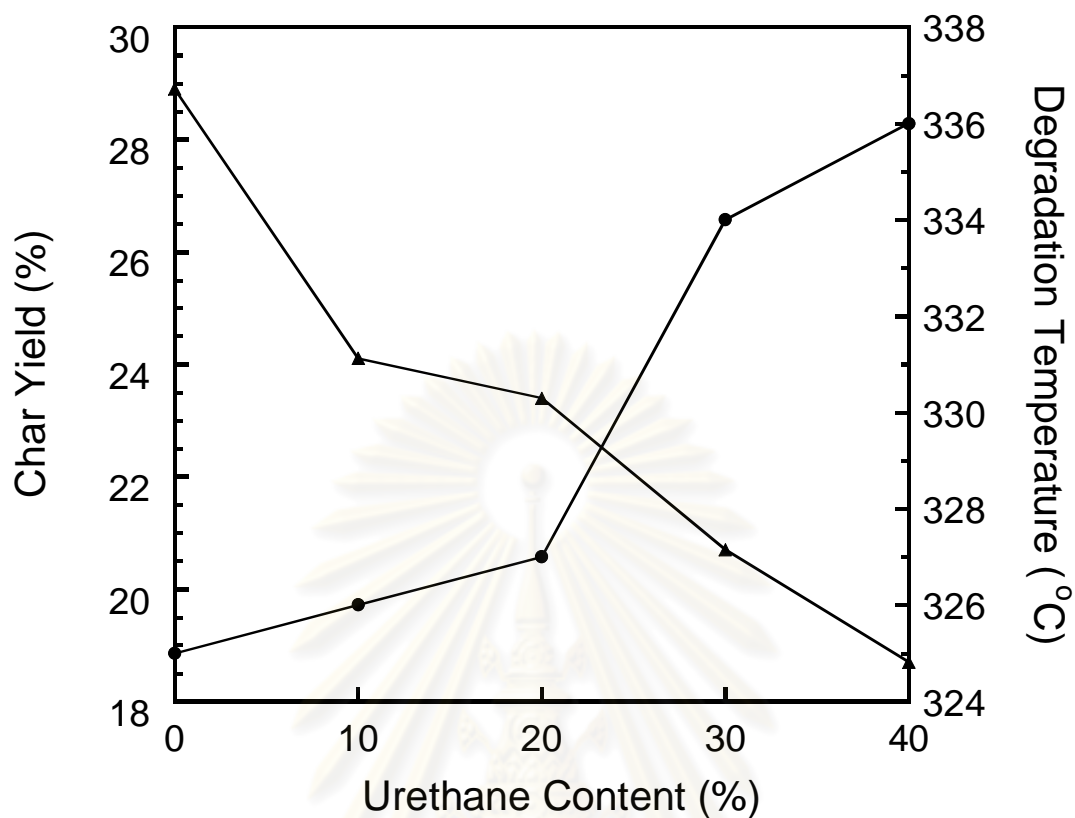


Figure 5.17 Thermal degradation of BA-a/PU alloys at various PU compositions :

(▲) Char yield and (●) Degradation temperature.

ศูนย์วิทยทรัพยากร
จุฬาลงกรณ์มหาวิทยาลัย

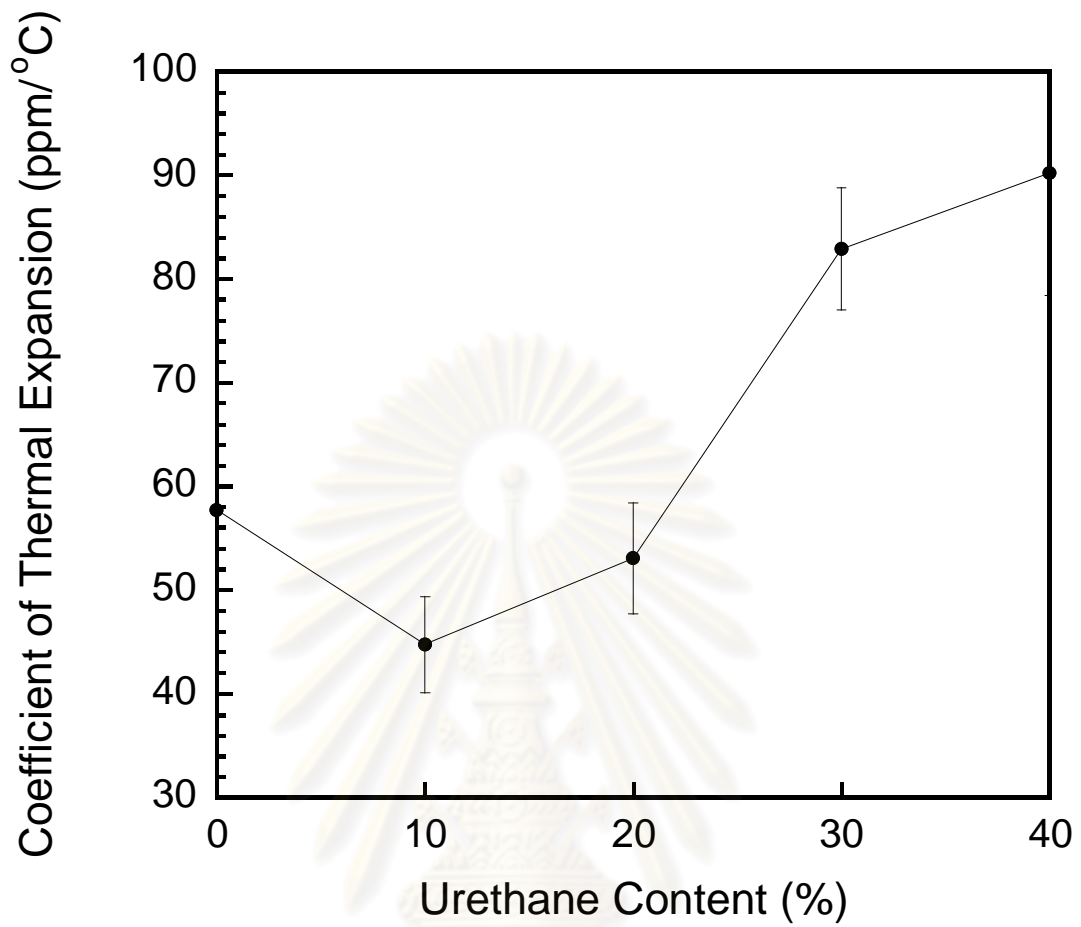


Figure 5.18 Effect of urethane content on coefficient of thermal expansion of BA-a/PU alloys at various PU compositions.

ศูนย์วิทยทรัพยากร
จุฬาลงกรณ์มหาวิทยาลัย

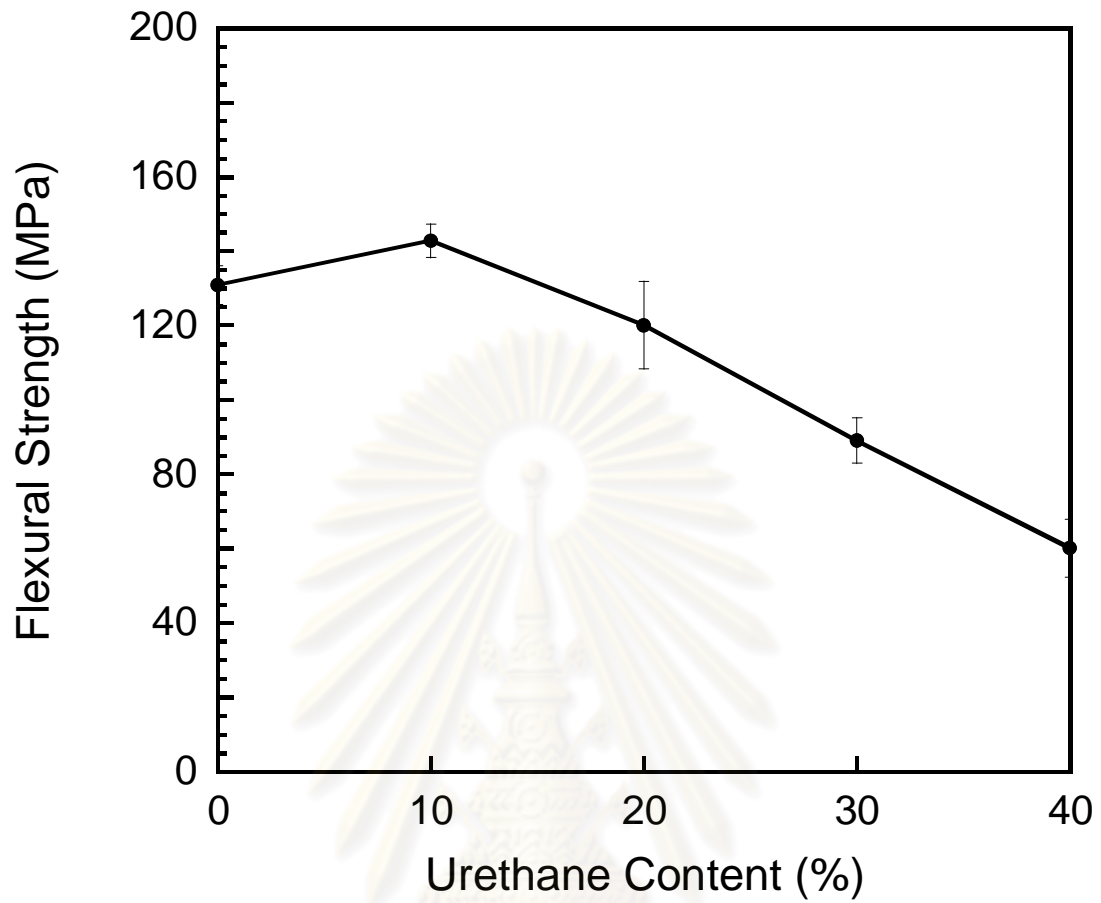


Figure 5.19 Effect of urethane content on flexural PU strength of BA-a/PU alloys at various compositions.

ศูนย์วิทยทรัพยากร
จุฬาลงกรณ์มหาวิทยาลัย

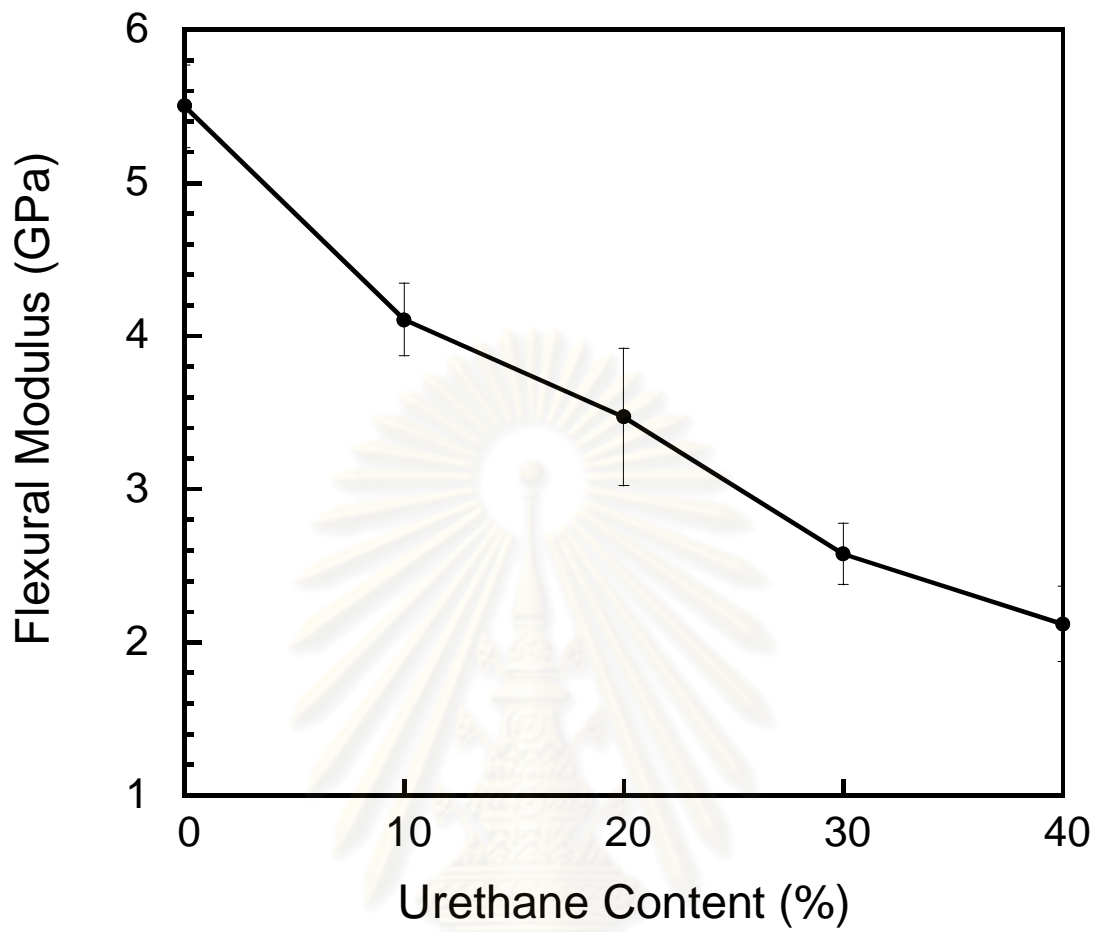


Figure 5.20 Effect of urethane content on flexural modulus of BA-a/PU alloys at various PU compositions.

ศูนย์วิทยทรัพยากร
จุฬาลงกรณ์มหาวิทยาลัย

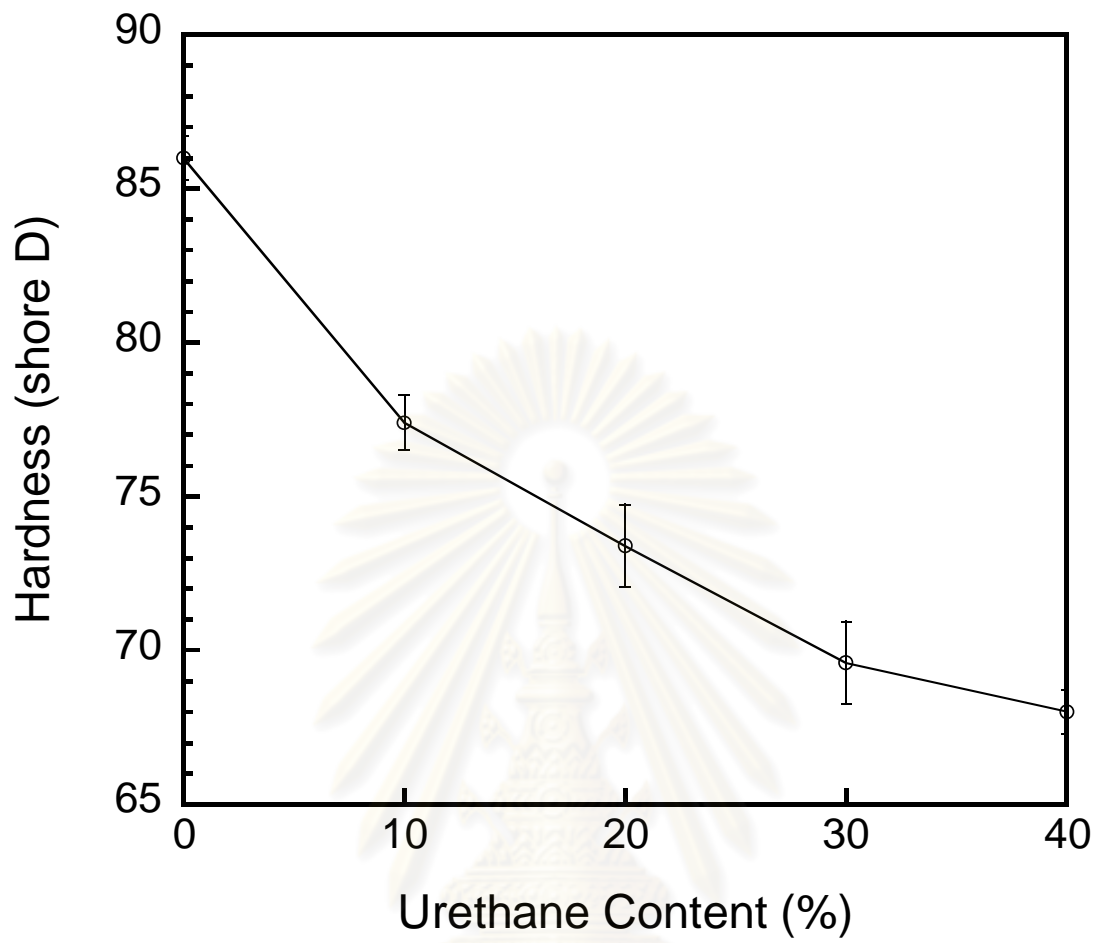


Figure 5.21 Effect of urethane content on surface hardness of BA-a/PU alloys at various PU compositions.

ศูนย์วิทยทรัพยากร
จุฬาลงกรณ์มหาวิทยาลัย

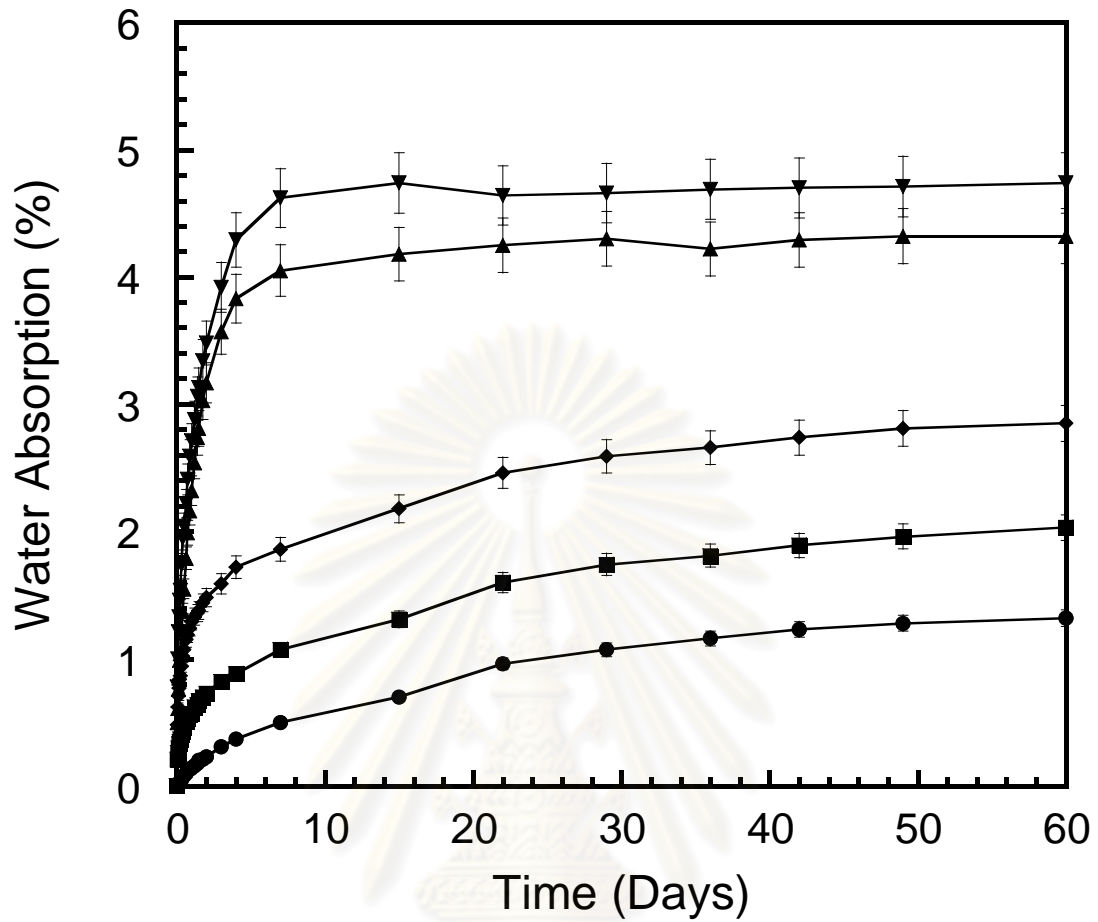


Figure 5.22 Percentage water absorption of BA-a/PU alloys at various PU compositions :

(●) BA-a/PU 100/0, (■) BA-a/PU 90/10, (◆) BA-a/PU 80/20, (▲) BA-a/PU 70/30
and (▼) BA-a/PU 60/40.

ศูนย์วิทยทรัพยากร
จุฬาลงกรณ์มหาวิทยาลัย

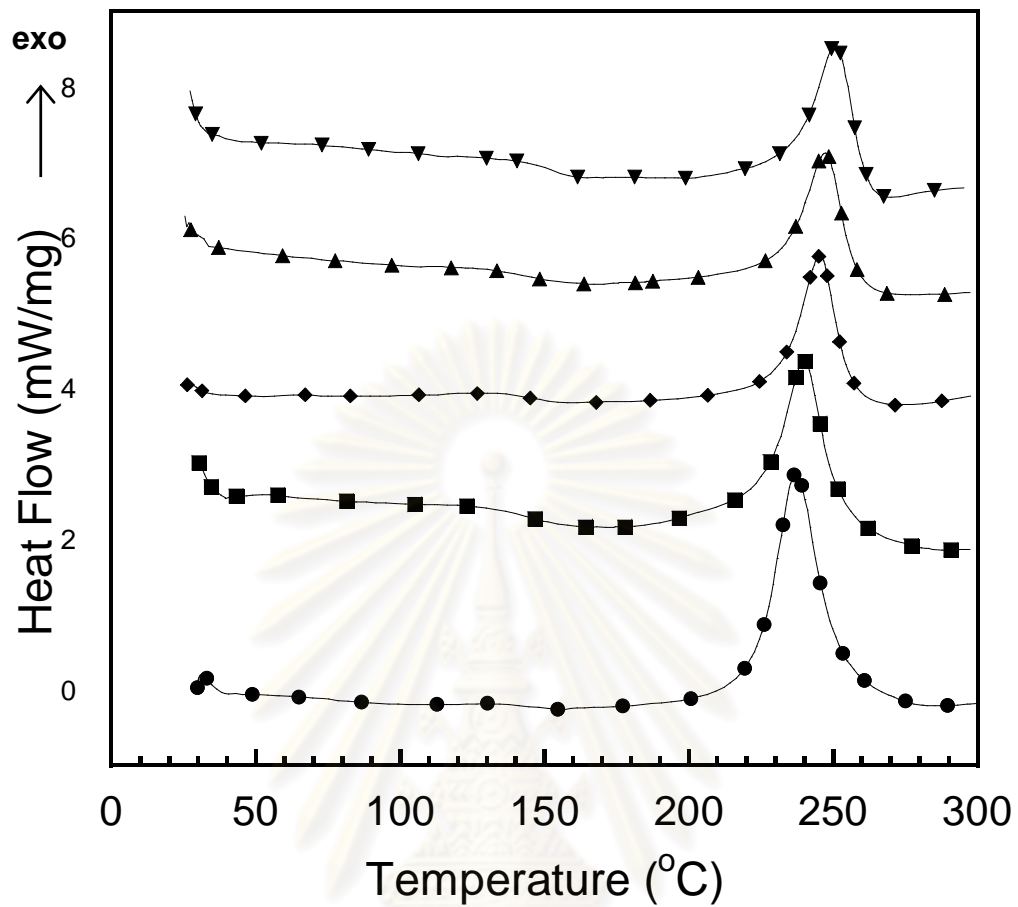


Figure 5.23 DSC thermograms of Zylon fiber composites at various PU compositions in the BA-a/PU alloys : (●) BA-a/PU 100/0, (■) BA-a/PU 90/10, (◆) BA-a/PU 80/20, (▲) BA-a/PU 70/30 and (▼) BA-a/PU 60/40.

ศูนย์วิทยทรัพยากร
จุฬาลงกรณ์มหาวิทยาลัย

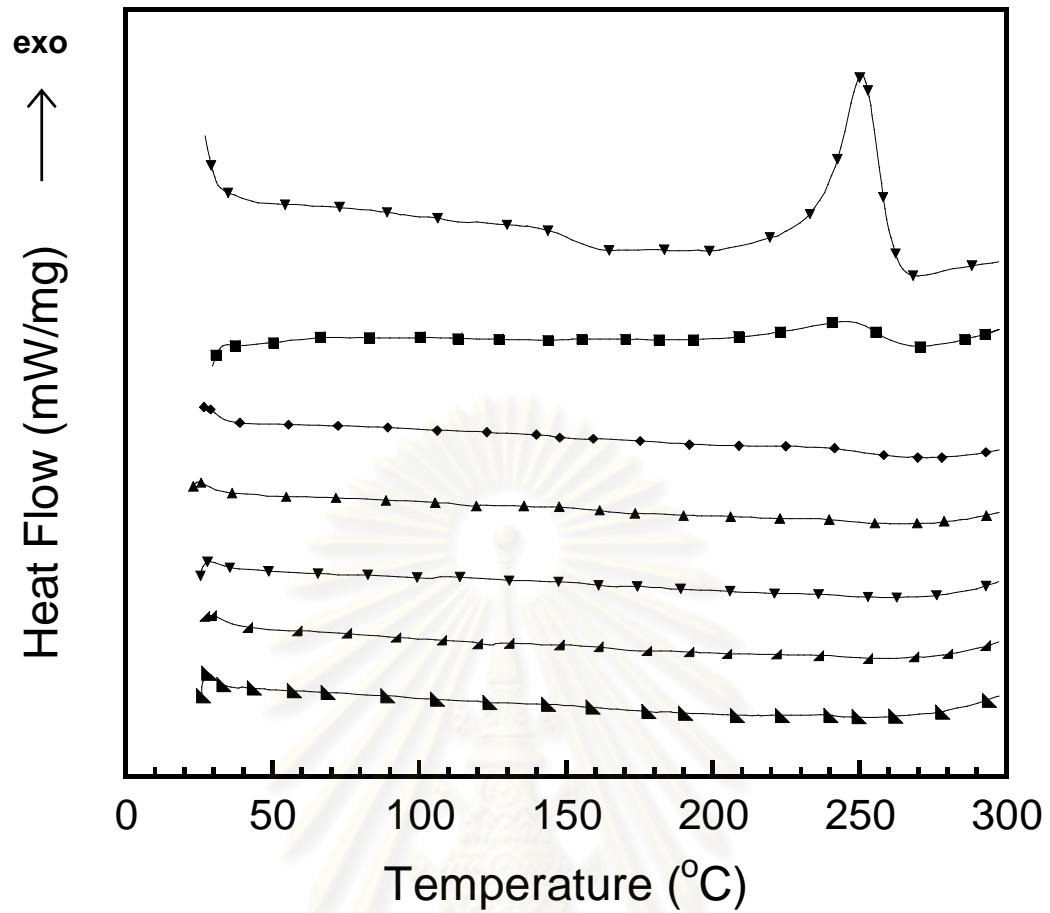


Figure 5.24 DSC thermograms of Zylon fiber composites at various curing conditions :

(●) uncured, (■) 150°C/1h, (◆) 170°C/1h, (▲) 180°C/1h, (▼) 190°C/1h,
 (▲) 200°C/1h and (▲) 200°C/2h.

ศูนย์วิทยทรัพยากร
 จุฬาลงกรณ์มหาวิทยาลัย

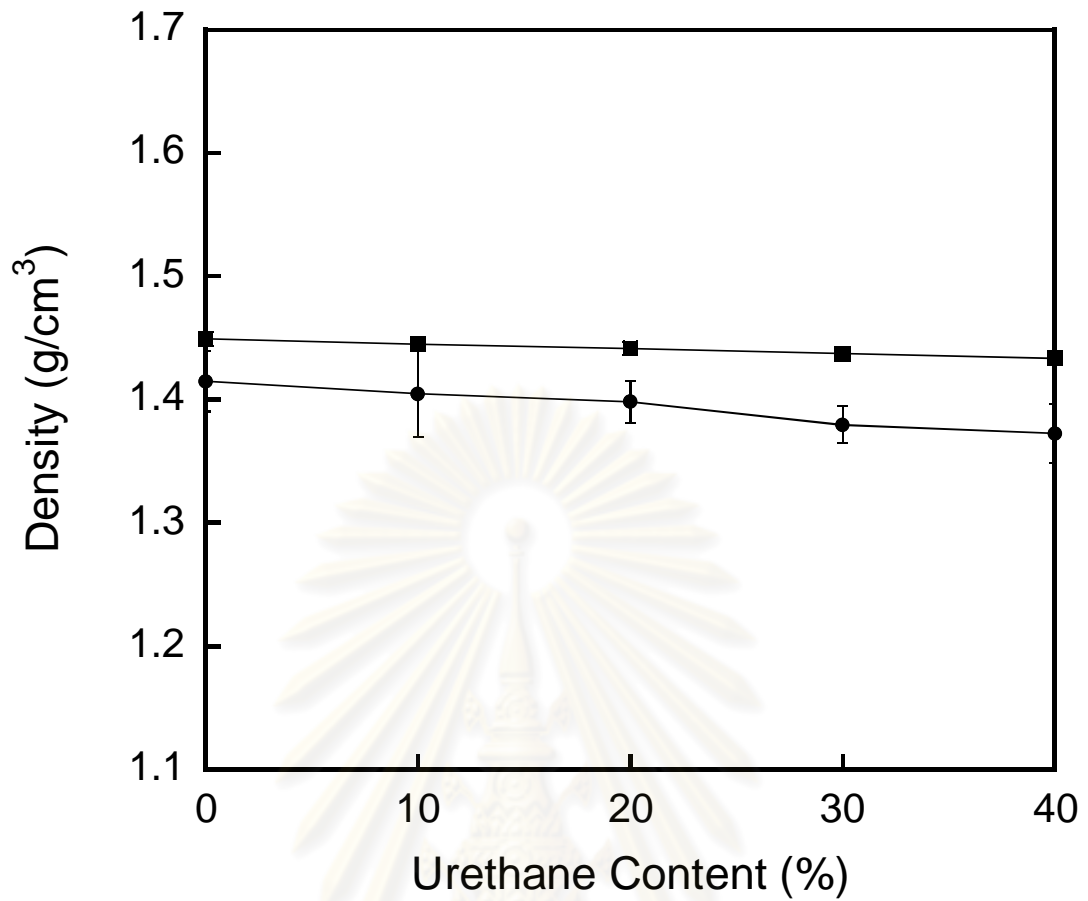


Figure 5.25 Density of Zylon fiber at various compositions :

(■) Theory density and (●) Actual density.

ศูนย์วิทยทรัพยากร
จุฬาลงกรณ์มหาวิทยาลัย

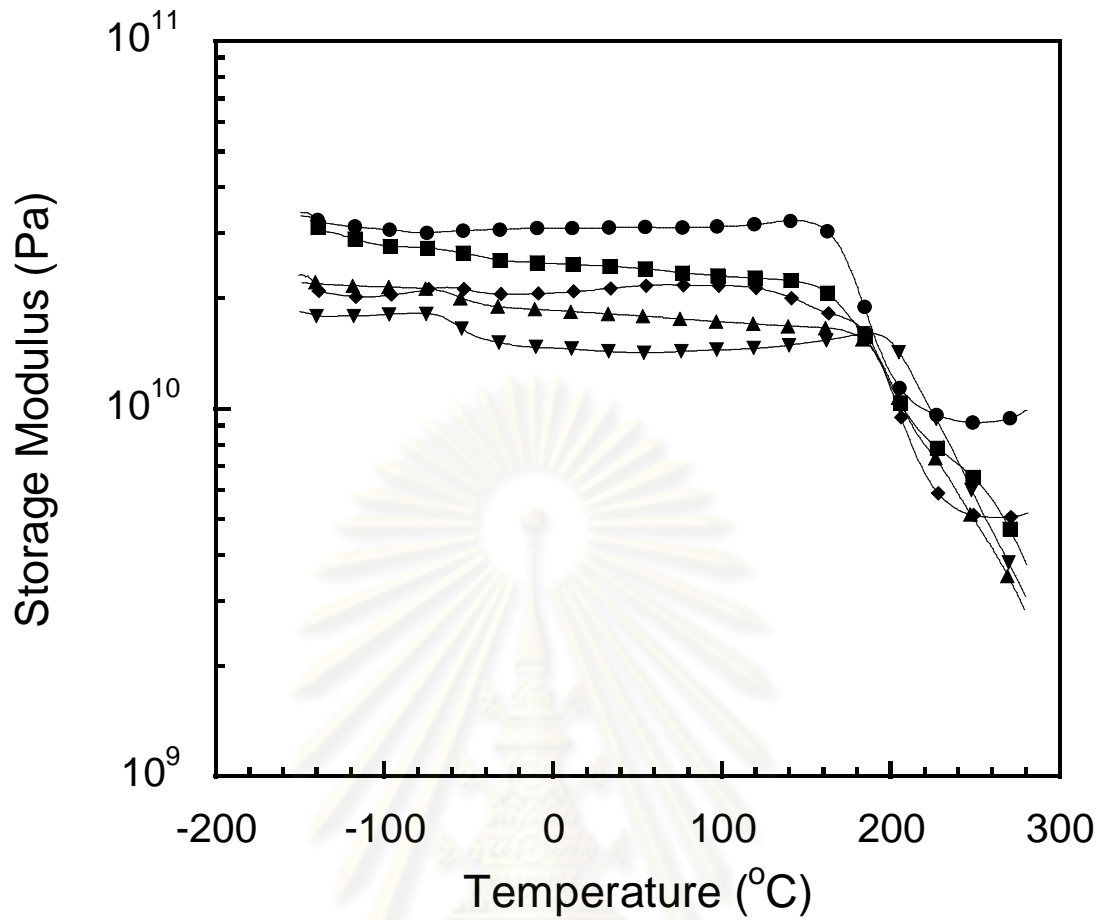


Figure 5.26 Storage modulus of Zylon fiber composites at various PU compositions in the BA-a/PU alloys : (●) BA-a/PU 100/0, (■) BA-a/PU 90/10, (◆) BA-a/PU 80/20, (▲) BA-a/PU 70/30 and (▼) BA-a/PU 60/40.

ศูนย์วิทยทรัพยากร
จุฬาลงกรณ์มหาวิทยาลัย

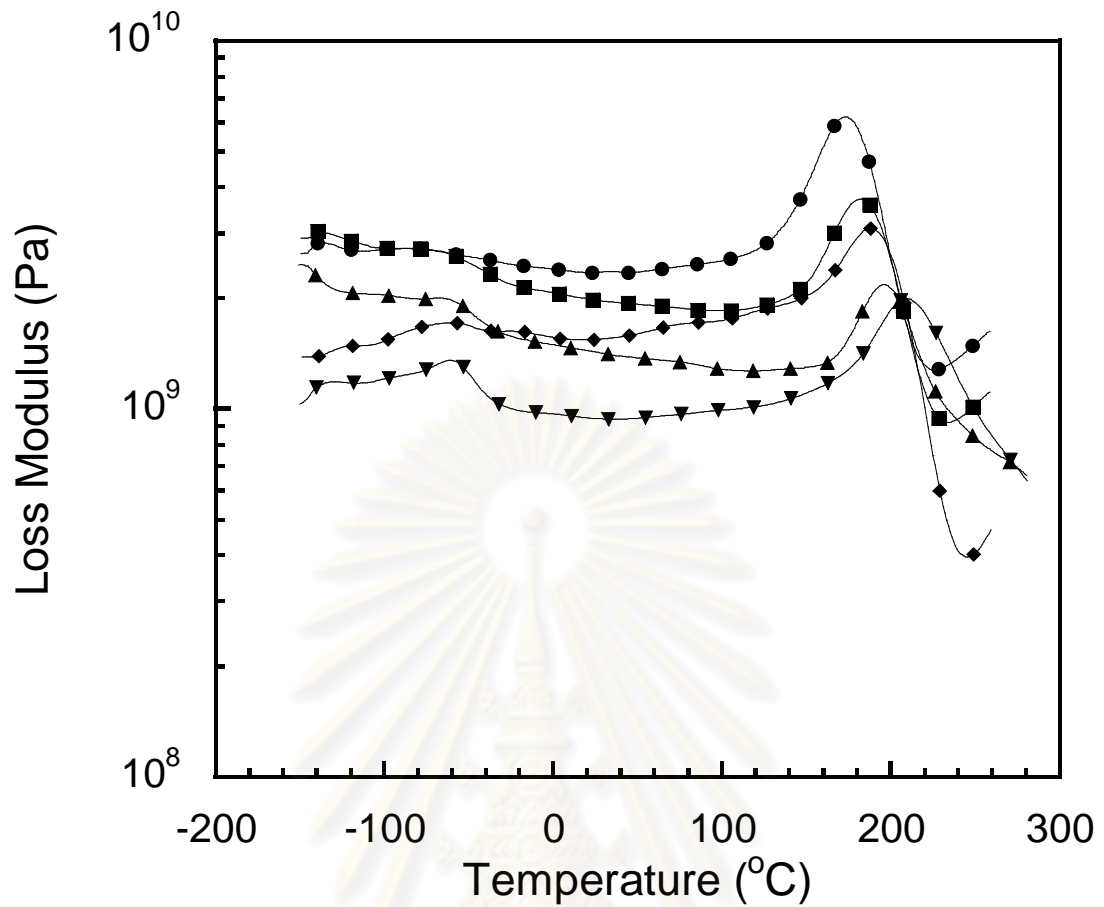


Figure 5.27 Loss modulus of Zylon fiber composites at various PU compositions in the BA-a/PU alloys : (●) BA-a/PU 100/0, (■) BA-a/PU 90/10, (◆) BA-a/PU 80/20, (▲) BA-a/PU 70/30 and (▼) BA-a/PU 60/40.

ศูนย์วิทยทรัพยากร
จุฬาลงกรณ์มหาวิทยาลัย

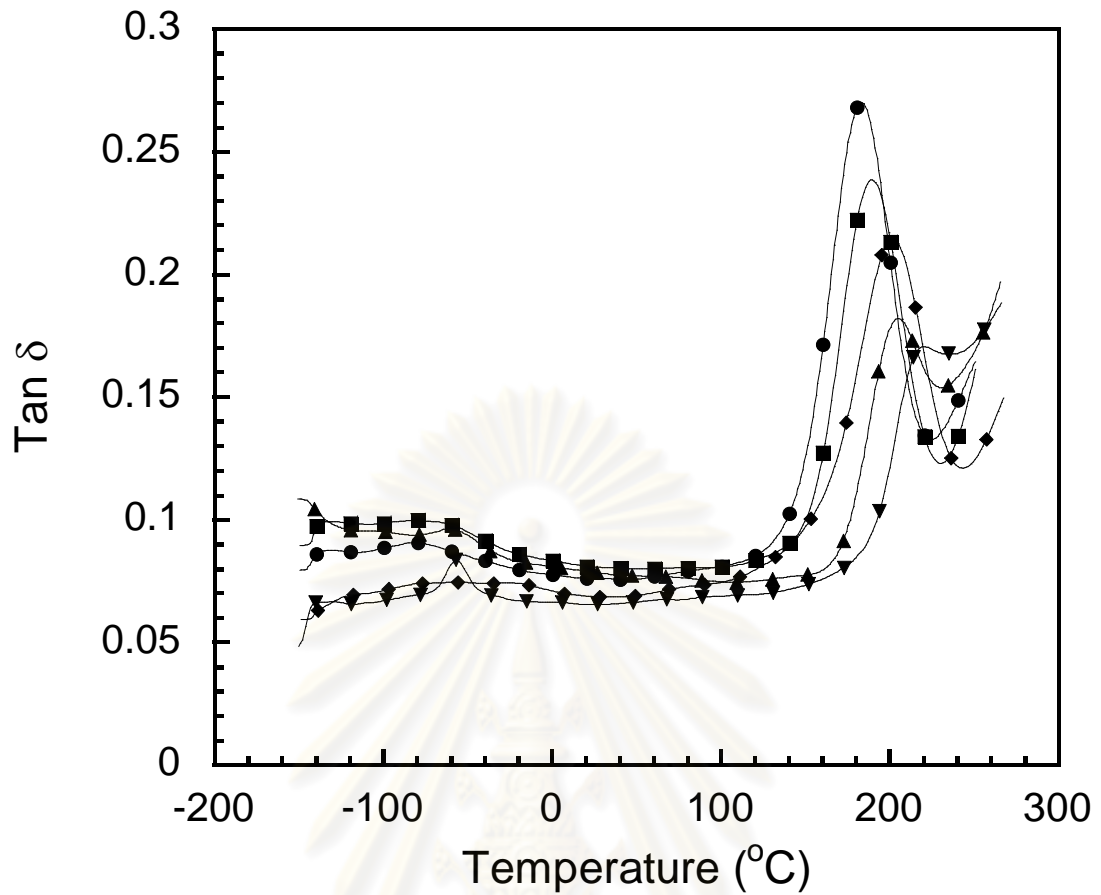


Figure 5.28 Tan δ of Zylon fiber composites at various PU compositions in the BA-a/PU alloys : (●) BA-a/PU 100/0, (■) BA-a/PU 90/10, (◆) BA-a/PU 80/20, (▲) BA-a/PU 70/30 and (▼) BA-a/PU 60/40.

ศูนย์วิทยทรัพยากร
จุฬาลงกรณ์มหาวิทยาลัย

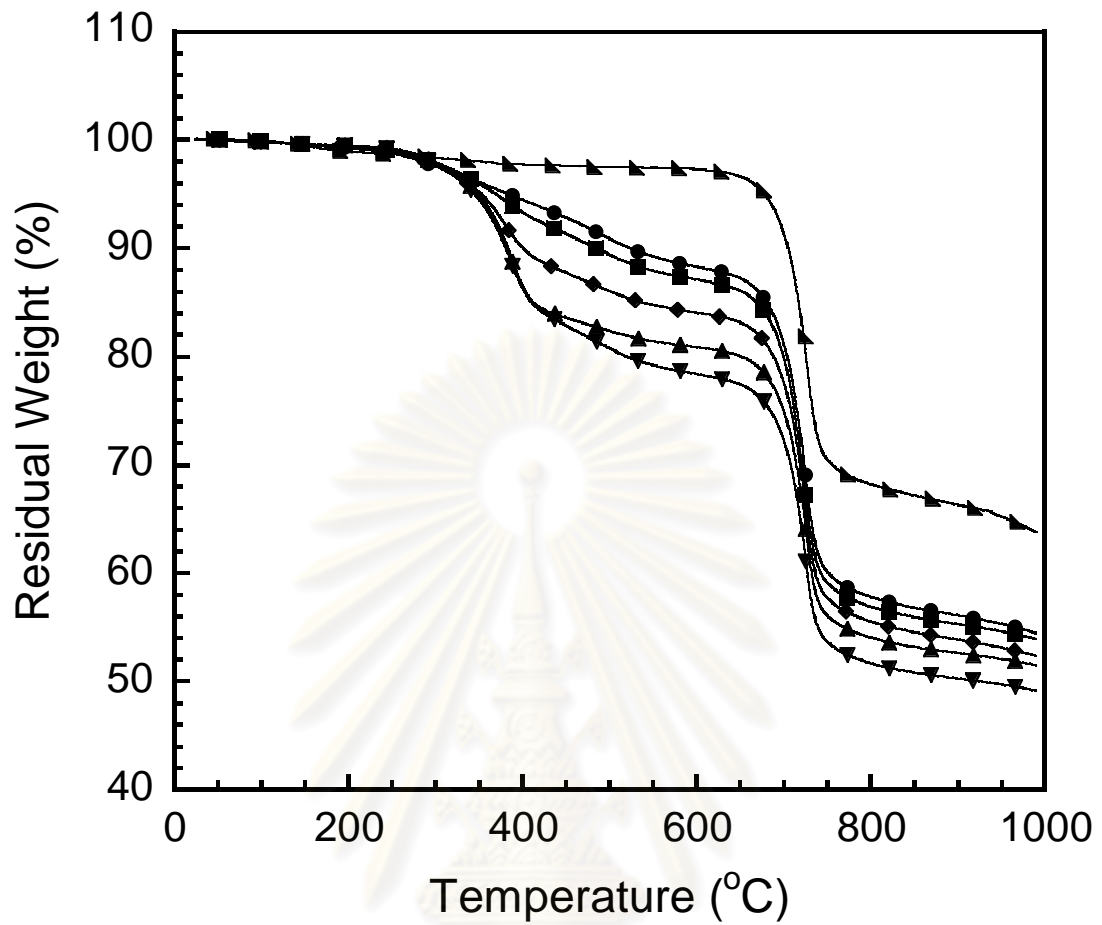


Figure 5.29 Thermal degradation of Zylon fiber composites at various PU compositions in the BA-a/PU alloys : (●) BA-a/PU 100/0, (■) BA-a/PU 90/10, (◆) BA-a/PU 80/20, (▲) BA-a/PU 70/30, (▼) BA-a/PU 60/40 and (▴) Zylon fiber.

ศูนย์วิทยทรัพยากร
จุฬาลงกรณ์มหาวิทยาลัย

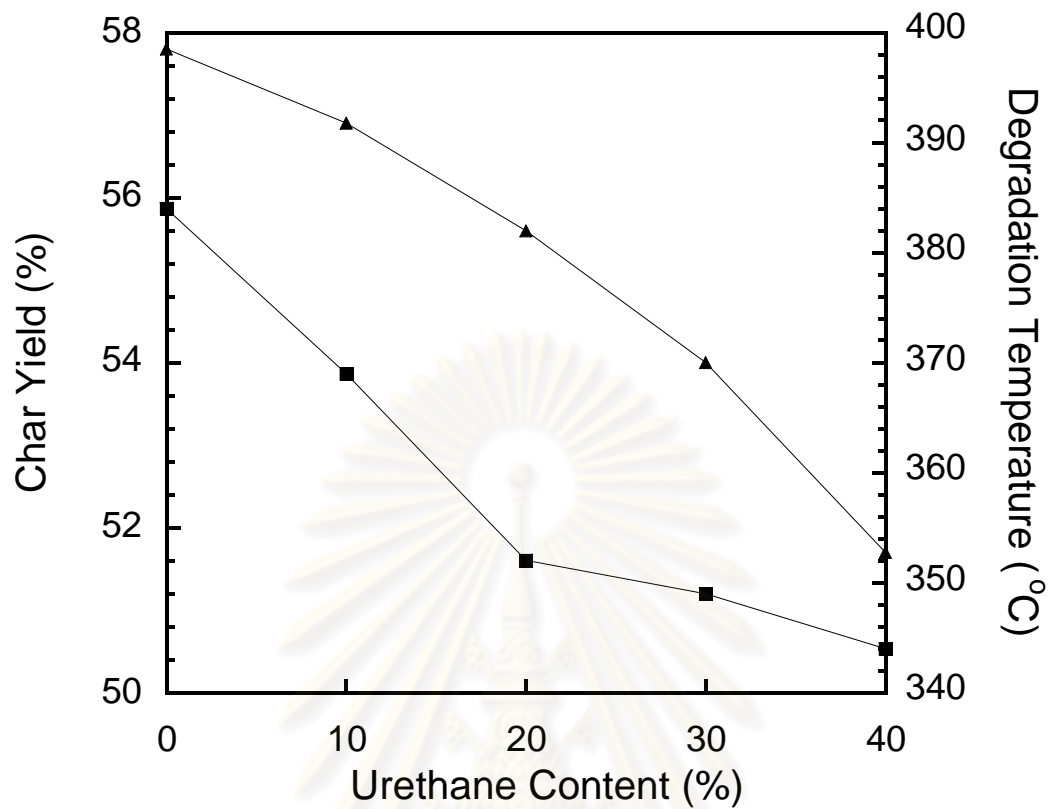


Figure 5.30 Thermal degradation of Zylon fiber composites at various PU compositions in the BA-a/PU alloys : (▲) Char yield and (■) Degradation temperature.

ศูนย์วิทยทรัพยากร
จุฬาลงกรณ์มหาวิทยาลัย

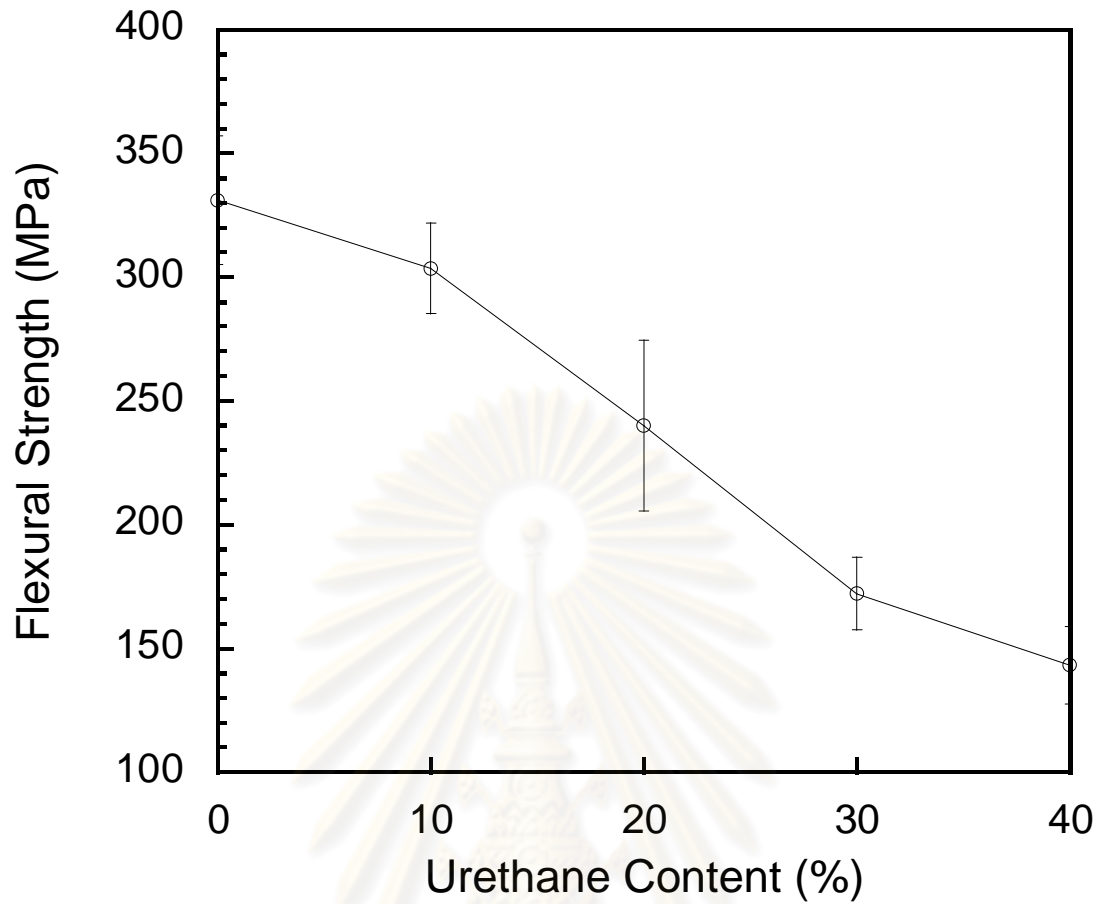


Figure 5.31 Effect of urethane content on in the BA-a/PU alloys flexural strength of their Zylon fiber composites at various compositions.

ศูนย์วิทยทรัพยากร
จุฬาลงกรณ์มหาวิทยาลัย

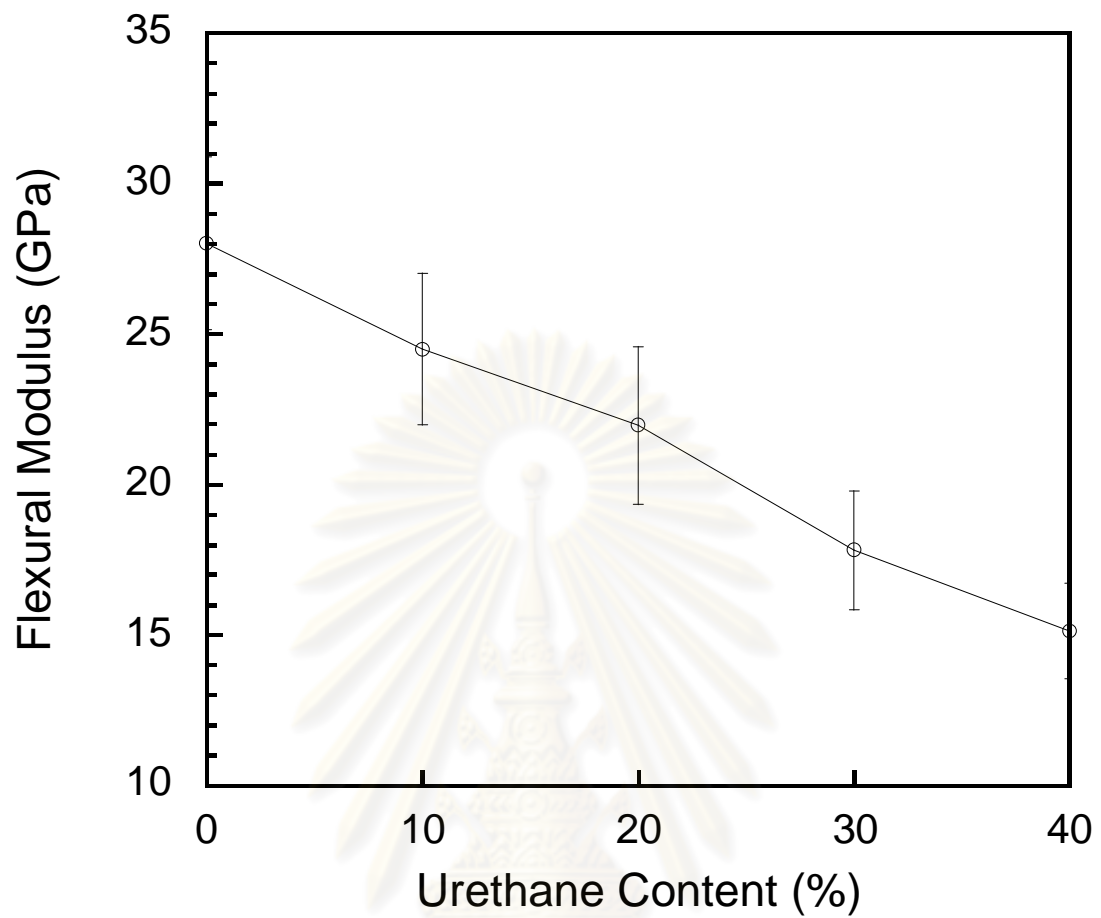


Figure 5.32 Effect of urethane content in the BA-a/PU alloys on flexural modulus of their Zylon fiber composites at various compositions.

ศูนย์วิทยทรัพยากร
จุฬาลงกรณ์มหาวิทยาลัย

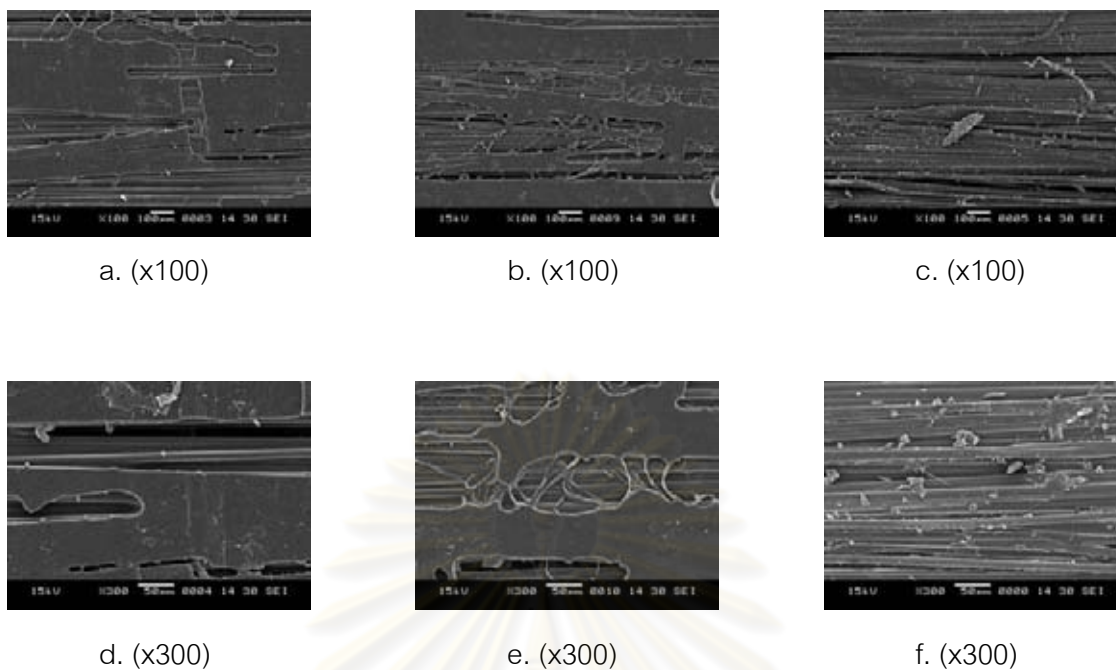


Figure 5.33: SEM micrographs of Zylon fiber-reinforced BA-a/PU composites at various matrix compositions : (a,d) BA-a, (b,e) 80/20 BA-a/PU and (c,f) 60/40 BA-a/PU.

CHAPTER VI

CONCLUSIONS

To widen the range of polybenzoxazine applications, polybenzoxazine alloying with urethane elastomer (PU) was developed. The alloy matrices at various compositions were also reinforced with Zylon fiber to obtain composite materials for high mechanical property applications. The essential characterizations in this research include processability, thermal stability, mechanical properties and physical properties of both the BA-a/PU alloy matrices and their Zylon fiber-reinforced composites.

An addition of urethane resin in BA-a/PU resin mixtures was found to widen their processing window by lowering their liquefying temperature and increasing their gel point. Additionally, the resin mixture curing reaction was observed to occur at higher temperature from the addition of the urethane prepolymer. The fully cured condition of the specimens could be achieved at 150°C for 1 hour, 170°C for 1 hour, 180°C for 1 hour, 190°C for 1 hour and 200°C for 2 hours. Synergism in glass transition temperature (T_g), obtained from both the midpoint temperature of the change in specific heat in the differential scanning calorimetry and from the peak of loss modulus (E'') in the dynamic mechanical analysis, was clearly observed. Moreover, degradation temperatures (T_d) also showed a synergistic behavior as the T_d of the alloys was observed to increase to the value greater than the T_d 's of both parent polymers with the mass fraction of the PU. Furthermore, the char yield of the BA-a/PU alloys was found to increase with the increasing amount of the BA-a fraction due to the higher char yield of the based polybenzoxazine than that of the urethane elastomer. In addition, the coefficient of thermal expansion (CTE) of the alloys was observed to show a minimum at the BA-a/PU = 90/10 mass ratio.

The flexural strength of the BA-a/PU alloys exhibited the ultimate value at BA-a/PU=90/10 mass ratio whereas the flexural modulus of the BA-a/PU alloys at various PU contents also showed a positive deviation from the rule of mixing. Last but not least, the hardness of the BA-a/PU polymer alloys was found to systematically decrease with increasing PU fraction.

These BA-a/PU polymer alloys were also proved to be useful as matrices of Zylon fiber for producing high performance composites with relatively high mechanical properties while still maintaining high thermal stability of the polymer matrices. The degradation temperature and the char yield of the composites were found to increase compared to the matrices. Finally, it was observed that the flexural strength and flexural modulus of the composites were significantly enhanced from those of the matrices possibly because the substantial interfacial strength between the reinforced Zylon fiber and the BA-a/PU matrices.



ศูนย์วิทยทรัพยากร
จุฬาลงกรณ์มหาวิทยาลัย

REFERENCES

- [1] Ishida, H. and Rodriguez, Y. Curing kinetics of a new benzoxazine based phenolic resin by differential scanning calorimetry. Polymer 36 (1995): 3151-3158.
- [2] Kimura, H.; Taguchi, S.; and Matsumoto, A. Studies on new type of phenolic resin (IX) curing reaction of bisphenol A-based benzoxazine with bisoxazoline and the properties of the cured resin. II. cure reactivity of benzoxazine. J. Appl. Polym. Sci. 79 (2000): 2331-2339.
- [3] Ghosh, N. N.; Kiskan, B.; and Yagci, Y. Polybenzoxazines-new high performance thermosetting resins: synthesis and properties. Prog. Polym. Sci. 32 (2007): 1344-1391.
- [4] Nair, C. P. R. Advances in addition-cure phenolic resins. Prog. Polym. Sci. 29 (2004): 401-498.
- [5] Espinosa, M. A.; Cadiz, V.; and Galia, M. Synthesis and characterization of benzoxazine-based phenolic resins: crosslinking study. J. Appl. Polym. Sci. 90 (2003): 470-481.
- [6] Ning, X.; and Ishida, H. Phenolic materials via ring-opening polymerization: synthesis and characterization of bisphenol-A based benzoxazines and their polymers. J. Polym. Sci., Part A: Polym. Chem. 32 (1994): 1121-1129.
- [7] Ishida, H.; and Allen, D. J. Mechanical characterization of copolymers based on benzoxazine and epoxy. Polymer 37 (1996): 4487-4495.
- [8] Ishida, H.; and Lee, Y. H. Synergism observed in polybenzoxazine and poly(ϵ -caprolactone) blends by dynamic mechanical and thermogravimetric analysis. Polymer 42 (2001): 6971-6979.
- [9] Takeichi, T.; and Guo, Y. Preparation and properties of poly(urethane-benzoxazine)s based on monofunctional benzoxazine monomer. Polym. J. 33 (2001): 437-443.
- [10] Takeichi, T.; Guo, Y.; and Agag. Synthesis and characterization of poly (urethane-benzoxazine) films as novel type of polyurethane/phenolic resin Composites. J. Polym. Sci., Part A: Polym. Chem. 38 (2000): 4165-4176.

- [11] Rimdusit, S.; Pirstpindvong, S.; Tanthapanichakoon, W.; and Damrongsakkul, S. Toughening of polybenzoxazine by alloying with urethane prepolymer and flexible epoxy: a comparative study. Polym. Eng. Sci. 45 (2005): 288-297.
- [12] Toyobo Co., Ltd. Technical information from the manufacturer Toyobo[online]. Available from: <http://www.toyobo.co.jp> [2007, October 25]
- [13] Mader, E., et al. Adhesion of PBO fiber in epoxy composites. J. Mater. Sci. 42 (2007): 8047–8052.
- [14] Riess, G.; Schwob J. M.; Guth, G.; and Lande, B. Advances in polymer synthesis. New York: Plenum Press, (1985).
- [15] Ishida, H.; and Allen, D. J. Physical and mechanical characterization of near-zero shrinkage polybenzoxazines J. Polym. Sci., Polym. Phys. Ed. 34 (1996): 1019-1030.
- [16] Takeichi, T.; Guo, Y.; and Rimdusit, S. Performance improvement of polybenzoxazine by alloying with polyimide: effect of preparation method on the properties. Polymer 46 (2005): 4909-4916.
- [17] Hepburn, C. Polyurethane elastomers. 2nd ed. London: Elsevier Science Publishing, 1992.
- [18] Wood, G. The ICI polyurethanes book. 1st ed. Singapore: John Wiley& Sons, 1987.
- [19] Wood, G. The ICI polyurethanes book. 2nd ed. Singapore: John Wiley&Sons, 1990.
- [20] O'Neil, J. M. Factors Contributing to the degradation of poly(p-phenylene benzobisoxazole) (PBO) fibers under elevated temperature and humidity conditions. Master's thesis, Department of Mechanical Engineering, Texas A&M University, 2006.
- [21] Smith, W. F.; and Hashemi, J. Foundations of materials science and engineering. 1st ed. New York: McGraw-Hill Companies Inc., 2006.
- [22] Jones, R. M. Mechanics of composite material. 1st ed. New York: McGraw-Hill, 1975.
- [23] Peters, S. T. Handbook of composites. 2nd ed. New York: Springer, 1997.
- [24] Kimura, H.; Murata, Y.; Matsumoto, A.; Hasegawa, K.; Ohtsaka, K.; and Fukuda, A. New Thermosetting resin from terpenediphenol-based benzoxazine and epoxy resin. J. Appl. Polym. Sci. 74 (1999): 2266-2273.

- [25] Rimdusit, S.; Kampangsaeree, N.; Tanthapanichakoon, W.; Takeichi, T.; and Suppakarn, N. Development of wood-substituted composites from highly filled polybenzoxazine–phenolic novolac alloys. Polym. Eng. Sci. 45 (2007): 140-149.
- [26] Rimdusit, S.; and Ishida, H. Synergism and multiple mechanical relaxations observed in ternary systems based on benzoxazine, epoxy, and phenolic resins. J. Polym. Sci., Polym. Chem. Ed. 38 (2000): 1687-1698.
- [27] Zhou, R.; Lu, D. H.; Jiang, Y. H.; and Li, Q. N. Mechanical properties and erosion wear resistance of polyurethane matrix composites. Wear 259 (2005): 676-683.
- [28] Huang, Y. K.; Frings, P. H.; and Hennes, E. Mechanical properties of Zylon/epoxy composite. Compos: Part B 33 (2002): 109-115.
- [29] Jang, J.; and Yang, H. Toughness improvement of carbon-fibre/polybenzoxazine composites by rubber modification. Compos. Sci. Technol. 60 (2000): 457-463.
- [30] Ishida, H.; and Chaisuwan, T. Mechanical property improvement of carbon fiber reinforce polybenzoxazine by rubber interlayer. Polym. Compos. 24 (2003): 597-607.
- [31] Jubsilp, C.; Takeichi T.; and Rimdusit S. Effect of novel benzoxazine reactive diluent on processability and thermomechanical characteristics of bi-functional polybenzoxazine. J. Appl. Polym. Sci. 104 (2007): 2928-2938.
- [32] Mark, J. E. Physical properties of polymer handbook. New York: AIP Press, 1996.
- [33] Ishida, H.; and Allen, D. J. Physical and mechanical characterization of near-zero shrinkage polybenzoxazines. J. Appl. Polym. Sci. 34 (1996): 1019-1030.
- [34] Nielsen, L. E. Mechanical properties of polymers and composites. 1st ed. New York: Marcel Dekker, 1974.
- [35] Nielsen, L. E.; and Landel, R. F. Mechanical properties of polymers and composites. 2nd ed. New York: Marcel Dekker, 1994.
- [36] Chartoff, R. P. Thermal characterization of polymeric materials. 2nd ed. San Diego: Academic, 1997.
- [37] Morgan, R. J.; Kong, F. M.; and Walkup. Structure-property relations of polyethertriamine-cured bisphenol-A-diglycidyl ether epoxies. J. C.M. Polym. 25 (1984): 375-386.

[38] Xiao, H. X.; and Frisch. K. C, Advances in urethane ionomer. Lancaster: Technomic Publishing, 1995.



ศูนย์วิทยทรัพยากร
จุฬาลงกรณ์มหาวิทยาลัย



APPENDICES

ศูนย์วิทยทรัพยากร
จุฬาลงกรณ์มหาวิทยาลัย

APPENDIX A

Thermal Properties of BA-a/PU Alloys

Appendix A-1 Liquefying and gel temperature of BA-a/PU mixtures.

PU content (wt.%)	Liquefying temperature (°C)	Gel temperature (°C)
0	71	196
10	67	205
20	60	210
30	57	215
40	51	219

Appendix A-2 Curing temperature of BA-a/PU mixtures.

PU content (wt.%)	Curing temperature (°C)
0	224
10	234
20	244
30	245
40	246

Appendix A-3 Glass transition temperature from DSC of BA-a/PU alloys.

PU content (wt.%)	Glass transition temperature (°C)
0	156
10	165
20	180
30	222
40	239

Appendix A-4 Degradation temperature (Td) of BA-a/PU alloys.

PU content (wt.%)	Td of BA-a/PU alloys	
	At 5 wt% loss	At 10 wt% loss
0	325	348
10	326	351
20	327	356
30	334	356
40	336	361

Appendix A-5 Char yield of BA-a/PU alloys.

PU content (wt.%)	Char yield at 800°C (%)
0	28.9
10	24.1
20	23.4
30	20.7
40	18.7

Appendix A-6 Coefficient of thermal expansion of BA-a/PU alloys.

PU content (wt.%)	Coefficient of thermal expansion (ppm/°C)
0	57.7
10	44.7
20	53.0
30	82.8
40	90.2

APPENDIX B

Mechanical Properties of BA-a/PU Alloys

Appendix B-1 Flexural strength of BA-a/PU alloys.

PU content (wt.%)	Flexural strength (MPa)
0	130
10	142
20	120
30	89
40	60

Appendix B-2 Flexural modulus of BA-a/PU alloys.

PU content (wt.%)	Flexural modulus (GPa)
0	5.5
10	4.1
20	3.4
30	2.5
40	2.1

ศูนย์วิทยทรัพยากร
จุฬาลงกรณ์มหาวิทยาลัย

APPENDIX C

Dynamic Mechanical Properties of BA-a/PU Alloys

Appendix C-1 Storage modulus of BA-a/PU alloys at 30°C.

PU content (wt.%)	Storage modulus (GPa)
0	5.2
10	3.8
20	3.2
30	2.5
40	1.8

Appendix C-2 Glass transition temperature from DMA of BA-a/PU alloys.

PU content (wt.%)	Glass transition temperature (°C)
0	166
10	177
20	192
30	220
40	245

ศูนย์วิทยทรัพยากร
จุฬาลงกรณ์มหาวิทยาลัย

APPENDIX D

Physical Properties of BA-a/PU Alloys

Appendix D-1 Surface hardness of BA-a/PU alloys.

PU content (wt.%)	Hardness (Shore D)
0	86
10	77
20	73
30	69
40	68

Appendix D2 Density of BA-a/PU alloys.

PU content (wt.%)	Actual density (g/cm ³)	Theoretical density (g/cm ³)
0	1.188	1.190
10	1.177	1.177
20	1.160	1.164
30	1.148	1.151
40	1.133	1.138

ศูนย์วิทยทรัพยากร
จุฬาลงกรณ์มหาวิทยาลัย

APPENDIX E

Thermal Properties of Zylon Fiber-Reinforced BA-a/PU Composites

Appendix E-1 Degradation temperature (Td) of Zylon fiber-reinforced BA-a/PU composites.

PU content (wt.%)	Td of Zylon fiber reinforced BA-a/PU alloys	
	At 5 wt% loss	At 10 wt% loss
0	384	523
10	369	484
20	352	400
30	349	383
40	344	380

Appendix E2 Char yield of Zylon fiber-reinforced BA-a/PU composites.

PU content (wt.%)	Char yield at 800°C (%)
0	57.8
10	56.9
20	55.6
30	54.0
40	51.7

APPENDIX F

Mechanical Properties of Zylon Fiber-Reinforced BA-a/PU Composites

Appendix F-1 Flexural strength of Zylon fiber-reinforced BA-a/PU composites.

PU content (wt.%)	Flexural strength (MPa)
0	330.9
10	303.5
20	240.5
30	172.1
40	143.2

Appendix F-2 Flexural modulus of Zylon fiber-reinforced BA-a/PU composites.

PU content (wt.%)	Flexural modulus (GPa)
0	28.0
10	24.5
20	21.9
30	17.8
40	15.1

APPENDIX G

Dynamic Mechanical Properties of Zylon Fiber-Reinforced BA-a/PU Composites

Appendix G-1 Storage modulus of Zylon fiber-reinforced BA-a/PU composites at 30°C.

PU content (wt.%)	Storage modulus (GPa)
0	30.8
10	24.3
20	21.1
30	18.0
40	14.3

Appendix G-2 Glass transition temperature of Zylon fiber-reinforced BA-a/PU composites.

PU content (wt.%)	Glass transition temperature (°C)
0	173
10	182
20	188
30	196
40	210

APPENDIX H

Physical Properties of Zylon Fiber-Reinforced BA-a/PU Composites

Appendix H-1 Density of Zylon fiber-reinforced BA-a/PU composites.

PU content (wt.%)	Actual density (g/cm ³)	Theoretical density (g/cm ³)
0	1.414	1.449
10	1.404	1.445
20	1.398	1.441
30	1.379	1.437
40	1.372	1.433



ศูนย์วิทยทรัพยากร
จุฬาลงกรณ์มหาวิทยาลัย

VITAE

Mr. Wanchat Bangsen was born in Songkhla Thailand on May 5, 1985. He obtained a high school diploma in 2002 from Hadyaiwittayalai School. In 2006, he received a Bachelor's Degree in Chemical Engineering from the Department of Chemical Engineering, Faculty of Engineering, King Mongkut's University of Technology North Bangkok. After that, he pursued his graduate study for a Master Degree in Chemical Engineering at the Department of Chemical Engineering, Faculty of Engineering, Chulalongkorn University.



ศูนย์วิทยทรัพยากร
จุฬาลงกรณ์มหาวิทยาลัย